This is to certify that the

dissertation entitled

STOCHASTIC MODELING AND AUTOMATIC CONTROL
OF GRAIN DRYERS:
OPTIMIZING GRAIN QUALITY

presented by

Qiang Liu

has been accepted towards fulfillment
of the requirements for

Ph.D. degree in Agricultural Engineering

F.W. Bakker-Arkema
Major professor

Date December 1, 1998

STOCHASTIC MODELING AND AUTOMATIC CONTROL OF GRAIN DRYERS: OPTIMIZING GRAIN QUALITY

By

Qiang Liu

A DISSERTATION

Submitted to
Michigan State University
in partial fulfillment of the requirements
for the degree of

DOCTOR OF PHILOSOPHY

Department of Agricultural Engineering

1998

ABSTRACT

STOCHASTIC MODELING AND AUTOMATIC CONTROL OF GRAIN DRYERS: OPTIMIZING GRAIN QUALITY

By

Qiang Liu

Quality damage to grain during high-temperature drying has become a severe problem for end users in many grain-processing industries. The problem can not be solved simply by decreasing the drying-air temperature because this will decrease the dryer capacity and the energy efficiency. The major objective of this research is to minimize the quality damage through improving the dryer design and control.

The objective was pursued in two directions, i.e. modeling of the drying process and developing of the control system. Stochastic maize drying and maize-quality models were developed, providing the necessary tools for optimizing dryer design; and, automatic moisture and quality controllers were developed to minimize grain-quality deterioration. Three aspects of maize quality were investigated, i.e. moisture distribution among grain kernels, protein denaturation and viability.

The stochastic nature of the moisture content of maize before and after drying was analyzed. The moisture content distribution of maize kernels at harvest and after thin-layer drying, appeared to be normally distributed, and after crossflow-drying to be skewed. Stochastic models correctly predicted the moisture content distribution in maize kernels

dried in different high-temperature dryer types, i.e. the average moisture content and its standard deviation of the dried grain.

The stochastic crossflow drying model, and the denatured protein and germination models, were combined to analyze the quality of individual kernels. The results served as a guide for operating crossflow dryers.

For the purpose of automatic *moisture control*, a distributed-parameter process model of crossflow drying was utilized to develop a model-predictive control system. The controller has a feedforward loop (i.e. the predictive model and the optimizer) and an feedback loop (i.e. the parameter estimator and the modifier). It was implemented and tested on a commercial crossflow dryer and controlled the moisture content of the maize at the outlet of the dryer to within ± 1.3% of the set point, at inlet moisture contents ranging from 21 to 32% w.b. and drying-air temperatures from 85 to120°C. The controller reacted properly to changes in the drying-air temperature.

The strategy of grain-quality control was analyzed. A neural network model was developed relating the quality of dried grain to various temperature/residence-time conditions. A control algorithm was selected which to varies the drying-air temperature with the objective of maintaining the grain quality close to the set point. Simulation tests showed that a more uniform grain quality is achieved by implementing the quality controller on a crossflow dryer.

ACKNOWLEDGMENTS

Being associated with Dr. Fred W. Bakker-Arkema was a great turn-point in my career. He has profoundly influenced my personal and professional life. His generous help will always be gratefully remembered.

Sincerely appreciation is extended to the guidance committee members: Dr. William Bickert, Agricultural Engineering; Dr. Lawrence Copeland, Crop and Soil Science; Dr. Clark J. Radcliffe, Mechanical Engineering; and Dr. R. Lal Tummala, Electrical and Computer Engineering. Thank you to William D. Crosby, ffi Corporation, Indianapolis, for serving as an outside examiner.

The financial support of ffi Corporation, Indianapolis, IN; MFS/York, Grand Island, NE and the Crop and Food Bioprocessing Center (CFBC) at Michigan State University, are greatly appreciated. Special thanks go to Mr. Curt Fankhauser, Chairman and CEO of ffi Corporation; Mr. Robert. E. Hines, former General Manager of MFS/York; and Prof. Kris A. Berglund, Director of the CFBC.

Also acknowledged is the willingness and tremendous cooperation received from the people at Jorgensen Farm Elevator without whom the experimental field tests would not have been successful. Special thanks go to Mr. Mike Turner, Manager of Jorgensen Farm Elevator.

Thanks also due to Jim E. Montross, James S. Labiak, Kyle E. Weidmayer for their help in the test. Special thanks to Lillian Agranian for her secretarial support.

Deep appreciation to my wife, Xiuli Qi, for her hard work, moral support and sacrifice, and to my lovely daughters, Xiaoxue Liu and Dana Xiaodan Liu.

TABLE OF CONTENT

INTRODUCTION **1**

OBJECTIVES 4

OUTLINE OF THE DISSERTATION 4

REFERENCES 8

CHAPTER 1. STOCHASTIC MODELING OF GRAIN DRYING: EXPERIMENTAL INVESTIGATION* **9**

ABSTRACT 9

1.1 INTRODUCTION 10

1.2 LITERATURE REVIEW 10

1.3 EXPERIMENTAL DETAILS 12

1.3.1 MOISTURE CONTENT MEASUREMENT OF INDIVIDUAL KERNELS 12

1.3.2 LABORATORY THIN-LAYER DRYING 13

1.3.3 COMMERCIAL CROSSFLOW DRYING 13

1.4 RESULTS 14

1.4.1 MOISTURE DISTRIBUTION AT HARVEST 14

1.4.2 MOISTURE DISTRIBUTION DURING DRYING 18

1.4.3 MOISTURE DISTRIBUTION DURING STORAGE 29

1.5 CONCLUSIONS 29

REFERENCES 31

CHAPTER 2. STOCHASTIC MODELING OF GRAIN DRYING: MODEL DEVELOPMENT* ... **32**

ABSTRACT 32

2.1 INTRODUCTION 33

2.2 THIN-LAYER DRYING MODEL 34

2.3 DEEP-BED (ONE-DIMENSIONAL) DRYING MODEL 35

2.4 DEEP-BED (TWO-DIMENSIONAL) DRYING MODEL 37

2.5. BASIS CONVERSION OF THE GRAIN MOISTURE CONTENT 38

2.6 MODEL VALIDATIONS 39

2.6.1 THIN-LAYER DRYING 39

2.6.2 CROSSFLOW DRYER 39

2.7 CONCLUSIONS 42

REFERENCES 44

APPENDIX 2A: THE MOISTURE CONTENT DISTRIBUTION OF GRAIN DRIED IN A ONE-DIMENSIONAL (CONCURRENT- OR COUNTER-FLOW) DEEP-BED DRYER 46

APPENDIX 2B: THE MOISTURE CONTENT DISTRIBUTION OF GRAIN DRIED IN A TWO-DIMENSIONAL (CROSSFLOW) DEEP-BED DRYER 49
SYMBOLS 52

CHAPTER 3. STOCHASTIC MODELING OF GRAIN DRYING: ANALYSIS OF CROSSFLOW DRYING* **53**

ABSTRACT 53
3.1 INTRODUCTION 54
3.2 CROSSFLOW DRYER SPECIFICATIONS 54
3.3 CROSSFLOW DRYER PERFORMANCE CHARACTERISTICS 55
3.4 STANDARD DEVIATION 60
3.5 AIR TEMPERATURE 64
3.6 AIRFLOW RATE 64
3.7 GRAIN INVERSION 64
3.8 CONCLUSION 70

CHAPTER 4. MODELING OF GRAIN QUALITY* **72**

ABSTRACT 72
4.1 INTRODUCTION 73
4.2 LITERATURE REVIEW 74
4.3 MODELS AND SIMULATION 81
4.3.1 QUALITY MODELS 81
4.3.2 QUALITY SIMULATION 82
4.3.3 MODEL VALIDATIONS 84
4.4 GAIN-QUALITY ANALYSIS 86
CONCLUSIONS 98
REFERENCES 100

CHAPTER 5. DISTRIBUTED-PARAMETER PROCESS MODEL FOR GRAIN DRYING **102**

ABSTRACT 102
5.1 INTRODUCTION 103
5.2 REVIEW OF GRAIN DRYING MODELS 104
5.3 MODEL DEVELOPMENT 106
5.3.1 ELEMENTAL DRYING MODELS (EDM) 106
5.3.2 FULL-SIZE DRYER MODEL 113
5.4 VALIDATION OF THE MODELS 114
5.5 DISCUSSION AND CONCLUSIONS 117
APPENDIX 5A: ONE-DIMENSIONAL CROSSFLOW DRYING MODEL 118

SYMBOLS 121
ABBREVIATIONS 122
REFERENCES 123

CHAPTER 6: DESIGN OF CONTROL ALGORITHM 125

ABSTRACT 125
6.1 INTRODUCTION 126
6.2 PROCESS CHARACTERISTICS AND REVIEW OF THE CONTROL STRATEGIES 127
6.3 MODEL-PREDICTIVE CONTROL STRATEGY 130
6.3.1 FEEDFORWARD LOOP 133
6.3.2 FEEDBACK LOOP (PARAMETER ESTIMATOR/MODIFIER) 136
6.4 SIMULATION TESTS AND TUNING OF THE CONTROLLER 138
6.4.1 VIRTUAL GRAIN DRYER AND CONTROLLER 138
6.4.2 FEEDFORWARD CONTROL 140
6.4.3 FEEDBACK CONTROL 145
6.4.4 ROBUSTNESS OF THE CONTROLLER 148
6.5 CONCLUSIONS 154
REFERENCES 159

CHAPTER 7. FIELD TESTS OF THE CONTROLLER 161

ABSTRACT 161
7.1 INTRODUCTION 162
7.2 IMPLEMENTATION 162
7.2.1 GRAIN DRYER 162
7.2.2 CONTROL SYSTEM 164
7.2.3 PROGRAMMING 166
7.3 RESULTS AND DISCUSSION 169
7.3.1 ON-LINE CALIBRATION OF THE MOISTURE SENSORS 169
7.3.2 CONTROL TESTS 170
7.4 CONCLUSIONS 186
REFERENCES 187

CHAPTER 8. GRAIN QUALITY CONTROL IN HIGH-TEMPERATURE DRYERS 188

ABSTRACT 188
8.1 INTRODUCTION 189
8.2 CONTROL-ORIENTED QUALITY MODELS 190
8.3 QUALITY CONTROL ALGORITHM 195
8.4 CONCLUSIONS 202

REFERENCES 204

CHAPTER 9. SUMMARY 205

9.1 STOCHASTIC DRYING MODELING 205
9.2 GRAIN-QUALITY MODELS 205
9.3 MOISTURE CONTROLLER 206
9.4 GRAIN-QUALITY CONTROLLER 206
9.5 SUGGESTIONS FOR FUTURE STUDY: 207

LIST OF TABLES

TABLE I.1 SHRINKAGE IN METRIC TONNES (MT) AND SHRINKAGE COST WHEN 25,400 MT (1,000,000 BU) OF MAIZE IS DRIED BELOW 15.5% W.B. (BROOKER ET AL., 1992). 3

TABLE I.2 ENERGY REQUIRED PER METRIC TONNE (MT) AND COST (AT DIFFERENT ENERGY PRICES) RESULTING FROM VARIOUS LEVELS OF OVERDRYING OF 25,400 MT (1,000,000 BU) OF 15.5% W.B. MAIZE (BROOKER ET AL., 1992) 3

TABLE 1.1 χ^2 TEST FOR NORMALITY IN THE MOISTURE CONTENT DISTRIBUTION OF MAIZE *AT HARVEST BEFORE SMOOTHING* OF THE DATA 16

TABLE 1.2 χ^2 TEST FOR NORMALITY IN THE MOISTURE CONTENT DISTRIBUTION OF MAIZE *AT HARVEST AFTER SMOOTHING* OF THE DATA IN TABLE 1.1. 17

TABLE 2.1 EXPERIMENTAL AND SIMULATED STANDARD DEVIATIONS (SD) OF MAIZE DRIED IN CROSSFLOW DRYERS. 45

TABLE 2.2 EXPERIMENTAL AND SIMULATED STANDARD DEVIATION (SD) DRIED IN CROSSFLOW DRYERS *EXCLUDING KERNELS AT MOISTURE CONTENTS LOWER THAN 9%.* 45

TABLE 3.1 DESIGN SPECIFICATIONS AND OPERATING CHARACTERISTICS OF THE STANDARD CROSSFLOW DRYER USED IN THE ANALYSIS OF THE MSU STOCHASTIC DRYING MODEL 54

TABLE 3.2 MOISTURE CONTENT (MC) AND STANDARD DEVIATION (SD) OF THE MOISTURE CONTENT (AVERAGE, AT AIR-INLET, AT AIR-OUTLET) OF MAIZE DRIED IN A CROSSFLOW DRYER *WITHOUT GRAIN-INVERSION* (AIR TEMPERATURE, 90°C; AIRFLOW RATE, 80 $M^3\ MIN^{-1}\ T^{-1}$). 69

TABLE 3.3 MOISTURE CONTENT (MC) AND STANDARD DEVIATION (SD) OF THE MOISTURE CONTENT (AVERAGE, AT AIR-INLET, AT AIR-OUTLET) OF MAIZE DRIED IN A CROSSFLOW DRYER *WITH GRAIN-INVERSION* (AIR TEMPERATURE, 90°C; AIRFLOW RATE, 80 $M^3\ MIN^{-1}\ T^{-1}$). 70

TABLE 4.1 EXPERIMENTAL AND PREDICTED TRANSMITTANCE AND DENATURATION OF PROTEIN AFTER DRYING OF MAIZE IN THREE COMMERCIAL CROSSFLOW DRYERS. 85

TABLE 4.2 EXPERIMENTAL AND PREDICTED GERMINATION OF MAIZE AFTER TWO HOURS OF DRYING IN A BATCH DRYER IN DRYING MAIZE TO 15% MC. 85

TABLE 4.3 DRYING CONDITIONS FOR THE GRAIN-QUALITY SIMULATION STUDY IN A CROSSFLOW DRYER. 85

TABLE 4.4A PREDICTED QUALITY OF MAIZE AFTER CROSSFLOW DRYING AT AN AIRFLOW RATE OF 40 CFM/BU (32 $M^3M^{-3}MIN^{-1}$) 88

TABLE 4.4B PREDICTED QUALITY OF MAIZE AFTER CROSSFLOW DRYING AT AN AIRFLOW RATE OF 60 CFM/BU (48 $M^3M^{-3}MIN^{-1}$). 88

TABLE 4.4C PREDICTED QUALITY OF MAIZE AFTER CROSSFLOW DRYING AT AN AIRFLOW RATE OF 80 CFM/BU (64 $M^3M^{-3}MIN^{-1}$). 89

TABLE 4.4D PREDICTED QUALITY OF MAIZE AFTER CROSSFLOW DRYING AT AN AIRFLOW RATE OF 100 CFM/BU (80 $M^3M^{-3}MIN^{-1}$). 89

TABLE 4.5 MAIZE QUALITY AFTER CROSSFLOW DRYING WITH AND WITHOUT AIR INVERSION AT THE MIDPOINT ALONG THE DRYING COLUMN WITH AN AIRFLOW RATE OF 60 CFM/BU (48 $M^3M^{-3}MIN^{-1}$). 99

TABLE 4.6 EFFECT OF THE STANDARD DEVIATION (SD) OF THE INLET MOISTURE CONTENT OF MAIZE ON THE FINAL GERMINATION AFTER CROSSFLOW DRYING (WITH AN AIRFLOW RATE OF 60 CFM/BU OR 48 $M^3M^{-3}MIN^{-1}$). 99

TABLE 5.1 THE SPECIFICATIONS OF THE ZIMMERMAN VT1210 AND VT4036 DRYERS. 115

TABLE 5.2 PREDICTED CAPACITY OF ZIMMERMAN VT1210 MAIZE DRYER USING THE C.O.D. MODEL AND P.E.D. MODEL. 116

TABLE 5.3 PREDICTED CAPACITY OF THE ZIMMERMAN VT4036 MAIZE DRYER USING THE C.O.D. MODEL AND P.D.E. MODEL. 116

TABLE 6.1 RESPONSE CHARACTERISTICS OF THE OUTLET MOISTURE CONTENT TO THE MODIFICATION OF THE DRYING CONSTANT FOR DIFFERENT VALUES OF THE FILTER FACTOR. 148

List of Figures

Fig. I.1 A schematic representation of the contents of the thesis. 7

Fig. 1.1 Typical frequency distribution of the kernel moisture content in maize reaching a dryer (average moisture content is 37.5 % d.b.). 15

Fig. 1.2 The frequency distribution of the raw data, smoothed data and the corresponding normal distribution of the moisture content of maize kernels in a typical maize sample reaching a dryer. 19

Fig. 1.3 Experimental thin-layer drying curves (each curve is the average of 60 kernels) of maize at three drying-air temperatures. 20

Fig. 1.4 The standard deviation at different average moisture contents (60 kernels as a group) during thin-layer drying of maize at three drying-air temperature. 21

Fig. 1.5 The moisture content distribution of 60 kernels at three drying stages during thin-layer drying at 60°C; the average moisture contents are 24.4 % (initial), 17.6 % and 14.9 % d.b., respectively, from left to right. 22

Fig. 1.6 The frequency distribution of the kernel dry mass of a typical maize sample. 24

Fig. 1.7 The drying curves of maize kernels grouped by dry weight during thin-layer drying of 60 kernels at 60°C. 25

Fig. 1.8 The standard deviation of the moisture content of maize kernels grouped by dry weight during drying at 60°C. 26

Fig. 1.9 Moisture distribution before and after drying of maize in a crossflow dryer (CF1); inlet average M.C.=33.0% d.b., stand. dev.=8.6% d.b., and outlet average M.C.=17.2% d.b., stand. dev. =7.1% d.b.. 27

Fig. 1.10 Moisture distribution before and after drying of maize in another crossflow dryer (CF2); at the inlet the average M.C. =34.0% d.b., stand. dev. =7.9% d.b., and at the outlet the average M.C. =18.6% d.b., stand. dev. =7.7% d.b. 28

Fig. 1.11 The change in the standard deviation over time of three maize samples after crossflow drying and storage at 20°C. The average moisture contents of samples are 22.4 % (Δ), 15.9 % (X) and 19.9 % (O) d.b., respectively. 30

Fig. 2.1 Predicted and experimental standard deviations of the moisture content of maize during single-kernel drying at 60°C and 70°C, respectively. 40

Fig. 2.2 Predicted and experimental standard deviations of the moisture content of maize during thin-layer drying at 80°C. 41

Fig. 2. A1 Simulated dryer exit moisture content distribution in a concurrent-flow maize dryer employing different thin-layer drying equations. 51

FIG. 3.1 THE AVERAGE MOISTURE CONTENT (AMC) OF MAIZE, THE DIFFERENCE BETWEEN THE AVERAGE MCS OF THE AIR-INLET AND AIR-OUTLET SUB-COLUMNS (AMCD), AND THE STANDARD DEVIATION ACROSS THE GRAIN COLUMN (SD), OF A CROSSFLOW DRYER OPERATING AT 90°C 56

FIG. 3.2 THE DRYING CURVES OF 25 % W.B. INITIAL MOISTURE CONTENT MAIZE AT DIFFERENT POSITIONS WITHIN THE GRAIN COLUMN OF A CROSSFLOW DRYER OPERATING AT 90°C. 57

FIG. 3.3 THE STANDARD DEVIATION OF THE MOISTURE CONTENT AT DIFFERENT POSITIONS WITHIN THE GRAIN COLUMN. MAIZE INITIALLY AT 25% (W.B.) MOISTURE CONTENT AND DRIED IN A CROSSFLOW DRYER OPERATING AT 90°C. 58

FIG. 3.4 THE MOISTURE DISTRIBUTION OF MAIZE BEFORE DRYING, AND AFTER ONE HOUR AND TWO HOURS OF CROSSFLOW DRYING AT 90°C. MAIZE INITIALLY AT 25% W.B. AVERAGE MOISTURE CONTENT WITH 3% W.B. STANDARD DEVIATION. 59

FIG. 3.5 THE STANDARD DEVIATION (SD) OF THE MOISTURE CONTENT OF MAIZE IN A CROSSFLOW DRYER FOR DIFFERENT INITIAL SD VALUES; THE DRYER OPERATES AT 90°C. 61

FIG. 3.6 THE MOISTURE DISTRIBUTION OF MAIZE DRIED IN A CROSSFLOW DRYER AT DIFFERENT AIR TEMPERATURES. MAIZE INITIALLY AT 25% W.B. AVERAGE MOISTURE CONTENT AND 3% W.B. STANDARD DEVIATION. 62

FIG. 3.7 THE STANDARD DEVIATION OF THE MOISTURE CONTENT IN MAIZE DRIED IN A CROSSFLOW DRYER AT DIFFERENT AIR TEMPERATURES. MAIZE INITIALLY AT 25% W.B. MOISTURE CONTENT. 63

FIG. 3.8 THE MOISTURE DISTRIBUTION OF MAIZE DRIED AT 90°C IN A CROSSFLOW DRYER AT DIFFERENT AIRFLOW RATES ($M^3\ MIN^{-1}\ T^{-1}$) . MAIZE INITIALLY AT 25% W.B. AVERAGE MOISTURE CONTENT WITH 3% W.B. STANDARD DEVIATION. 65

FIG. 3.9 THE STANDARD DEVIATION OF MAIZE DRIED AT 90°C IN A CROSSFLOW DRYER AT DIFFERENT AIRFLOW RATES ($M^3MIN^{-1}T^{-1}$). MAIZE INITIALLY AT 25% W.B. MOISTURE CONTENT. 66

FIG. 3.10 THE MOISTURE DISTRIBUTION OF MAIZE BEFORE DRYING, AND AFTER ONE HOUR AND TWO HOURS OF CROSSFLOW DRYING AT 90°C. THE MAIZE IS INITIALLY AT 25% W.B. MOISTURE CONTENT AND IS INVERTED AFTER 1 HOUR OF DRYING. 67

FIG. 3.11 THE STANDARD DEVIATION (SD) OF THE MOISTURE CONTENT OF MAIZE DRIED AT 90°C IN A CROSSFLOW DRYER WITH AND WITHOUT GRAIN-INVERSION. THE MAIZE IS INITIALLY AT 25% W.B. MOISTURE CONTENT 68

FIG. 4.1 EXPERIMENTAL (POINTS) AND PREDICTED (LINES) GERMINATION VS. TIME OF MAIZE AT FOUR LOCATIONS (AT THE AIR INLET, AT 1/2, 2/3 AND AIR OUTLET) IN THE GRAIN COLUMN 87

FIG. 4.2 DENATURED PROTEIN VS. DRYING AIR TEMPERATURE IN MAIZE DRIED IN A CROSSFLOW DRYER WITH AN INITIAL MOISTURE CONTENT OF 20% W. B. AT AIRFLOW RATES OF 32, 48, 64, 80 AND 96 $M^3M^{-3}MIN^{-1}$. 92

FIG. 4.3 DENATURED PROTEIN VS. AIRFLOW RATE IN MAIZE DRIED IN A CROSSFLOW DRYER WITH AN INITIAL MOISTURE CONTENT OF 20% W.B. AND AT DRYING AIR TEMPERATURES OF 50, 60, 70, 80, 100 AND 120°C. 93

FIG. 4.4 DENATURED PROTEIN VS. INLET MOISTURE CONTENT IN MAIZE DRIED IN A CROSSFLOW DRYER AT AN AIRFLOW RATE OF 48 $M^3M^{-3}MIN^{-1}$ AND AT DRYING AIR TEMPERATURES OF 50, 60, 70, 80, 100 AND 120°C. 94

FIG. 4.5 GERMINATION VS. DRYING AIR TEMPERATURE IN MAIZE DRIED IN A CROSSFLOW DRYER AT AN AIRFLOW RATE OF 48 $M^3M^{-3}MIN^{-1}$ AND WITH INLET MOISTURE CONTENTS OF 17.5, 20, 25, 30 AND 35%W.B.. 95

FIG. 4.6 GERMINATION VS. AIRFLOW RATE IN MAIZE DRIED IN A CROSSFLOW DRYER WITH AN INITIAL MOISTURE CONTENT OF 20% AND AT DRYING AIR TEMPERATURES OF 50, 60, 70, 80, 100 AND 120°C.96

FIG. 4.7 GERMINATION VS. INLET MOISTURE CONTENT IN MAIZE DRIED IN A CROSSFLOW DRYER AT AN AIRFLOW RATE OF 48 $M^3M^{-3}MIN^{-1}$ AND AT DRYING AIR TEMPERATURES OF 50, 60, 70, 80, 100 AND 120°C. 97

FIG. 5.1 SCHEMATIC OF CROSSFLOW DRYING. 107

FIG. 5.2 DRYING PROCESSES ON A PSYCHROMETRIC CHART. 109

FIG. 5A.1 LINEAR APPROXIMATION OF EQ. 5A.2 AT INLET DRYING-AIR TEMPERATURE OF 100°C (OR 672°R). 119

FIG. 6.1 MODEL-PREDICTIVE CONTROL OF GRAIN DRYERS. 132

FIG. 6.2 CONTROL PANEL OF THE VIRTUAL GRAIN DRYER FOR CONTROL TEST 139

FIG. 7.2 IMPLEMENTATION OF THE CONTROLLER 165

FIG. 7.3 FLOWCHART OF THE CONTROL PROGRAM. 168

FIG. 7.4 COMPARISON OF THE READINGS OF THE TRIME SENSORS AND THE BURROWS METER: (A) INLET MOISTURE, AND (B) OUTLET MOISTURE 171

FIG. 7.5 MEASURED AND PREDICTED OUTLET MOISTURE CONTENTS AND THE VALUE OF THE MULTIPLIER OF THE MAIZE DRYING CONSTANT IN A CROSSFLOW DRYER OPERATING UNDER ZAE CONTROL (DRYING-AIR TEMPERATURE = 105°C, SET POINT =14.5% W.B., FILTER FACTOR β = 0.5). 173

FIG. 7.6 INLET AND OUTLET MOISTURE CONTENTS, AND THE AUGER SPEED DURING AUTOMATIC CONTROL OF A CROSSFLOW DRYER WITH ZAE CONTROL (DRYING-AIR TEMPERATURE = 105°C, FILTER FACTOR β = 0.5, INITIAL MULTIPLIER γ_0 = 0.7, RESIDENCE TIME=2.5-3.5 HOURS). 174

FIG. 7.7 INLET AND OUTLET MOISTURE CONTENTS, AND THE AUGER SPEED DURING AUTOMATIC CONTROL OF A VT1210 DRYER WITH ZAE CONTROL (DRYING-AIR TEMPERATURE = 105°C, FILTER FACTOR β = 0.5, INITIAL MULTIPLIER γ_0 = 0.6, RESIDENCE TIME =2.0-2.5 HOURS). 176

FIG. 7.8 MEASURED AND PREDICTED OUTLET MOISTURE CONTENTS, AND THE MODEL ERROR (I.E. THE MEASURED MINUS THE PREDICTED OUTLET MOISTURE CONTENTS) DURING THE TEST SHOWN IN FIG. 7.7. 177

FIG. 7.9 INLET AND OUTLET MOISTURE CONTENTS, AND THE AUGER SPEED, DURING AUTOMATIC CONTROL OF A VT1210 DRYER WITH ZAE CONTROL AND AN INLET MOISTURE FILTER (DRYING-AIR TEMPERATURE =

105°C, FILTER FACTOR β = 0.5, INITIAL MULTIPLIER γ_0 = 0.7, SET POINT = 15% W.B., RESIDENCE TIME=2-2.5 HOURS). 179

FIG. 7.10 INLET AND OUTLET MOISTURE CONTENTS, AND THE AUGER SPEED, DURING AUTOMATIC CONTROL OF A VT1210 DRYER WITH LSE CONTROL (DRYING-AIR TEMPERATURE = 105°C, FILTER FACTOR β = 0.5, INITIAL MULTIPLIER γ_0 = 0.7, RESIDENCE TIME = 2.5-3.0 HOURS). 180

FIG. 7.11 INLET AND OUTLET MOISTURE CONTENTS, AND THE AUGER SPEED DURING AUTOMATIC CONTROL OF A CROSSFLOW DRYER WITH LSE CONTROL AND THE INLET MOISTURE FILTER (DRYING-AIR TEMPERATURE = 105°C, FILTER FACTOR β = 0.5, INITIAL MULTIPLIER γ_0 = 0.7, RESIDENCE TIME = ABOUT 2.5 HOURS)..... 181

FIG. 7.12 RESPONSE TO A STEP CHANGE IN THE DRYING-AIR TEMPERATURE OF A VT1210 DRYER FROM 105 TO 85°C WITH ZAE CONTROL (SET POINT =15% W.B., FILTER FACTOR β = 0.5, INITIAL MULTIPLIER γ_0 = 0.7, RESIDENCE TIME = ABOUT 2.5 HOURS). 183

FIG. 7.13 RESPONSE TO A STEP CHANGE IN THE DRYING-AIR TEMPERATURE OF A VT1210 DRYER FROM 85 TO 105°C WITH LSE CONTROL (SET POINT = 15% W.B., FILTER FACTOR β = 0.5, INITIAL MULTIPLIER γ_0 = 0.7, RESIDENCE TIME = 2.5-3.0 HOURS). 184

INTRODUCTION

Grain is usually harvested at high moisture contents to minimize field losses. The grain moisture needs to be reduced to a safe level for storage. Therefore, artificial drying has become prevalent on farms or at elevators.

Depending on the temperature of the drying-air, artificial drying is categorized into natural-air drying (i.e. using ambient air), low-temperature drying (the ambient air is heated a few degrees), and high-temperature drying. High-temperature drying is popular because of its high drying capacity. The principle high-temperature dryer types are: crossflow, mixed-flow and concurrent-flow dryers. The drying-air temperature ranges from 50-300°C (Brooker et al., 1992), depending on the dryer type and type of grain.

The application of high-temperature drying has significantly increased the harvest/drying rate of farmers. However, severe damage to grain quality, both physically and bio-chemically, may happen in the drying process. For instance, an average 10-20% of protein in maize is usually denatured in a conventional high-temperature dryer (Chang et al., 1989). In the wet-milling industry, the drying conditions have a 2-3 times greater effect on the starch recovery rate than variety and maturity (Le Bras, 1982); in fact, if the drying-air temperature in a mixed-flow dryer is higher than 100°C, the maize becomes unacceptable for wet-milling (Lasseran, 1988).

The diversity of maize utilization has increased rapidly in last a few years. Only 9.9% of US maize was consumed as food and alcohol in 1986 but doubled in 1996, reaching a total of 1650 million bushels a year (USDA, 1997). Additional non-food maize products, such as maize-based biodegradable plastics, salt substitutes and ethanol-

containing products, have come on the market recently because of their environmental, health-related and economic benefits. The non-food uses of maize demand high quality grain.

Dryer design needs to be improved to produce high-quality grain for non-feed industries. Conventional high-temperature grain dryers in the US have been mainly designed for feed grain. The research has focused on dryer capacity and energy efficiency; grain quality became a major concern only in the late 1980s. Limited number of experimental and modeling studies have thus far been conducted to quantify the major factors causing quality damage to grain in the drying process.

Adequate control of the dryer is essential to reduce the quality damage because of overdrying and underdrying of the grain. Overdrying causes breakage and stress-cracks in maize kernels. Overdrying is also costly because of the unnecessary loss in weight and the extra energy consumption. Table I.1 lists the shrinkage of 25,400 MT of maize (1,000,000 bu) caused by overdrying 0.25-2.00% beyond 15.5%, and the cost of the shrinkage at two price levels (Brooker et al., 1992). Thus, the shrinkage in overdrying 25,400 MT by 1.0% moisture results in a weigh loss of 297 MT, and costs $17,544 when maize sells for $59.1/MT, and $29,240 when maize sells for $98.4/MT. The additional energy needed in the drying process and the extra energy cost are tabulated in Table I.2. The data show that 1.0% overdrying requires an additional 87.8 MJ/MT in energy and costs $10,570 per 25,400 MT, assuming the energy cost is $5.00/1,055 MJ.

A limited number of research studies have been conducted on moisture control, but only a few control algorithms have been implemented on commercial dryers. More work is needed on moisture control to better address the non-linearity and long delay of

Table I.1 Shrinkage in metric tonnes (MT) and shrinkage cost when 25,400 MT (1,000,000 bu) of maize is dried below 15.5% w.b. (Brooker et al., 1992).

Overdrying, %	Shrinkage	Cost ($) at two prices	
	MT	59.1/MT	98.4/MT
0.25	74.9	4,425	7,375
0.50	149.4	8,823	14,705
1.00	297.1	17,544	29,240
1.50	443.1	26,163	43,605
2.00	587.3	34,682	57,803

Table I.2 Energy required per metric tonne (MT) and cost (at different energy prices) resulting from various levels of overdrying of 25,400 MT (1,000,000 bu) of 15.5% w.b. maize (Brooker et al., 1992)

Overdrying, %	Energy required	Natural gas cost ($/ 1055MJ)	
	MJ/MT	5.00/MT	7.00/MT
0.25	22.1	2,655	3,717
0.50	44.1	5,305	7,427
1.00	87.8	10,570	14,798
1.50	132.2	15,920	22,288
2.00	180.5	21,730	30,422

the grain drying process. As grain quality becomes of greater concern, a new issue in grain dryer operation is the control of the drying-air temperature to optimize grain quality.

Objectives

The major objectives of the research conducted in this study were:

1. To develop stochastic grain drying models, predicting the average and the standard deviation of the moisture content of individual maize kernels in a drying process.
2. To develop grain quality models which quantify the quality deterioration of maize in the drying process.
3. To develop a moisture controller which minimizes the overdrying and underdrying during the drying process.
4. To develop a grain-quality controller which controls the drying-air temperature during the drying process according to specific grain-quality requirements.

The investigations are primarily concerned with crossflow drying of maize because the crossflow dryer is prevalent in the US, and maize is the major grain type. However, the results will be applicable to other dryer types and other grains.

Outline of the dissertation

The thesis is divided into four parts. Part I, Chapters 1, 2 and 3, present the development of the stochastic grain drying models. Part II, Chapter 4, covers the quality

simulation. Part III, Chapters 5, 6 and 7, describe the moisture controller. And, Part IV, Chapter 8, discusses the grain-quality controller.

Part I: Stochastic Modeling of Grain Drying

In Chapters 1-3, the stochastic nature of the moisture content of maize before and after drying is explored. Chapter 1 presents experimental data of the moisture content distribution in maize at harvest time, after thin-layer drying, and after crossflow drying. In Chapter 2, the stochastic models are developed of the moisture-content distribution in maize dried in concurrent-flow, counter-flow and crossflow dryers. In Chapter 3, the process of maize drying in a crossflow dryer is analyzed stochastically.

Part II: Modeling of Grain Quality

In Chapter 4, the stochastic drying model and the denatured protein and germination models are combined to simulate the quality of individual kernels in grain crossflow dryers. The relationship between the drying conditions and the grain quality after drying is analyzed.

Part III: Moisture Control of Grain Dryers

A control-oriented grain drying model is developed in Chapter 5. Chapter 6 covers the design of the control algorithms, and the tuning and simulation tests of the controller. Chapter 7 presents the implementation and field testing of the controller on a commercial maize dryer.

Part IV: Grain Quality Control

Chapter 8 discusses the development of the quality-control model and the associated control algorithm.

The relationship between the various parts of the thesis is shown in Fig. I.1.

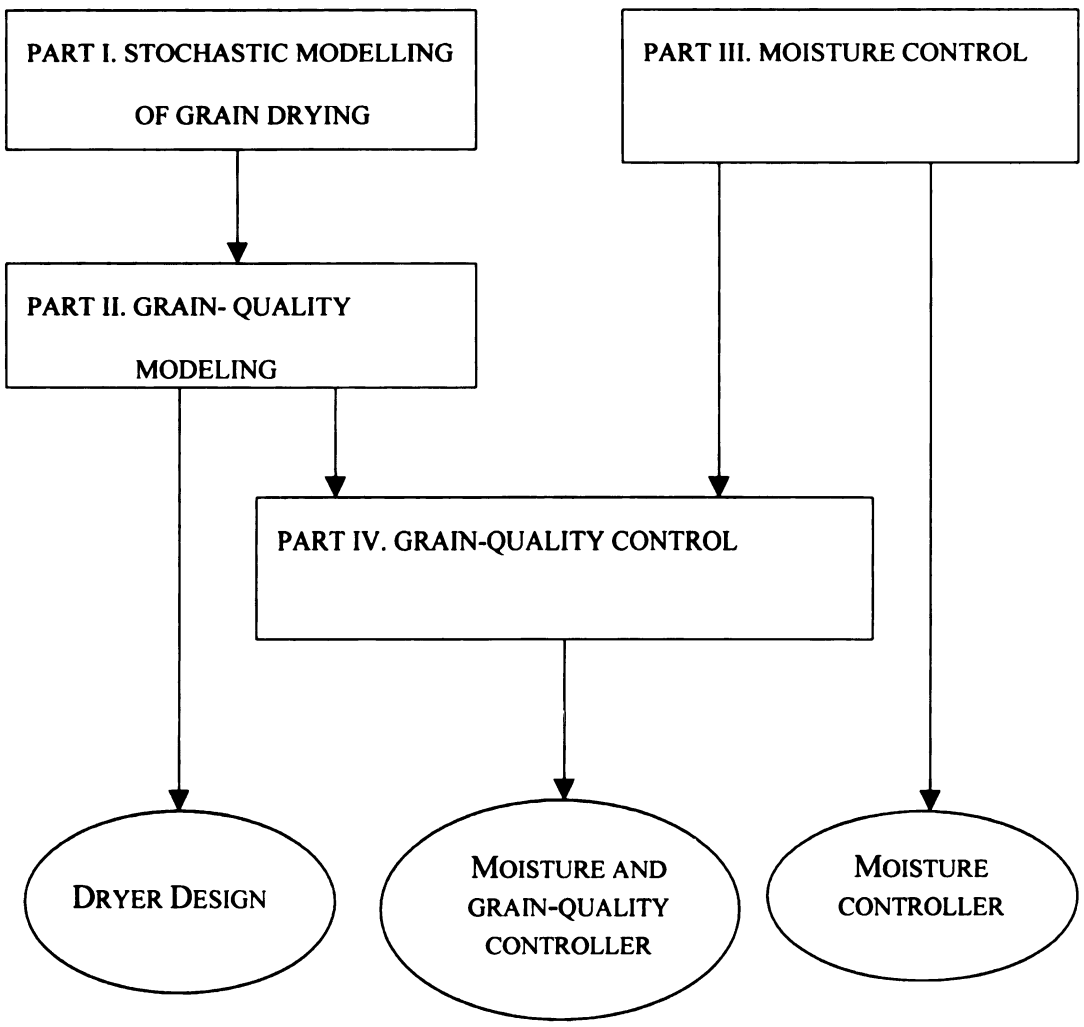

Fig. I.1 A schematic representation of the contents of the thesis.

References

Brooker D.B., Bakker-Arkema, F.W., Hall, C.W. 1992. Drying and Storage of Grains and Oilseeds. Van Nostrand Reinhold, New York, NY.

Chang, C. H. and M. R. Paulsen. 1989. Moisture distribution and starch recovery of commercially dried maize. Paper No. 89-6525, American Society of Agricultural Engineers, St. Joseph, MI.

Lasseran, J. C., A. Le Bras. 1988. Improvement of drying techniques to better grain quality for processing industries. Paper No. 88-323. Presented at the International Conference on Agricultural Engineering, Ag Eng 88, Paris, France. March 2-5, 1988.

Le Bras, A.1982. Maize drying and its resulting quality for wet-milling industry. In: Maize: Recent Progress in Chemistry and Technology. Academic Press, Inc., New York, NY.

USDA. 1997. Feed Situation and Outlook. Economic Research Service, U.S. Department of Agriculture, Washington, DC.

CHAPTER 1. STOCHASTIC MODELING OF GRAIN DRYING: EXPERIMENTAL INVESTIGATION*

Abstract

Previous research has shown that the variance in the moisture content of individual maize kernels is significant at harvest. In this series of three Chapters, the stochastic nature of the moisture content of maize before and after drying is explored. Chapter 1 presents experimental data of the moisture content distribution of maize kernels in samples taken at harvest time, after thin-layer drying, and after crossflow drying. The moisture content in recently harvested, and in thin-layer dried maize appears to be normally distributed and in crossflow-dried maize to be skewed. In the Chapter 2, stochastic models are developed of the distribution of the moisture content in maize kernels dried in concurrent-flow, counter-flow and crossflow dryers, and in Chapter 3 one of the models is used to analyze the process of grain drying in a crossflow dryer.

*This paper was published in 1997 in the Journal of Agricultural Engineering Research 66:267-273.

1.1 Introduction

The term "grain moisture content" refers in the grain market, and in grain-drying technology, to the average moisture content of a sample of kernels. Recent studies have established that a significant variance in moisture content exists among individual grain kernels (Montross et al., 1994). Thus, the variation in the moisture content between the kernels should be considered in the evaluation of the processes of grain drying and grain storage, in addition to the average moisture content.

Present grain drying models assume an uniform initial moisture content of the grain kernels; they are routinely used in the simulation, design and control of grain dryers (Brooker et al., 1992). The object of the present study is to develop stochastic models for the *average moisture content and variance* in grain dryers operating under non-uniform initial moisture content of the kernels. Chapter 1 presents the experimental results, Chapter 2 the development of several stochastic models, and Chapter 3 the analysis of crossflow drying employing a stochastic model.

1.2 Literature Review

Oxley (1948) was among the first to measure the moisture content of individual grain kernels (i.e. wheat); the standard deviation of the moisture content was in the range of 0.7-7.8% w.b. at harvest and decreased to 0.1-0.4% w.b. after one month of storage, and rapid drying produced a skewed distribution in the kernel moisture content. Lasseran (1987) measured a range in kernel moisture of 23-39% w.b. in freshly-harvested maize at an average of 30.2% w.b. (and with a standard deviation of 3.8% w.b.); immediately after drying in a mixed-flow dryer to an average of 16.6% w.b. moisture, the kernel moisture

content ranged from 6-29% w.b. (with a standard deviation of 4.0% w.b.). Kocher et al. (1990) established that the moisture range of 20% w.b. rough rice at harvest is 10-23% w.b., with a standard deviation between 4-6% w.b.; the mean moisture content of the rice kernels is different from the mode.

Banaszek and Siebenmorgen (1990) studied the drying of individual rice kernels selected from various maturity groups; differences in moisture content and drying rate were determined to be related to kernel width, thickness and initial moisture content. Regner (1995) measured the mass distribution of the kernels in samples of wheat and its effect on drying rate; light kernels dried faster than heavier kernels but the effect of the kernel mass was small compared with that of the drying air temperature.

Montross et al. (1994) determined that at harvest time the smaller tip kernels on an ear of maize are on average at a lower moisture content than the larger bottom kernels; at an average sample moisture of 24-25% w.b., the difference is 5-7% w.b., with a range in the individual kernel moisture of 8-37% w.b. (and in the standard deviation of 0.6-9.0% w.b.). The authors also measured the moisture content distribution in maize dried in commercial cross-flow, concurrent-flow and mixed-flow dryers; maize exiting a high-temperature dryer, regardless of type, was found to have a standard deviation in the moisture content of 3-5% w.b..

1.3 Experimental Details

1.3.1 Moisture content measurement of individual kernels

For the commercial dryer tests, the moisture contents of single maize kernels in a sample were determined in a single-kernel moisture meter manufactured by Shizuoka Seiki, Inc. (Japan). Each kernel is automatically guided to a metallic crusher; the moisture content (w.b.) is obtained by converting its electric resistance or conductance into a moisture value. The moisture meter also calculates the average moisture content of 100 kernels, the frequency in each 0.5% w.b. moisture range, and the standard deviation of the moisture content of the sample. Calibration studies of the average moisture content readings of the meter have shown excellent agreement between the meter and the oven methods (Tsai et al., 1987).

During the thin-layer drying tests, the mass of individual maize kernels was measured with a Mettler PM 400 digital balance with a precision of 0.001 g. Since the dry mass of a single kernel of maize is about 0.3 g, the relative error of the measurement is approximately 0.33%. The dry mass of each kernel was determined subsequently by the standard oven method (ASAE standard, 1989).

In general, the moisture content in this paper is expressed on a dry basis. In some cases, the moisture content is also given on a wet basis because its more frequent use in commerce.

1.3.2 Laboratory thin-layer drying

The thin-layer dryer contains a 0.15m x 0.15m x 0.21m drying platform to which air is directed at a velocity of 1.2 m/s. The position of individual kernels is numbered. The change of the mass of each kernel is measured after predetermined drying times.

The grain samples consisted of hand-picked ears of Dekalb 458 maize. It was stored in a 4°C cooler immediately following the harvest. The ears were kept in the laboratory for 24 hrs, and then were shelled manually just before the start of a drying. Each sample consisted of 20 arbitrarily selected kernels. The kernels started start a drying test 30 s apart. After predetermined drying periods (i.e. multiples of 10 min), each kernel was weighed. The tests were conducted at temperatures of 60 °C, 70 °C and 80 °C ± 1 and an absolute humidity of 0.008 kg/kg ± 0.001. Each test was replicated three times.

1.3.3 Commercial crossflow drying

Maize was dried experimentally in two commercial crossflow dryers, CF1 and CF2.

CF1 is a cylindrical crossflow dryer with a capacity of 141 m^3/h of wet grain at 5% w.b. moisture removal. The diameter of the dryer is 5.03 m, and the thickness of the grain column is 0.305m. The height of the drying section is 16.26 m, and the airflow in the drying section is 294,000 m^3/h. The grain column is turned midway through the drying section. The height of the cooling section is 5.58 m, and the airflow in the cooling section is 147,000 m^3/h. The exhaust air from the cooling section is re-circulated to the drying section.

CF2 is a rectangular three-stage 7.32 m x 0.305 m crossflow dryer with a capacity of 60 m^3/h of wet grain at 5% w.b. moisture removal. The air temperatures in the first two

stages may differ. The third stage is the cooling section. The thickness of the grain column is 0.305 m. The height of stage one is 2.44 m; of stage two 1.55 m, and of stage three 0.98 m. The airflow both in the first and second stages is 36,000 m^3/h, and in the cooling stage 30,000 m^3/h.

Samples were taken every half hour at the inlet and outlet of the dryers after they had reached steady-state; the moisture content of individual kernels was measured with the individual kernel moisture meter immediately after the samples were taken. The residence time of grain in the dryer was considered in taking the outlet samples to match them with the inlet samples. The averages of the moisture data of three consecutive samples from the dryer inlet or outlet were used for analysis.

1.4 Results

1.4.1 Moisture distribution at harvest

The distribution of the moisture content in a typical maize sample reaching a dryer is shown in Fig. 1.1; the sample had an average moisture content of 37.5% d.b.. Table 1.1 shows the Chi-Square (χ^2) results for the normality test of the moisture content distribution in twenty samples ranging in average moisture content from 19.5 to 38.9% d.b.. The standard deviation in the moisture content in these samples varied from 0.8 to 11.3% d.b., with the higher average moisture contents usually displaying the higher standard deviations.

Table 1.1 shows that the moisture distribution of only 5 of the 20 maize samples passed the test for normality. This is due (it is believed) to the severe fluctuation in the frequency values in adjacent moisture content ranges. This was confirmed after the data

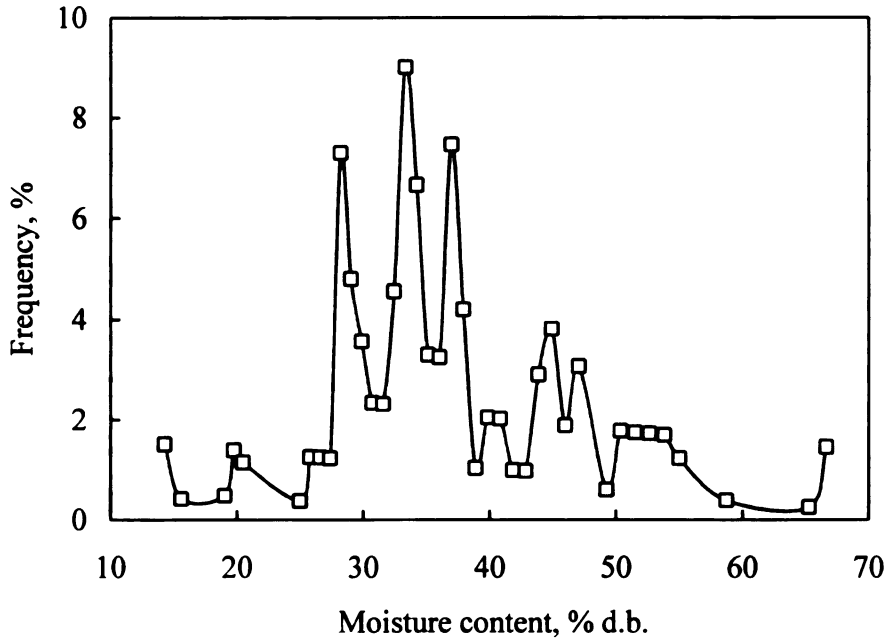

Fig. 1.1 Typical frequency distribution of the kernel moisture content in maize reaching a dryer (average moisture content is 37.5 % d.b.).

Table 1.1 χ^2 test for normality in the moisture content distribution of maize *at harvest before smoothing* of the data.

SAMPLE NUMBER	AVERAGE MC (% D.B.)	STANDARD DEVIATION (% D.B.)	DEGREES OF FREEDOM	$\chi^2_{0.05}$ VALUE	χ^2_{SAMPLE} VALUE	TEST RESULTS
1	38.9	11.3	14	23.7	49.3	Fail
2	37.8	11.0	14	23.7	39.3	Fail
3	37.6	10.5	12	21.1	20.8	Pass
4	37.3	12.1	13	22.4	35.1	Fail
5	33.6	11.9	13	22.4	31.3	Fail
6	31.9	8.8	11	19.7	42.5	Fail
7	31.0	5.9	11	19.7	18.5	Pass
8	29.3	11.5	20	31.4	56.5	Fail
9	29.2	5.4	11	19.7	45.7	Fail
10	28.7	3.7	14	23.7	104.2	Fail
11	25.5	5.3	10	18.3	48.2	Fail
12	25.3	5.9	12	21.3	29.5	Fail
13	25.3	6.0	12	21.0	63.4	Fail
14	25.0	4.1	14	23.7	29.8	Fail
15	24.6	4.6	12	21.0	33.5	Fail
16	23.7	4.5	14	23.7	51.7	Fail
17	23.1	2.2	8	15.5	9.4	Pass
18	21.5	2.3	6	12.6	97.8	Fail
19	19.7	1.3	4	9.5	6.6	Pass
20	19.5	0.8	3	7.8	6.2	Pass

Table 1.2 χ^2 test for normality in the moisture content distribution of maize *at harvest after smoothing* of the data in Table 1.1.

SAMPLE NUMBER	AVERAGE MC (% D.B.)	STANDARD DEVIATION (% D.B.)	DEGREES OF FREEDOM	$\chi^2_{0.05}$ VALUE	χ^2_{SAMPLE} VALUE	TEST RESULTS
1	38.9	11.3	14	23.7	15.2	Pass
2	37.8	11.0	14	23.7	14.3	Pass
3	37.6	10.5	12	21.1	8.9	Pass
4	37.3	12.1	13	22.4	13.2	Pass
5	33.6	11.9	13	22.4	10.5	Pass
6	31.9	8.8	11	19.7	17.0	Pass
7	31.0	5.9	11	19.7	7.4	Pass
8	29.3	11.5	20	31.4	20.4	Pass
9	29.2	5.4	11	19.7	17.8	Pass
10	28.7	3.7	14	23.7	21.1	Pass
11	25.5	5.3	10	18.3	16.4	Pass
12	25.3	5.9	12	21.3	10.4	Pass
13	25.3	6.0	12	21.0	20.3	Pass
14	25.0	4.1	14	23.7	11.6	Pass
15	24.6	4.6	12	21.0	12.3	Pass
16	23.7	4.5	14	23.7	19.4	Pass
17	23.1	2.2	8	15.5	7.9	Pass
18	21.5	2.3	6	12.6	11.5	Pass
19	19.7	1.3	4	9.5	5.3	Pass
20	19.5	0.8	3	7.8	6.4	Pass

were smoothed with a Fast Fourier Transform (FFT) filter. The procedure removes any linear trend in the data, and then uses the FFT technique to filter the data (Press et al., 1986). The linear trend was reinserted at the end. The number of the data points smoothed each time was 10. Each of the maize samples then passed the χ^2 test for normal distribution (see Table 1.2). Fig. 1.2 shows, in addition to the raw and smoothed data curves, the normal distribution curve of the frequency of the kernel moistures in a typical maize sample reaching a dryer.

1.4.2 Moisture distribution during drying

(1) Thin-layer drying

Fig. 1.3 shows the average moisture content of three maize samples during drying at three temperatures; the change in the value of the standard deviation *during the drying process* (i.e. at different average moisture contents) of the three samples in Fig. 1.3 is illustrated in Fig. 1.4. It appears that the standard deviation of the moisture content decreases during the course of drying, at least at 60°C and 70°C while at 80°C this decrease is less pronounced. The rate of decrease in the standard deviation in the high average moisture content range is larger than in the low average moisture content range.

Fig. 1.5 illustrates the narrowing of the kernel-moisture distribution during the drying of maize from 24.4% d.b. down to 14.9% d.b.. This is because the lower moisture-content kernels dry more slowly than the kernels at the average moisture, and the kernels at the higher than average moisture content dry faster. Note that the distribution of the kernel moisture remains essentially normal during the drying process, i.e. normal.

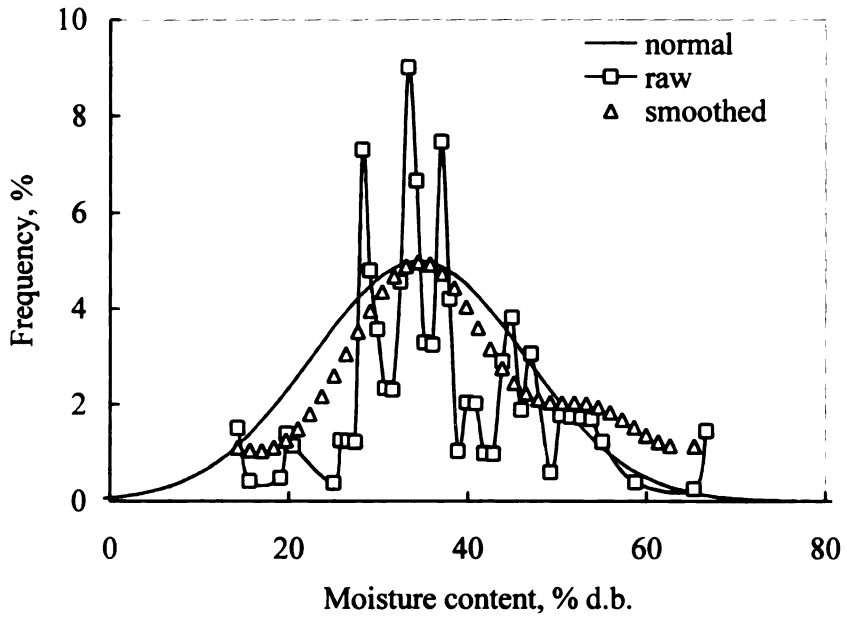

Fig. 1.2 The frequency distribution of the raw data, smoothed data and the corresponding normal distribution of the moisture content of maize kernels in a typical maize sample reaching a dryer.

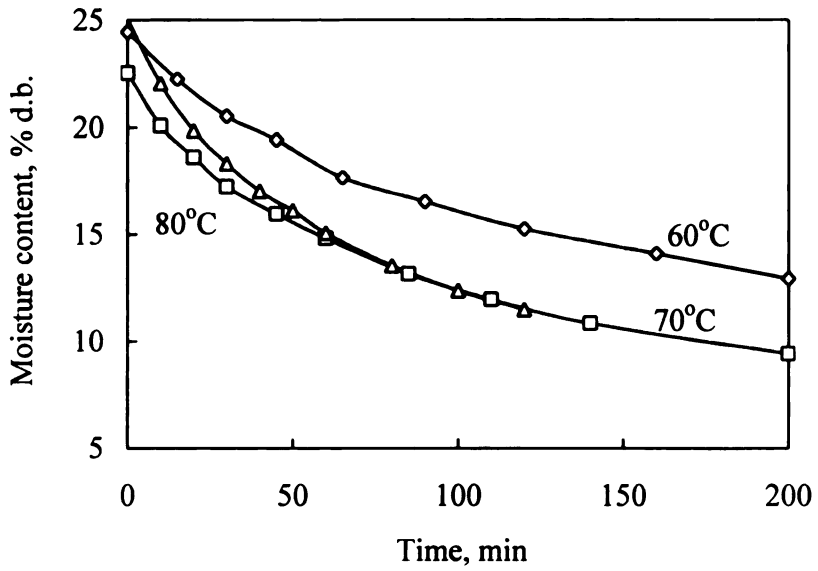

Fig. 1.3 Experimental thin-layer drying curves (each curve is the average of 60 kernels) of maize at three drying-air temperatures.

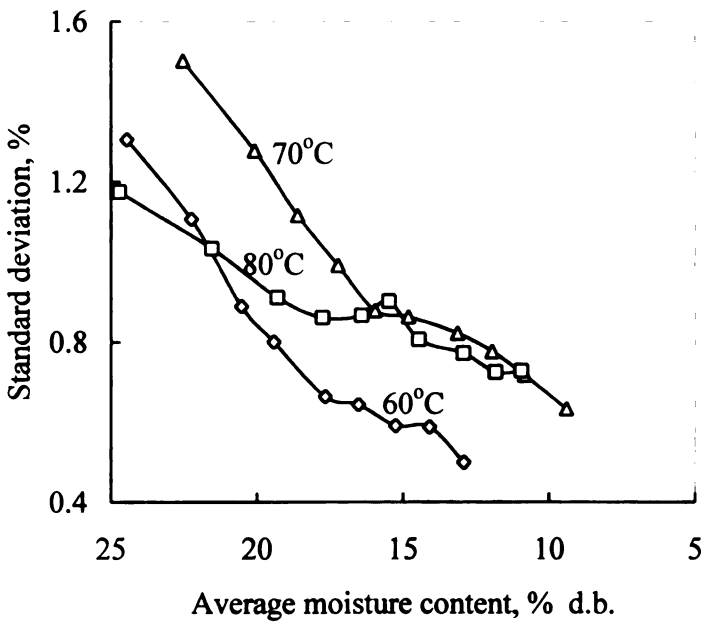

Fig. 1.4 The standard deviation at different average moisture contents (60 kernels as a group) during thin-layer drying of maize at three drying-air temperature.

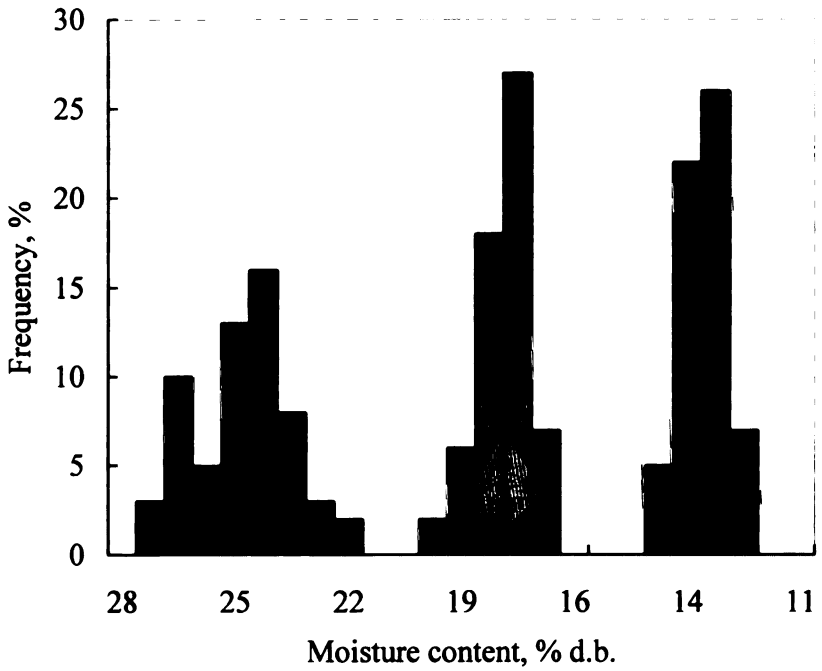

Fig. 1.5 The moisture content distribution of 60 kernels at three drying stages during thin-layer drying at 60°C; the average moisture contents are 24.4 % (initial), 17.6 % and 14.9 % d.b., respectively, from left to right.

The frequency distribution of the kernel dry mass of a typical maize sample is shown in Fig. 1.6; the individual kernel mass varied from 0.21 to 0.45 g, with the maximum frequency occurring at 0.31 g.

In order to test the effect of kernel mass on the drying process, some samples were separated into three kernel-mass categories--large, medium and small. The drying behavior of three categories and of the whole sample is illustrated in Figs. 1.7 and 1.8; Fig. 1.7 shows the drying curves, Fig. 1.8 the standard deviations of the moisture content. The lighter (i.e. smaller) kernels dry only slightly faster than the heavier (i.e. larger) kernels. The standard deviation in each of the three categories is similar in value than that of the whole sample. Thus, the distinct difference in kernel mass within a lot of maize does not affect the standard deviation during drying.

(2) Crossflow drying

The inlet and outlet moisture content distributions of maize in crossflow dryer CF1 are illustrated in Fig. 1.9. The average inlet moisture content was 33.0% d.b. (SD = 8.6% d.b.) and the average outlet moisture content 17.2% d.b. (SD = 7.1% d.b.).

Fig. 1.10 shows the moisture distributions in a second crossflow dryer CF2, in which maize at an average initial moisture content of 34.0% d.b. was dried to an average of 18.6% d.b. The standard deviation of the maize before drying was 7.9% d.b. and immediately after drying 7.7% d.b..

The higher value of the standard deviation in the moisture content after drying than before drying is due to the uneven drying treatment of the kernels in a crossflow dryer. Kernels near the air-inlet in the drying column are usually overheated and overdried, while

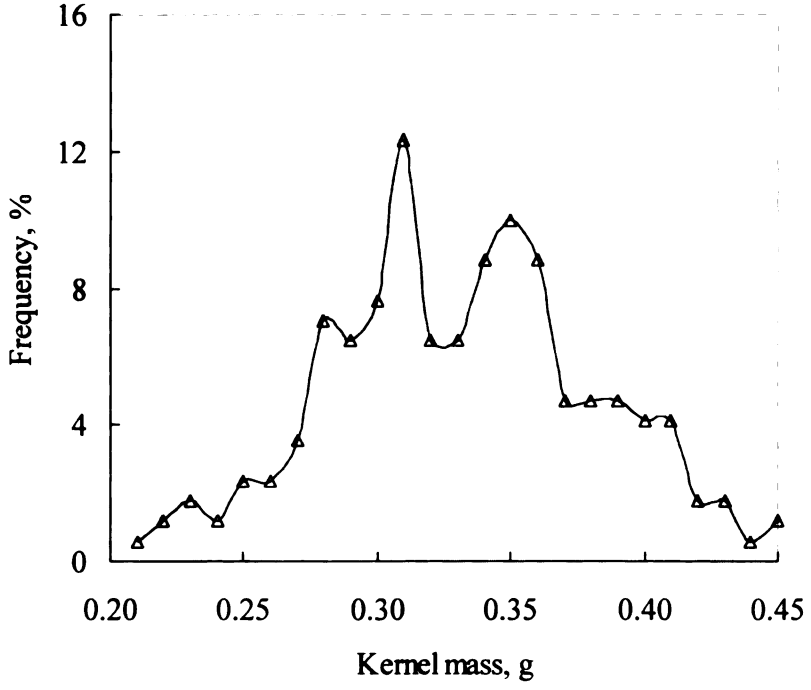

Fig. 1.6 The frequency distribution of the kernel dry mass of a typical maize sample.

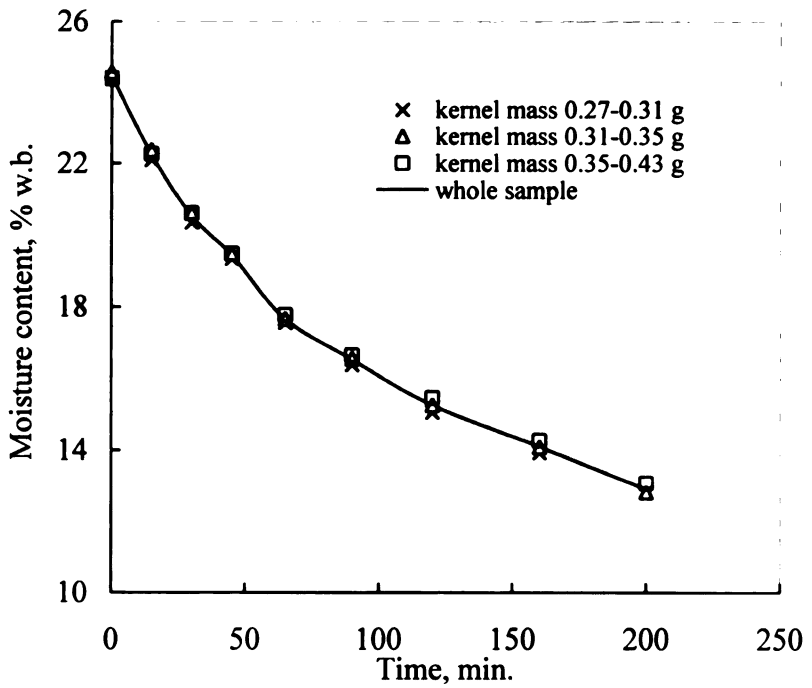

Fig. 1.7 The drying curves of maize kernels grouped by dry weight during thin-layer drying of 60 kernels at 60°C.

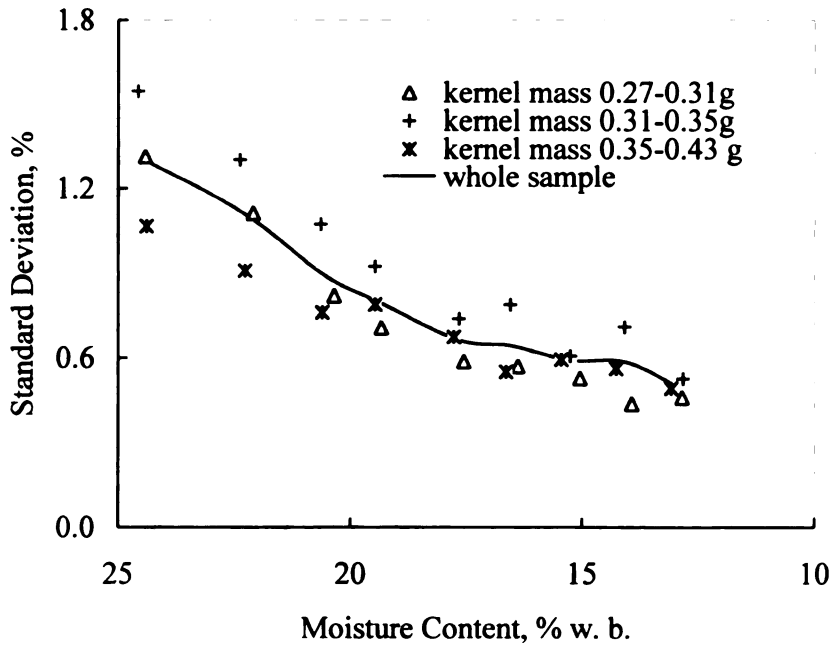

Fig. 1.8 The standard deviation of the moisture content of maize kernels grouped by dry weight during drying at 60°C.

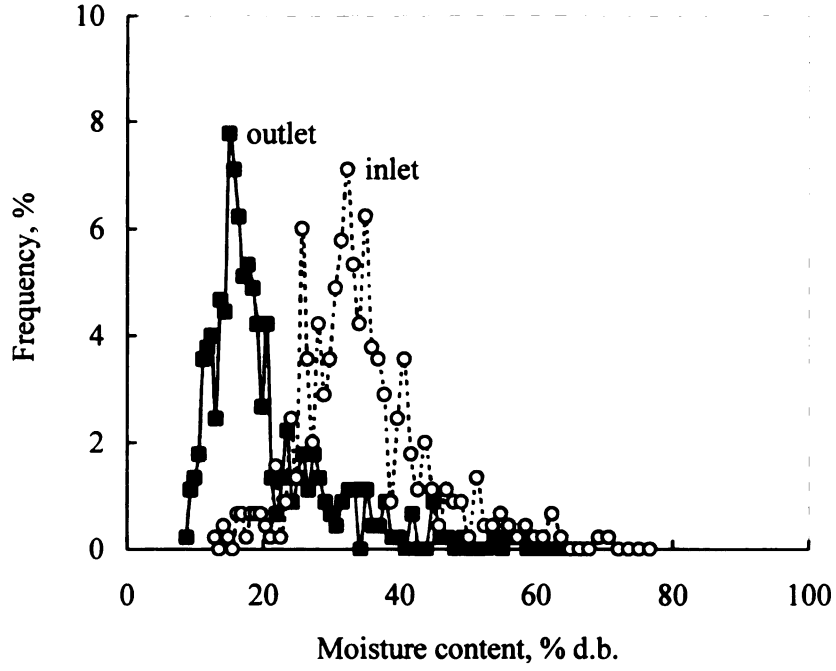

Fig. 1.9 Moisture distribution before and after drying of maize in a crossflow dryer (CF1); inlet average m.c.=33.0% d.b., stand. dev.=8.6% d.b., and outlet average m.c.=17.2% d.b., stand. dev. =7.1% d.b..

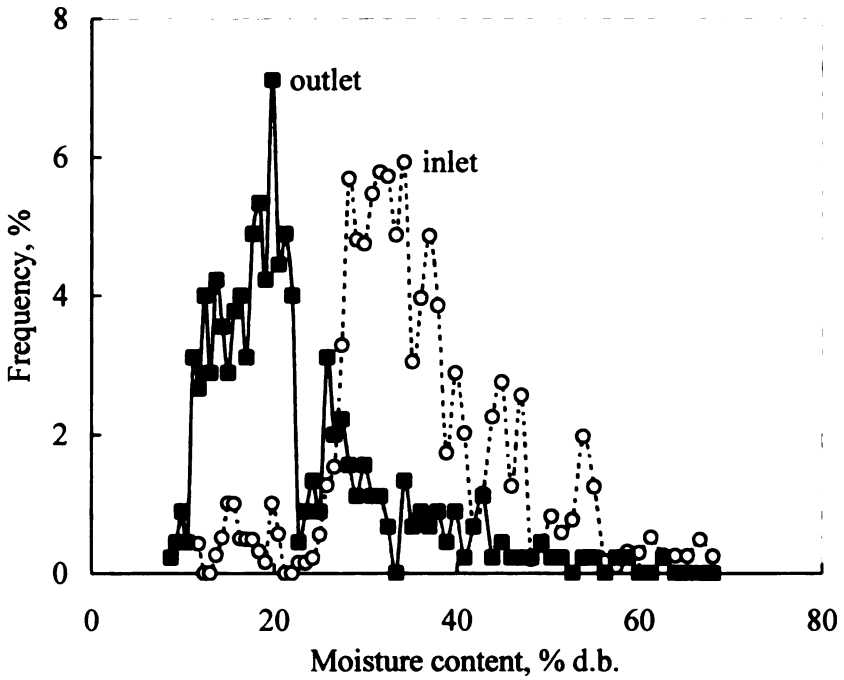

Fig. 1.10 Moisture distribution before and after drying of maize in another crossflow dryer (CF2); at the inlet the average m.c. =34.0% d.b., stand. dev. =7.9% d.b., and at the outlet the average m.c. =18.6% d.b., stand. dev. =7.7% d.b..

kernels at the outlet side of the column are underheated and underdried. The moisture content distribution in crossflow-dried maize is skewed because the kernels entering the dryer at the air-outlet side of the grain column are often not dried at all.

1.4.3 Moisture distribution during storage

Fig. 1.11 shows the decrease in the standard deviation of the moisture content of three maize samples during storage in plastic bag at about 20 °C. Within 24 hs, the standard deviation in each of the samples diminished to 1-2% w.b., regardless of the initial standard deviation. After 150 hs storage, the standard deviation equilibrated to 0.6-0.9% w.b..

1.5 Conclusions

(1) The moisture content distribution of maize after harvest can approximately be expressed by a normal distribution. The distribution is not normal after drying of maize in a crossflow dryer.

(2) After thin-layer drying, the kernel-moisture distribution is still normal, but with a smaller standard deviation than before drying. The difference in kernel mass does not affect the moisture distribution and the standard deviation.

(3) After cross-flow drying, the moisture distribution is skewed to the low end of the moisture content range while displaying a tail at in the high moisture range.

(4) The range of the moisture content in stored maize diminishes after drying. The standard deviation decreases rapidly, and equilibrates to a value of 0.6-0.9 % w.b..

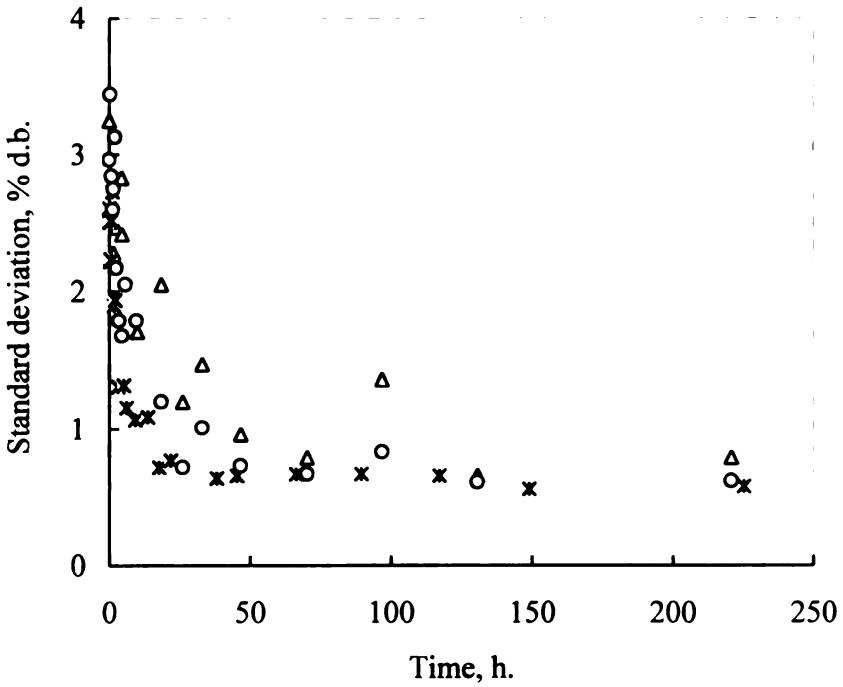

Fig. 1.11 The change in the standard deviation over time of three maize samples after crossflow drying and storage at 20°C. The average moisture contents of samples are 22.4 % (Δ), 15.9 % (✕) and 19.9 % (O) d.b., respectively.

References

Montross, M. D., F. W. Bakker-Arkema, C. L. Leppanen and R. E. Hines. 1994. Moisture content variation and grain quality of maize dried in different high-temperature dryers. Paper No. 94-6590. ASAE, St. Joseph, MI.

Brooker, D. B., F. W. Bakker-Arkema and C. W. Hall. 1992. Drying and Storage of Grains and Oilseeds. Van Nostrand Reinhold, New York, NY.

Oxley, T. A. Study water content of single kernels of wheat. Cereal Chemistry 1948, 25(2):111-127

Lasseran, J. C. 1987. Grain drying in France. Paper No. 87-6014. ASAE, St. Joseph, MI.

Kocher, M. F., T. J. Siebenmorgen, R. J. Morman and B. R. Wells. 1990. Rice kernel moisture content variation at harvest. Transactions of the ASAE 33(2):541-547.

Banaszek, M. M. and T. J. Siebenmorgen. 1990. Individual rice kernel drying curves. Paper No. 90-6589. ASAE, St. Joseph, MI, 1990

Regner, S. Kernel mass related properties of cereal grains. 1995. Ph.D. Thesis. Swedish University of Agricultural Sciences, Uppsala, Sweden.

Tsai, C., R. Yamashita and R. Goto. 1987. Moisture distribution of cereal grain in postharvest processing. Japanese Society of Agricultural Machinery 46(6):599-604

ASAE. Standard S352.2. 1989. ASAE, St. Joseph, MI.

Press, W. H., B. P. Flannery, S. A. Teukolsky and W. T. Vetterling. 1986. Numerical Recipes: The Art of Scientific Computing. Cambridge University Press, Cambridge, MA.

CHAPTER 2. STOCHASTIC MODELING OF GRAIN DRYING: MODEL DEVELOPMENT*

Abstract

In Chapter 1 of this series of three chapters, it was shown that the moisture content in maize reaching a dryer is approximately normally distributed. In Chapter 2, stochastic drying models are developed for grain initially with an initial normal distribution in moisture content. It is shown that the moisture content is still normally distributed after one-dimensional drying (i.e. concurrent- or counter-flow drying), but is skewed after two-dimensional drying (i.e. crossflow drying). The models predict for dried grain, both the average moisture content and its standard deviation to an acceptable accuracy.

*This paper was published in 1997 in the Journal of Agricultural Engineering Research 66:275-280.

2.1 Introduction

Drying models are routinely used in the design and analysis of grain dryers (Brooker et al., 1992). For instance, the Michigan State University (MSU) grain-drying models which are of the deterministic type, calculate the average moisture content of the grain exiting a dryer. The assumption is made that the moisture content of each grain kernel entering a dryer is equal to the average moisture content. This assumption has proven to be an over-simplification (see Chapter 1), and thus the traditional deterministic grain-drying models need to be modified to stochastic-type models which accept non-uniform inlet moisture content data.

Stochastic parameter data have been employed by Sokhansanj (personal communication, 1996) to account for the effect of random variation of some of the physical constants in the grain drying model of a batch dryer. However, the model was not used to simulate the distribution of the moisture content in individual grain kernels.

Ryniecki et al. (1994) developed a stochastic model for near-ambient in-bin grain drying. The stochastic nature of the ambient temperature and relative humidity was considered to be the sole stochastic effect in the drying process; the variability in the initial grain moisture content of the grain kernels was not accounted for.

Three stochastic grain-dryer models are presented in this paper, a thin-layer drying model, a concurrent- or counter-flow model, and a crossflow model.

2.2 Thin-layer Drying Model

The change in the moisture content of a thin layer of grain dried under constant air conditions can be expressed by the following empirical equation (Brooker et al., 1992):

$$\frac{M_f - M_e}{M_o - M_e} = f(T, \phi, \tau) \tag{2.1}$$

where M_o is the initial dry-basis moisture content, M_f the dry-basis moisture content at drying time τ, and M_e the dry basis equilibrium moisture content at the air temperature T and relative humidity ϕ.

or

$$M_f = AM_o + B \tag{2.2}$$

where $A = f(T, \phi, \tau)$ and $B = M_e[1-f(T, \phi, \tau)]$. Thus, A and B are independent of grain moisture content. If the initial moisture content can be represented by a normal distribution of $N[E(M_o), \sigma_o]$, the moisture content after drying is also of the normal type $N[E(M_f), \sigma_f]$ (Press et al., 1986), where

$$E(M_f) = AE(M_o) + B \tag{2.3}$$

and

$$\sigma_f = A\sigma_o \tag{2.4}$$

2.3 Deep-bed (one-dimensional) Drying Model

Concurrent- or counter-flow drying are examples of one-dimensional deep-bed drying. In the deterministic MSU drying models (Brooker et al., 1992), a set of mathematical equations describes the grain temperature and moisture content, and the air temperature and humidity, within a small element in the grain bed. In the simulation of a one-dimensional deep-bed dryer, the grain bed is divided into thin layers (elements); the model is solved for each thin-layer by considering the outlet conditions of one layer to be the inlet conditions of the next layer downstream. After the model is solved for all layers, the grain and the air conditions in the grain bed are obtained. It is assumed in the deterministic dryer models that the moisture content of the grain kernels is uniform. In the MSU stochastic dryer models it is postulated that the moisture content in a lot of grain is non-uniform, and normally distributed when grain reaches the dryer.

The simulation of the one-dimensional drying of grain with a normal-type initial kernel moisture content distribution is accomplished in two steps:

(1) Calculate the distributions of the air temperature and humidity within the grain-bed with the deterministic drying model, assuming the initial moisture content of all kernels is equal to the average initial moisture content.

(2) Determine the moisture and grain temperature changes throughout the bed for the kernels with any initial moisture content other than the average, employing the deterministic model again, *but under the air temperature and humidity distributions determined in step 1.*

Thus, it is assumed that the air temperature and humidity at a particular position in the drying bed have the same values which they would have had if all kernels had initially

been at the average moisture content. This assumption is reasonable because the air conditions in a grain bed are determined by the average condition of all the kernels encountered by the air.

In a one-dimensional deep-bed dryer, such as a concurrent-flow (CCF) dryer, the air temperature and air humidity distributions are one-dimensional, and thus it can be assumed that each kernel encounters the same drying conditions passing through the dryer. If the initial grain moisture content distribution is normal, the final grain moisture content distribution is also normal, i.e. $N[E(M_f), \sigma_f]$ (see Appendix 2A). Also,

$$E(M_f) = CE(M_o) + D \tag{2.5}$$

$$\sigma_f = C\sigma_o \tag{2.6}$$

where C and D are dependent on the air temperature and humidity distributions in the drying-bed.

Two runs of the deterministic dryer simulation program are required to determine the final distribution of the grain moisture content in a one-dimensional dryer. If $E(M_o)$ is the average of the initial grain moisture content, the average final moisture content $E(M_f)$ is determined in a run of the deterministic dryer program (step 1). The air temperature and humidity distributions are stored in a data file. Next, a second initial moisture content, i.e. M_o^+ different from $E(M_o)$, is selected (such as letting $M_o^+ = E(M_o) - \sigma_o$), and the dryer program is run again under the air conditions now stored in the data file. A second dryer-exit moisture content M_f^+ is obtained (step 2), and the standard deviation of the exit moisture content is calculated. Thus, from Eq A6:

$$M_f^+ = CM_o^+ \tag{2.7}$$

and from Eq. 2.7 and Eq. 2.5:

$$\begin{aligned} M_f^+ - E(M_f) &= (CM_o^+ + D) - [CE(M_o) + D] \\ &= C[M_o^+ - E(M_o)] \end{aligned} \tag{2.8}$$

Then

$$C = \frac{M_f^+ - E(M_f)}{M_o^+ - E(M_o)} \tag{2.9}$$

Finally, substituting Eq. 9 into Eq. 6:

$$\sigma_f = \frac{M_f^+ - E(M_f)}{M_o^+ - E(M_o)} \sigma_o \tag{2.10}$$

Thus, the moisture content distribution of the grain at the dryer exit in a one-dimensional dryer is $N[E(M_f), \sigma_f]$.

2.4 Deep-bed (two-dimensional) Drying Model

A crossflow dryer is an example of a two-dimensional dryer. In a two-dimensional deterministic drying model, the grain column is divided into a number of equal-depth sub-columns in the direction of airflow. The thickness of a sub-column is small so that the changes in the air temperature and humidity in the sub-column are negligible, i.e. the changes in the air temperature and humidity are assumed to be in the grainflow direction only (as in the one-dimensional model).

$$E(M_f) = \frac{1}{m}\sum_{i=1}^{m} E(M_{fi}) \tag{2.11}$$

The same method employed for the one-dimensional stochastic drying model is used to determine the dryer-exit moisture content distribution of a sub-column in the two-dimensional model. If the initial grain moisture content is normal, the exit grain moisture content of each sub-column is normal. The average moisture content of the grain exiting the grain column is the result of the average of the sub-columns. If the column is divided into *m* sub-columns, the average exit-grain moisture content and its standard deviation in a crossflow dryer are (see Appendix 2.B):

and

$$\sigma_f = \sqrt{\frac{1}{m}\sum_{i=1}^{m}\sigma_{fi}^2 + \frac{1}{m}\sum_{i=1}^{m}[E(M_{fi})]^2 - [E(M_f)]^2} \tag{2.12}$$

2.5. Basis Conversion of the Grain Moisture Content

As the wet-basis moisture content of grain is normally used in commercial transactions, a program is developed to convert the average and standard deviation of the moisture content from dry basis to wet basis. Assuming the moisture content is normally distributed on a dry basis, the distribution of the moisture content on a wet basis is not normal because the conversion of the moisture content from dry basis to wet basis is not linear, i.e.:

$$M_w = \frac{M_d}{1 - M_d} \tag{2.13}$$

The Monte Carlo technique (Press et al., 1986) is used in the conversion, i.e. randomly generating 1000 dry-basis moisture contents with the known distribution function, then converting each moisture content to a wet basis with Eq. 13, and finally calculating the average moisture content and the standard deviation on wet basis.

2.6 Model Validations

2.6.1 Thin-layer drying

Figs. 2.1 and 2.2 show the experimental and predicted standard deviations during the thin-layer drying of maize at 60°C, 70°C and 80°C. [Note: The experimental data have been presented in Chapter 1.] The predicted standard deviations decrease approximately linearly with average moisture content. The standard errors between the experimental and simulated results are 0.11, 0.06 and 0.10 at 60°C, 70°C and 80°C, respectively. The relative error is in the range of 10% to 15%. The systematic error is small, except in the low moisture content range of the 80°C run. A possible explanation is that the drying rate is high at 80°C, and thus a small error in the drying time causes a relatively large error in the calculated moisture content and its standard deviation.

2.6.2 Crossflow dryer

Table 2.1 shows the experimental and predicted standard deviations for two crossflow dryers (CF1 and CF2). [Note: The specifications of the crossflow dryers are presented in Chapter 1.] The dryer capacities were determined by simulation, i.e. by matching the experimental dryer-exit moisture content to that obtained by simulation.

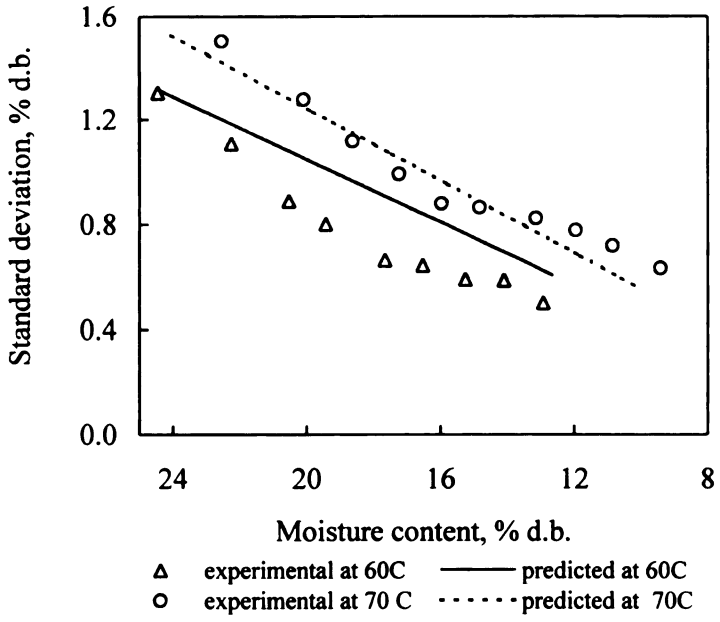

Fig. 2.1 Predicted and experimental standard deviations of the moisture content of maize during single-kernel drying at 60°C and 70°C, respectively.

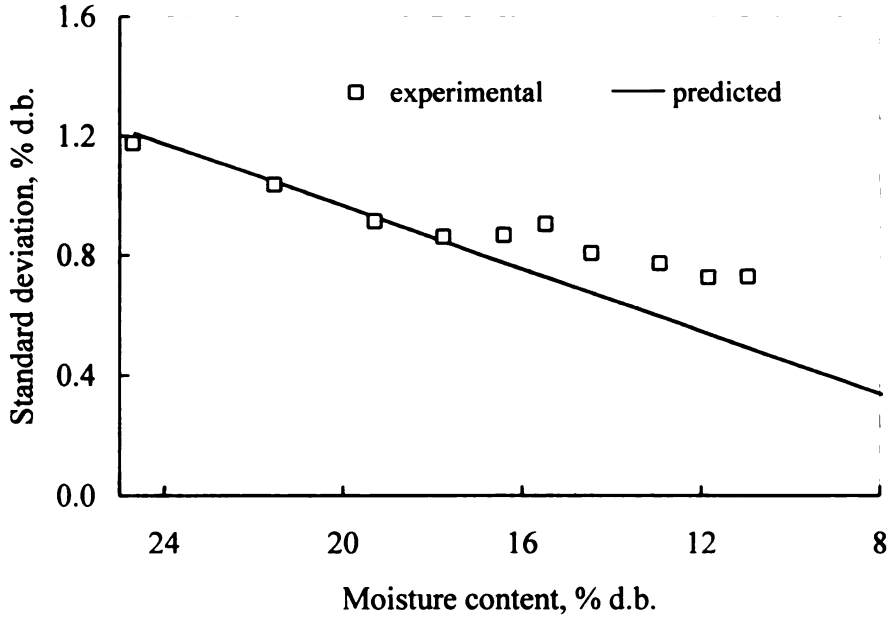

Fig. 2.2 Predicted and experimental standard deviations of the moisture content of maize during thin-layer drying at 80°C.

[This procedure is justified since model validation for dryer capacity at average inlet/outlet moisture contents has been proven elsewhere (Brooker et al., 1992).]

The data in Table 2.1 show that the predicted dryer-outlet standard deviations are higher than the experimental values. The average relative error is 29.9% and is believed to be caused mainly by the limited range of the single-kernel moisture meter (i.e. the rated moisture range is 9%-40 % w.b.). This means that the meter incorrectly measured the moisture content of the kernels below 9% w.b. and above 40% w.b. Since some crossflow-dried kernels have a moisture content well below 9% w.b. (Brooker et al., 1992), the measured standard deviation is smaller than the predicted value.

Table 2.2 shows the comparison of the experimental and predicted standard deviations when *kernels with a predicted value of less than 9% w.b. moisture are excluded* in the determination of the standard deviation. The relative error between the experimental and theoretical standard deviation values now ranges from -8.8% to 17.1% with an average error of 11.6%. Based on the data in Table 2.2, it is concluded that the MSU stochastic crossflow drying model shows acceptable agreement with the experimental results.

2.7 Conclusions

Chapter 1 in this series of three papers showed experimentally that there is a wide range in the moisture content amongst maize kernels before or after drying, and that the conventional deterministic grain-dryer models should be complemented with stochastic models.

This Chapter presents the MSU stochastic models for one-dimensional concurrent-flow and two-dimensional crossflow drying. The models simulate, in addition to the average final moisture content, the moisture content distribution and standard deviation of the grain leaving these dryers.

Acceptable agreement was found between the experimental and simulated data. Thus, it now is possible to predict the moisture content range and distribution of a lot of maize kernels dried in concurrent-flow and crossflow dryers.

References

Brooker, D. B., F. W. Bakker-Arkema and C. W. Hall. 1992. Drying and Storage of Grains and Oilseeds. Van Nostrand Reinhold, New York, NY.

Ryniecki, A., A. Molinska and D. S. Jayas. 1994. Stochastic modeling of grain moisture content for near-ambient drying. Paper No. 94-6594, Am. Soc. of Agric. Eng., St. Joseph, MI.

Kreyszig, E. 1972. Advanced Engineering Mathematics. John Wiley and Sons, New York, NY.

Pabis, S. and S. M. Henderson. 1961. Grain drying theory: II. A critical analysis of the drying curve of shelled maize. J. of agric. Eng. Res. 6: 272-277.

Misra, M. K. and D. B. Brooker. 1980. Thin-layer drying and rewetting equations for shelled yellow corn. Transactions of the ASAE 23(5): 1254-1260.

Thompson, T. L., R. M. Peart and G. H. Foster. 1968. Mathematical simulation of corn drying - A new model. Transactions of the ASAE 11(4):582-586.

Press, W. H., B. P. Flannery, S. A. Teukolsky and W. T. Vetterling. 1986. Numerical Recipes: The Art of Scientific Computing. Cambridge University Press, Cambridge, MA.

Table 2.1 Experimental and simulated standard deviations (SD) of maize dried in crossflow dryers.

	DRYING CONDITIONS AND EXPERIMENTAL RESULTS						SIMULATED RESULTS		
TEST NO.	DRYER	AIR TEMPS (°C)	MC_{IN} (% W.B.)	SD_{IN} (% W.B.)	MC_{OUT} (% W. B.)	SD_{OUT} (% W.B.)	MC_{OUT} (% W.B.)	SD_{OUT} (% W.B.)	REL. ERROR* OF SD_{OUT} (%)
1	CF1	90	22.9	4.57	15.7	4.87	15.7	5.67	16.4
2	CF1	102	26.2	5.86	14.3	5.70	14.4	6.00	5.3
3	CF1	105	22.2	4.19	12.7	3.68	12.6	5.52	50
4	CF2 3-stage	1^{st}-120 2^{nd}-100 3^{rd}-65	24.4	4.12	14.7	5.15	14.8	7.71	49.7
5	CF2 3-stage	1^{st}-88 2^{nd}-88 3^{rd}-7	18.7	3.31	14.4	3.59	14.5	4.59	27.9

* Rel. Error of Sd_{out} = (simulated SD_{out} - experimental SD_{out}) / (experimental SD_{out})

Table 2.2 Experimental and simulated standard deviation (SD) dried in crossflow dryers *excluding kernels at moisture contents lower than 9%.*

TEST NO.	1	2	3	4	5
DRYER	CF1	CF1	CF1	CF2	CF2
EXPERIMENTAL SD_{OUT} (%)	4.87	5.70	3.68	5.15	3.59
SIMULATED SD_{OUT} (%)	5.23	5.25	4.31	5.90	3.96
REL. ERROR OF SD_{OUT} (%)	7.4	-8.8	17.1	14.6	10.3

Appendix 2A: The Moisture Content Distribution of Grain Dried in a One-dimensional (concurrent- or counter-flow) Deep-bed Dryer

Assume the distribution of the moisture content in the grain entering the dryer is normal, i.e. $N[E(M_o), \sigma_o]$. The grain bed is divided into n thin layers in the direction of the grain flow. The thin-layer drying equation at constant air conditions is (Brooker et al., 1992):

$$\frac{M - M_e}{M_o - M_e} = e^{-k\tau} \tag{2A.1}$$

where M_e, k are functions of the air conditions.

For any thin layer of grain i, the relationship between the layer-exit moisture content, M_{i+1}, and the layer-inlet moisture content, M_i, is:

$$\frac{M_i - M_{ei}}{M_o - M_{ei}} = e^{-k_i \tau_{eq}} \tag{2A.2}$$

$$\frac{M_{i+1} - M_{ei}}{M_o - M_{ei}} = e^{-k_i(\tau_{eq} + \Delta\tau)} \tag{2A.3}$$

Eliminating τ_{eq} in Eqs A2 and A3 results in:

$$M_{i+1} = M_i e^{-k_i \Delta\tau} + (1 - e^{-k_i \Delta\tau}) M_{ei} \tag{2A.4}$$

where M_{ei} and k_i are functions of T_i and ϕ_i.

Therefore, the exit moisture content of any grain layer is a function of the air temperature and humidity, and the initial grain moisture content, i.e. :

$$
\begin{aligned}
M_1 &= M_0 e^{-k_0\Delta\tau} + (1 - e^{-k_0\Delta\tau})\, M_{e0} \\
M_2 &= M_1 e^{-k_1\Delta\tau} + (1 - e^{-k_1\Delta\tau})\, M_{e1} \\
&= M_0 e^{-(k_0 \cdot k_1)\Delta\tau} + (1 - e^{-k_0\Delta\tau}) e^{-k_1\Delta\tau}\, M_e 0 + (1 - e^{-k_1\Delta\tau})\, M_{e1} \\
&\cdots \\
M_n &= M_0 e^{-(k_0 \cdot k_1 \cdot \ldots \cdot k_{n-1})\Delta\tau} \\
&\quad + (1 - e^{-k_0\Delta\tau}) e^{-(k_1 \cdot k_2 \cdot \ldots \cdot k_{n-1})\Delta\tau}\, M_{e0} \\
&\quad + (1 - e^{-k_1\Delta\tau}) e^{-(k_2 \cdot k_3 \cdot \ldots \cdot k_{n-1})\Delta\tau}\, M_{e1} \\
&\quad \cdots \\
&\quad + (1 - e^{-k_{n-1}\Delta\tau})\, M_{e(n-1)}
\end{aligned}
\tag{2A.5}
$$

Therefore, the dryer-exit (i.e. final) grain moisture content is

$$
M_f = M_n = CM_o + D \tag{2A.6}
$$

where

$$
\begin{aligned}
C &= e^{-(k_0 \cdot k_1 \cdot \ldots \cdot k_{n-1})\Delta\tau} \\
D &= (1 - e^{-k_0\Delta\tau}) e^{-(k_1 \cdot k_2 \cdot \ldots \cdot k_{n-1})\Delta\tau}\, M_{e0} \\
&\quad + (1 - e^{-k_1\Delta\tau}) e^{-(k_2 \cdot k_3 \cdot \ldots \cdot k_{n-1})\Delta\tau}\, M_{e1} \\
&\quad \cdots \\
&\quad + (1 - e^{-k_{n-1}\Delta\tau})\, M_{e(n-1)}
\end{aligned}
\tag{2A.7}
$$

Note that C and D are functions of the air temperature and humidity within the drying bed only.

Since C and D are independent on M_o, M_f is the normal distribution with (Press et al., 1986):

$$
E(M_f) = CE(M_o) + D \tag{2A.8}
$$

$$
\sigma_f = C\sigma_o \tag{2A.9}
$$

If the thin-layer drying equation (i.e. 2A.1) is not an exponential equation, or if the drying constant k is a function of the grain temperature or the moisture content, the above derivation is not strictly correct. Fig. 2A.1 shows the simulated grain moisture content distributions after drying in a one-dimensional (i.e. concurrent-flow) dryer when three different thin-layer drying equations (i.e. exponential equation (Pabis, et al., 1961), Page equation (Misra et al., 1980) and Thompson equation (Thompson et al., 1968)) are employed. It is clear that the final grain moisture content distributions are close. Therefore, the form of the thin-layer drying equation has only a limited effect on the final moisture content distribution.

Appendix 2B: The Moisture Content Distribution of Grain Dried in a Two-dimensional (crossflow) Deep-bed Dryer

The grain column is divided into m sub-columns in the direction perpendicular to the air flow. In each sub-column the grain flowrate is G. The distribution of the exit-grain moisture content in sub-column i is normal, i.e. $N_i[E(M_{fi}), \sigma_{fi}]$ (see Appendix 2A).

Within sub-column i, the probability density and the probability of the moisture content are

$$f_i(X) = \frac{1}{\sqrt{2\pi}\,\sigma_{fi}} e^{-[X-E(M_{fi})]^2/2\sigma_{fi}^2} \qquad (2B.1)$$

and

$$P_i(X) = \frac{g_i}{G} = \int_{-\infty}^{x} f_i(X)dX \qquad (2B.2)$$

where $g_i(x)$ is the grain flowrate with a moisture content less than or equal to X in the sub-column i.

The dryer-exit moisture content is the average of the exit moistures of the sub-columns. The probability and probability density of the moisture content of the grain leaving the dryer are

$$P(X) = \frac{\sum_{i=1}^{m} g_i}{\sum_{i=1}^{m} G} = \frac{1}{m}\sum_{i=1}^{m}\frac{g_i}{G} = \frac{1}{m}\sum_{i=1}^{m} P_i(X) \qquad (2B.3)$$

and

$$f(X) = \frac{d}{dx}[P(X)] = \frac{1}{m}\sum_{i=1}^{m} f_i(X) \qquad \text{(2B. 4)}$$

Therefore, the average dryer-exit grain moisture content and standard deviation are:

$$E(M_f) = \frac{1}{m}\sum_{i=1}^{m} E(M_{fi}) \qquad \text{(2B. 5)}$$

and

$$\begin{aligned}
\sigma_f^2 &= E(M_f^2) - [E(M_f)]^2 \\
&= \frac{1}{m}\sum_{i=1}^{m} \int_{-\infty}^{+\infty} X^2 f_i(X)dX - [E(M_f)]^2 \\
&= \frac{1}{m}\sum_{i=1}^{m} (\sigma_{fi}^2 + [E(M_{fi})]^2) - [E(M_f)]^2 \\
&= \frac{1}{m}\sum_{i=1}^{m} \sigma_{fi}^2 + \frac{1}{m}\sum_{i=1}^{m} [E(M_{fi})]^2 - [E(M_f)]^2
\end{aligned} \qquad \text{(2B. 6)}$$

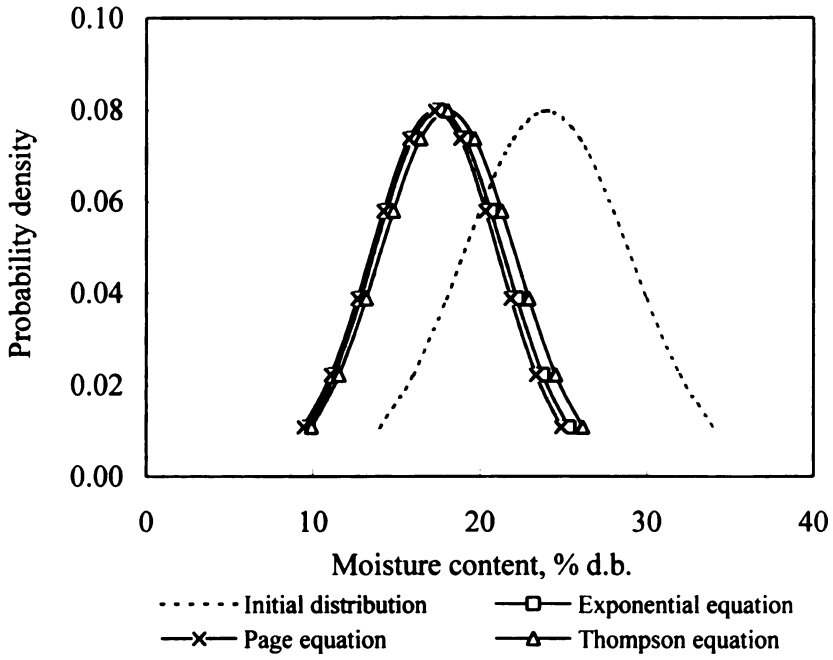

Fig. 2. A1 Simulated dryer exit moisture content distribution in a concurrent-flow maize dryer employing different thin-layer drying equations.

Symbols

A, B, C, D	coefficients
G	grain flowrate in sub-column, dry matter, kg s^{-1}
E	average value
M, M'	moisture content, decimal, d.b.
N	normal distribution
P	probability
T	air temperature, °C
X	grain moisture content, decimal, d.b.
f	probability density function
g	flowrate of grain with moisture content lower than or equal to X, dry matter kg kg s^{-1}
k	drying constant, s^{-1}
N	relative humidity, %
τ	drying time, s
σ	standard deviation
∇	increment

Subscripts

d	dry basis
e	equilibrium
eq	equivalent
i	inlet or layer number
f	final
o	initial
w	wet basis

CHAPTER 3. STOCHASTIC MODELING OF GRAIN DRYING:

ANALYSIS OF CROSSFLOW DRYING*

Abstract

In Chapter 3 of the papers on stochastic dryer modeling of grain drying, the MSU stochastic drying model is used to investigate the distribution of the kernel moisture content during the crossflow drying of maize. It is shown that the standard deviation of the moisture content gradually increases during the drying process, and becomes larger when the drying temperature is increased or the airflow rate is decreased. A grain-inverter placed in a crossflow dryer is demonstrated to have a beneficial effect by decreasing the value of the standard deviation of the moisture content of the grain leaving the dryer.

*This paper was published in 1997 in the Journal of Agricultural Engineering Research 66:281-286.

3.1 Introduction

In Chapters 1 and 2 of this study the stochastic character of the process of grain drying has been accounted for and has been modelled. First, experimental data were collected to show the wide variation in moisture content among the kernels in pre-dried and post-dried samples of maize. Next, stochastic models were developed for the moisture distribution in the maize before and after drying. In this Chapter in the series, the MSU stochastic crossflow model is employed to assess the effect of several design parameters (i.e. air temperature, airflow rate, grain reversal) on the moisture content distribution in crossflow-dried maize.

3.2 Crossflow Dryer Specifications

The analysis of crossflow grain drying is performed with a commercial-sized crossflow dryer operating without a cooler (i.e. in a dryeration-type process). The design specifications along with the operating conditions of the dryer are tabulated in Table 3.1.

Table 3.1 Design specifications and operating characteristics of the standard crossflow dryer used in the analysis of the MSU stochastic drying model.

COLUMN LENGTH, m	10.0
COLUMN THICKNESS, m	0.305
GRAIN VELOCITY, m h^{-1}	5.0
AIR TEMPERATURE, °C	70, 90, 110
AMBIENT AIR CONDITIONS, °C AND % RH	70 and 60
AIRFLOW RATE, m^3 min^{-1} t^{-1}	60, 80, 100
INITIAL MOISTURE CONTENT, % (W.B.)	25.0
INITIAL STANDARD DEVIATION, % W.B.	2.0, 3.0, 4.0

The thickness of the grain column is 0.305 m, a standard value in crossflow maize dryers. The length of the grain column is 10.0 m and the airflow rate is 80 $m^3 min^{-1} t^{-1}$, resulting in a moisture content decrease of maize of 10-12% w.b. after 2 h of drying under normal drying conditions (i.e. at 90-100°C).

To analyze the effect of the major operating parameters in a crossflow dryer receiving 25% w.b. maize, the air temperature (70, 90, 110°C), the airflow rate (60, 80, 100 $m^3 min^{-1} t^{-1}$), and the initial standard deviation of the moisture content of maize entering the dryer (2, 3, 4% w.b.), were varied. The selected values of each of these parameters fall within the range encountered at commercial elevator sites in the U. S. A. As wet basis is usually used in grain commerce, the moisture content and the standard deviation of maize are presented on a wet basis in this paper.

3.3 Crossflow Dryer Performance Characteristics

Fig. 3.1 shows the simulated operating characteristics of the crossflow dryer as calculated by the MSU stochastic crossflow drying model presented in Chapter 2. Maize at an average moisture content (AMC) of 25.0% w.b. is dried to an average 11.9% w.b. in 2 h at 90 °C. As the maize moves slowly through the dryer, the average moisture content difference (AMCD) between the maize at the air-inlet and -outlet sides of the drying column increases from zero to 9.1% w.b.. The standard deviation (SD) of the moisture content of the maize across the column increases slightly from 3.0% w.b. to 3.4% w.b., with the maximum of 3.9% w.b. occurring after about 60 minutes of drying.

Figs. 3.2 and 3.3 show the change in the moisture content and the standard deviation, respectively, at four positions within the grain column during the drying

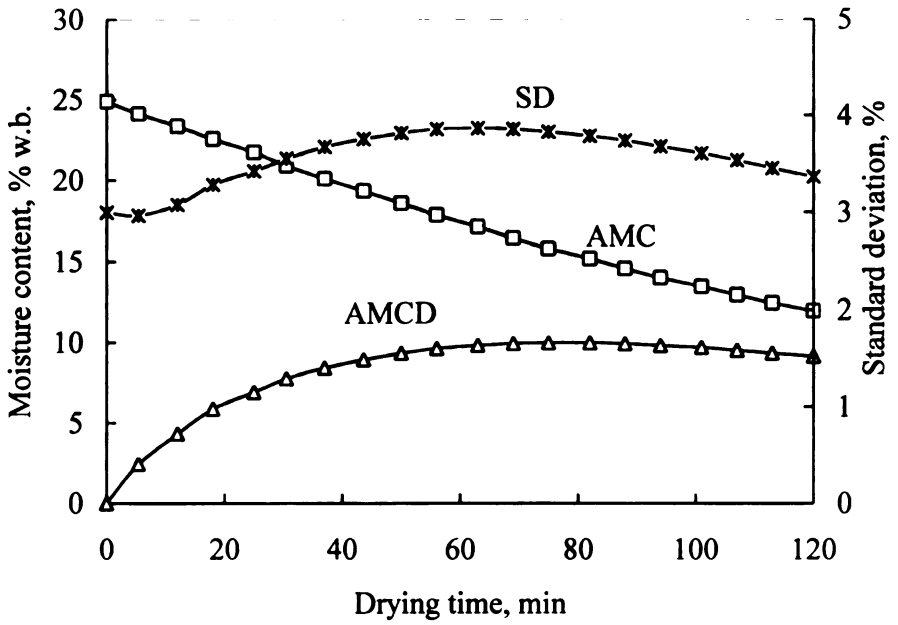

Fig. 3.1 The average moisture content (AMC) of maize, the difference between the average MCs of the air-inlet and air-outlet sub-columns (AMCD), and the standard deviation across the grain column (SD), of a crossflow dryer operating at 90°C.

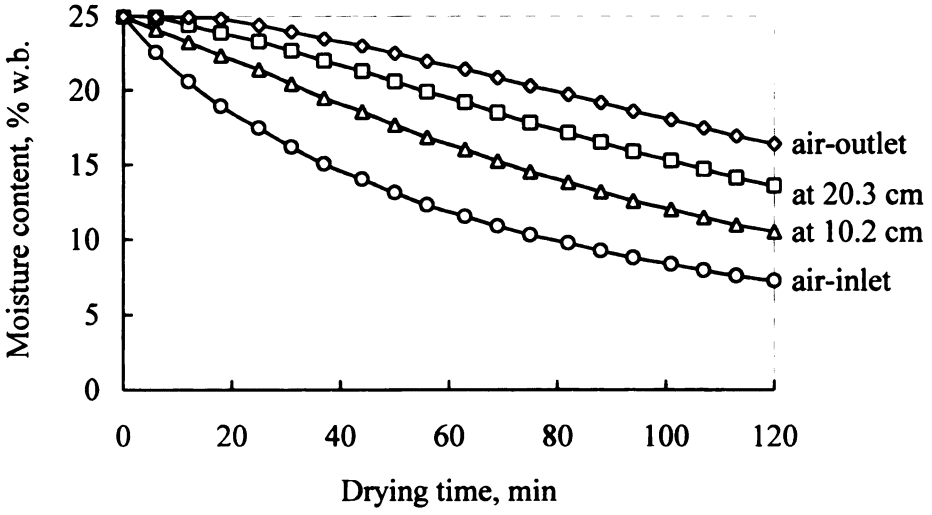

Fig. 3.2 The drying curves of 25 % w.b. initial moisture content maize at different positions within the grain column of a crossflow dryer operating at 90°C.

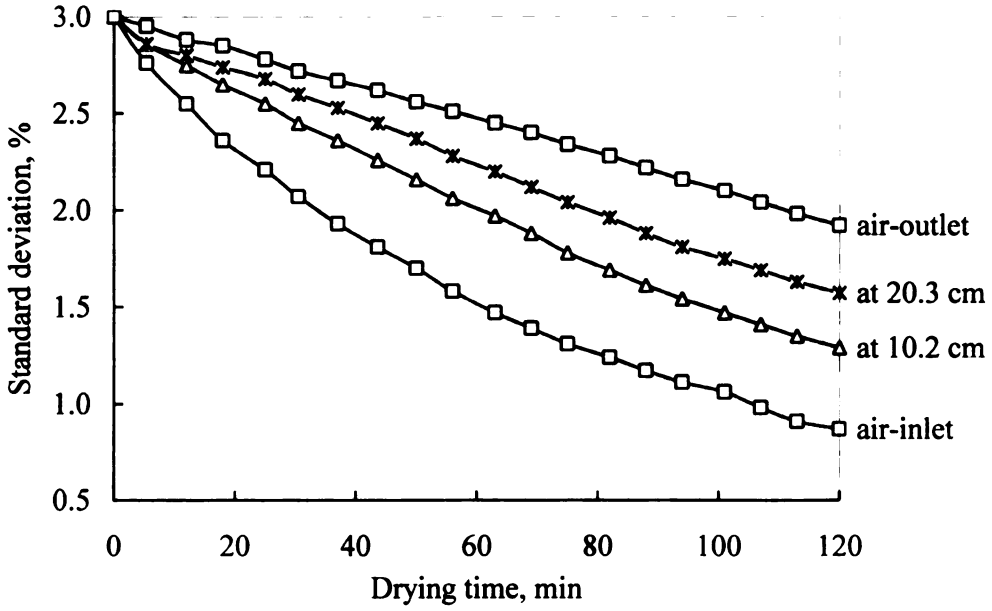

Fig. 3.3 The standard deviation of the moisture content at different positions within the grain column. Maize initially at 25% (w.b.) moisture content and dried in a crossflow dryer operating at 90°C.

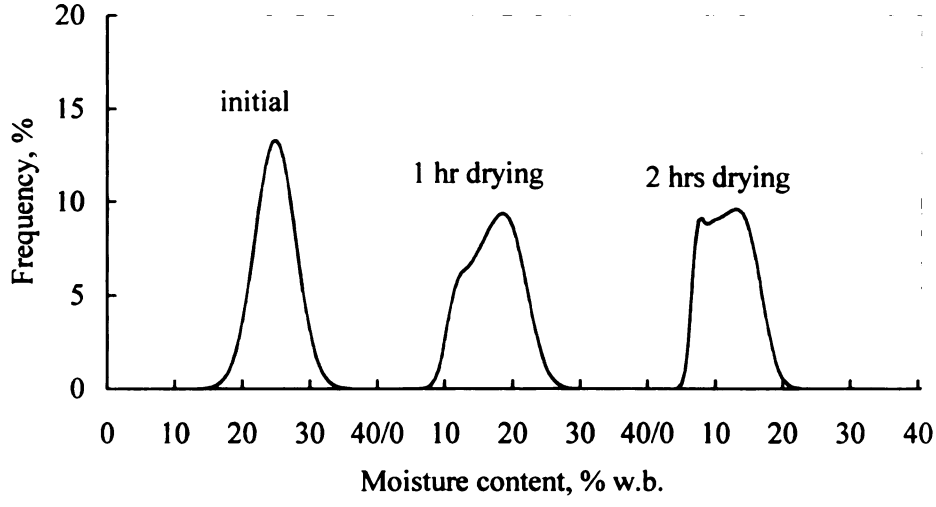

Fig. 3.4 The moisture distribution of maize before drying, and after one hour and two hours of crossflow drying at 90°C. Maize initially at 25% w.b. average moisture content with 3% w.b. standard deviation.

process, i.e. at the air-inlet and -outlet sides, and at two intermediate locations within the grain column. The maize at the air-inlet side dries faster (to MC_{final} = 7.0% w.b. in 2 h), and the standard deviation decreases more quickly (to SD_{final} = 0.8% w.b. in 2 h) than the grain flowing through the dryer at the air-outlet side of the grain column (MC_{final} = 16.0% w.b., SD_{final} = 1.9% w.b.).

The change in the moisture content distribution of the maize as it flows through the crossflow dryer is illustrated in Fig. 3.4. The shape of the frequency distribution curve changes --fewer kernels are at or near the average moisture content after 1 h and 2 h of drying than at the start of the drying process. The maximum frequency has shifted to the higher moisture content range, and the frequency curve has changed from a normal to bi-modal distribution. Thus, a sample of crossflow-dried maize can be expected to contain a relatively large number of low and high moisture-content kernels.

3.4 Standard Deviation

The standard deviation in the moisture content of the maize entering a crossflow dryer influences the standard deviation of the maize exiting the dryer, as is illustrated in Fig. 3.5. The standard deviation is affected by (1) the standard deviation within each sub-column, and (2) the standard deviation due to non-uniform heat-transfer/mass-transfer treatment of the grain across the grain column. During the initial minutes of drying the standard deviation changes little, but rapidly increases to a maximum value after about 1 h of drying. Subsequently, the standard deviation gradually decreases to about 3.0% w.b..

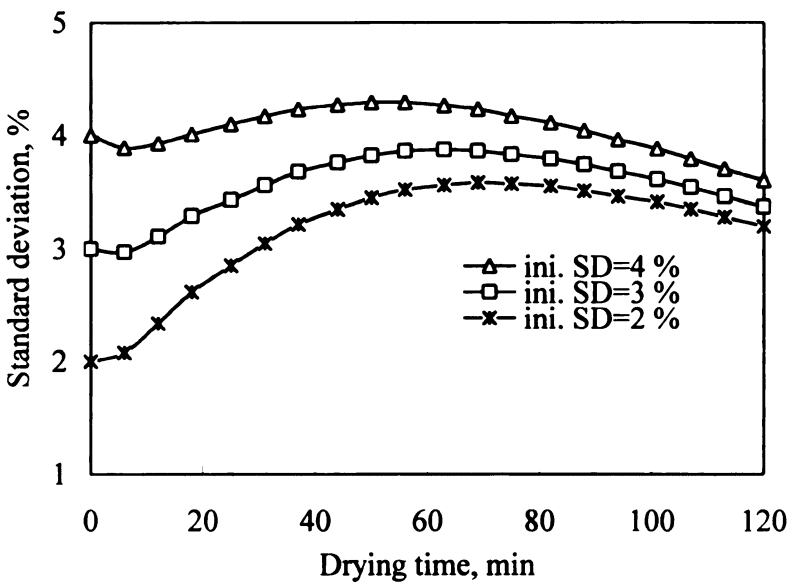

Fig. 3.5 The standard deviation (SD) of the moisture content of maize in a crossflow dryer for different initial SD values; the dryer operates at 90°C.

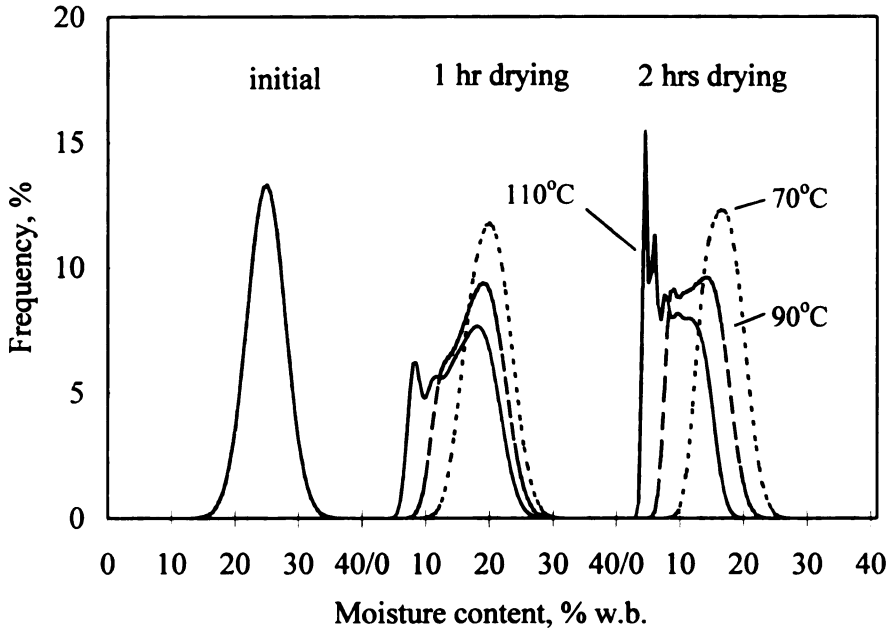

Fig. 3.6 The moisture distribution of maize dried in a crossflow dryer at different air temperatures. Maize initially at 25% w.b. average moisture content and 3% w.b. standard deviation.

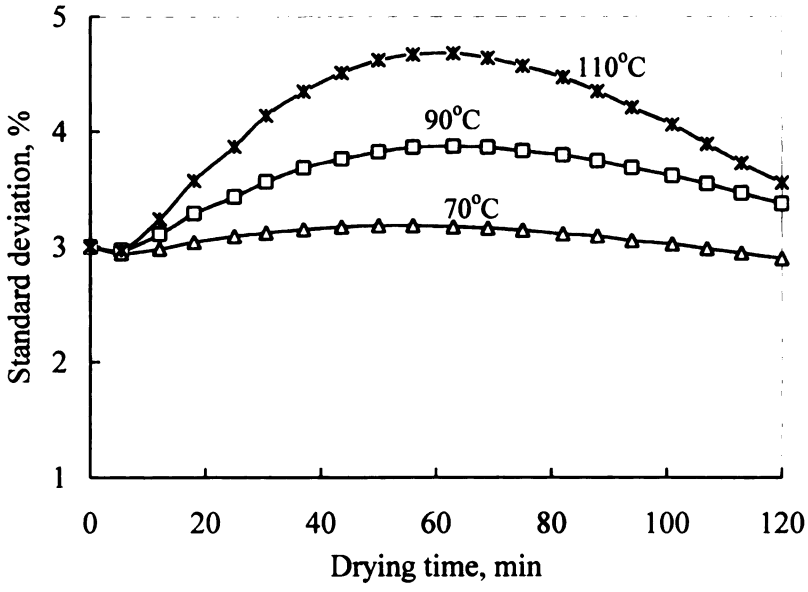

Fig. 3.7 The standard deviation of the moisture content in maize dried in a crossflow dryer at different air temperatures. Maize initially at 25% w.b. moisture content.

3.5 Air temperature

The air temperature is a significant parameter in the operation of crossflow dryers. Fig. 3.6 shows the frequency distribution of the moisture content of 25% w.b. maize as it is dried at three temperatures. The multi-hump, non-normal character of the frequency curve (Fig. 3.6) is pronounced at high drying temperatures, and it is curious that at 70°C the moisture content distribution after 1 h and 2 h is approximately normal.

Fig. 3.7 exhibits the change in the standard deviation under these conditions. Air temperature, as expected, affects the standard deviation of maize during the process of crossflow drying. While the change in the standard deviation at 70°C is negligible, at 90-110°C the standard deviation increases substantially during the first hour of drying and then decreases to about 0.5% w.b. above the initial value.

3.6 Airflow Rate

The effect of the airflow rate on the moisture distribution is similar to that of the drying air temperature. This is illustrated in Figs. 8 and 9. At the higher airflow rates, the standard deviation and the range in the moisture content are smaller than at lower airflow. Again, the non-normal distribution of the moisture content during and after the crossflow drying is evident.

3.7 Grain Inversion

Inverting the grain column at the midway point of the drying column has long been advocated as a means of alleviating the overdrying and underdrying of grain in

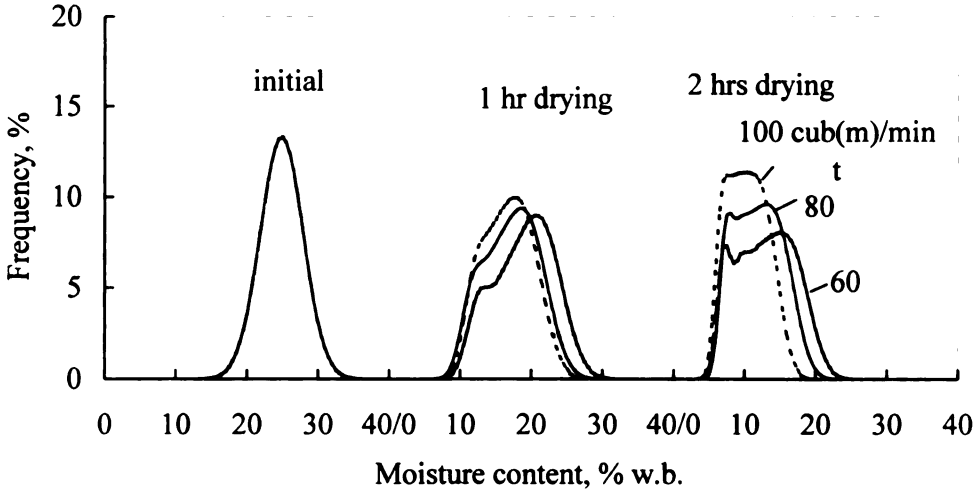

Fig. 3.8 The moisture distribution of maize dried at 90°C in a crossflow dryer at different airflow rates ($m^3\ min^{-1}\ t^{-1}$). Maize initially at 25% w.b. average moisture content with 3% w.b. standard deviation.

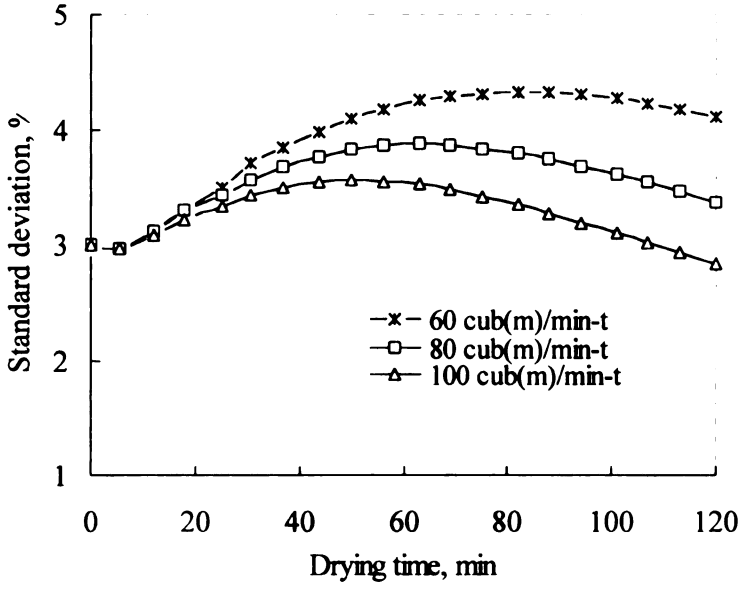

Fig. 3.9 The standard deviation of maize dried at 90°C in a crossflow dryer at different airflow rates ($m^3min^{-1}t^{-1}$). Maize initially at 25% w.b. moisture content.

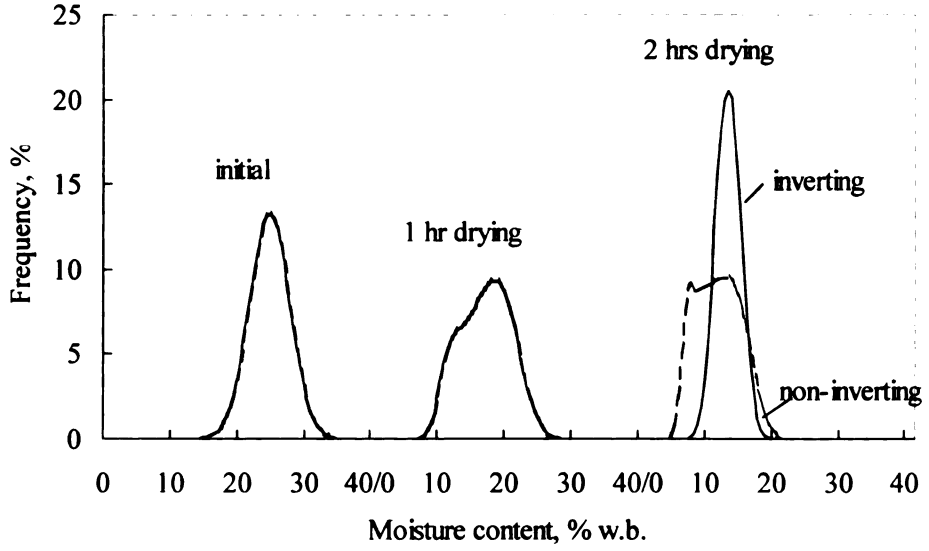

Fig. 3.10 The moisture distribution of maize before drying, and after one hour and two hours of crossflow drying at 90°C. The maize is initially at 25% w.b. moisture content and is inverted after 1 hour of drying.

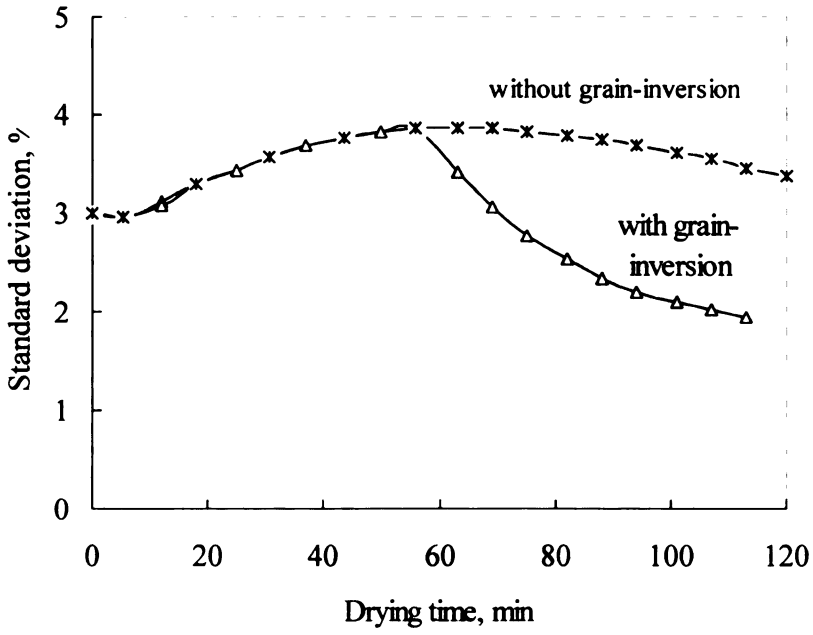

Fig. 3.11 The standard deviation (SD) of the moisture content of maize dried at 90°C in a crossflow dryer with and without grain-inversion. The maize is initially at 25% w.b. moisture content.

crossflow dryers. Figs. 10 and 11 provide proof of this beneficial effect. The moisture content range of maize dried in a conventional (non-inverting) crossflow dryer is wider than of maize dried in a dryer fitted with a grain-inverter (see Fig. 3.10). Also, the standard deviation in the moisture content of maize dried in a grain-inverting dryer is substantially lower than of the maize dried in a non-inverting model (see Fig. 3.11).

The advantages of inverting grain in a crossflow dryer are also illustrated in Tables 3.2 and 3.3. Without the grain-inverter the maize dries slightly faster than in the dryer with the inverter, i.e. in 120 min to 11.9% w.b. instead of to 12.6% w.b.. A large difference between the two designs occurs in the standard deviation of the exit moisture of the two dryers, 3.4% w.b. without the inverter and only 1.9% w.b. with the device. Also, note the considerable overdrying occurring of the maize exiting the dryer without the inverter at the air-inlet side of the column, i.e. a moisture content of the exit grain of well below 10% w.b..

Table 3.2 Moisture content (MC) and standard deviation (SD) of the moisture content (average, at air-inlet, at air-outlet) of maize dried in a crossflow dryer *without grain-inversion* (air temperature, 90°C; airflow rate, 80 m^3 min^{-1} t^{-1}).

TIME (MIN)	MC_{AV} (% W.B.)	MC_{IN} (% W.B.)	MC_{OUT} (% W.B.)	SD_{AV} (% W.B.)	SD_{IN} (% W.B.)	SD_{OUT} (% W.B.)
0	25.0	25.0	25.0	3.0	3.0	3.0
25	21.7	17.5	24.4	3.4	2.2	2.8
50	18.6	13.1	22.5	3.8	1.7	2.6
75	15.8	10.3	20.3	3.8	1.3	2.3
100	13.4	8.4	18.0	3.6	1.1	2.1
120	11.9	7.3	16.4	3.4	0.9	1.9

Table 3.3 Moisture content (MC) and standard deviation (SD) of the moisture content (average, at air-inlet, at air-outlet) of maize dried in a crossflow dryer *with grain-inversion* (air temperature, 90°C; airflow rate, 80 m^3 min^{-1} t^{-1}).

TIME (MIN.)	MC_{AV} (% W.B.)	MC_{IN} (% W.B.)	MC_{OUT} (% W.B.)	SD_{AV} (% W.B.)	SD_{IN} (% W.B.)	SD_{OUT} (% W.B.)
0	25.0	25.0	25.0	3.0	3.0	3.0
25	21.7	17.5	24.4	3.4	2.2	2.8
50	18.6	13.1	22.5	3.8	1.7	2.6
75	16.3	17.1	12.3	2.7	2.1	1.6
100	14.1	12.9	11.9	2.1	1.6	1.5
120	12.6	10.7	11.4	1.9	1.3	1.4

*air temperature, 90°C; airflow rate, 80 m^3 min^{-1} t^{-1}

3.8 Conclusion

Deterministic grain drying models provide insight into the course of the *average* moisture content of grain during the drying process, and predict the average moisture content as it exits from a dryer. *Stochastic* drying models furnish *additional* information, namely the *distribution* of the moisture content during and immediately after drying.

Deterministic grain dryer models assume a *uniform* inlet moisture content while the stochastic models presume a more realistic *normal distribution* of the moisture content in the grain entering a dryer. Only stochastic modelling can provide essential design information on the degree of overdrying *and* of underdrying occurring in crossflow dryers.

Wet and dry millers in particular will profit from the information provided by the stochastic dryer models with respect to the uniformity of their base product, i.e. maize.

But also, livestock feeders will benefit because of the capability for assessing the likely breakage susceptibility, and thus the storability, of their feed.

Finally, the MSU stochastic drying models are important tools in the design of grain drying systems. This has been illustrated in this paper in the analysis of grain inverters in crossflow maize dryers.

CHAPTER 4. MODELING OF GRAIN QUALITY*

Abstract

The objective of this chapter is to develop simulation models of grain-quality deterioration during crossflow drying. The stochastic drying model and the denatured protein and germination models are combined to simulate the quality loss of individual kernels in crossflow dryers. The results of this study lead to a better understanding of grain-quality deterioration, and provide an improved tool for dryer design and control.

*Part of the content was published in ASAE Paper No: 97-6030 and was presented at the 1997 ASAE Annual International Meeting sponsored by ASAE, Minneapolis Convention Center, Minneapolis, Minnesota, August 10-14, 1997.

4.1 Introduction

Grain is usually harvested at high moisture content to minimize field losses. High-temperature dryers are widely used to quickly reduce the moisture to a safe storage level. The drying-air-temperature ranges from 50 to 300°C, depending on dryer type, the crop to be dried, and the quality requirements (Brooker et al., 1992). In general, higher drying-air-temperatures result in higher capacities and energy efficiencies, but degrade the grain quality. Therefore, the drying air temperature is a compromise between the throughput of the dryer and the grain quality.

Three reasons make it difficult to predict or control the grain quality in a drying process: a) the grain quality during drying is affected by multiple factors including the drying-air temperature, drying time and grain moisture content; b) no dryer (crossflow, mixed-flow, and concurrent-flow) treats grain uniformly; and c) the moisture content of each grain kernel is distributed stochastically around an average, and thus each kernel has a different reaction to the drying treatment. Therefore, the drying conditions for various dryers are generally determined by rules-of-thumb, and this may lead to substantial quality damage of the grain.

The objective of this Chapter is to develop a simulation model of the grain quality in crossflow grain dryers. The model will be used to improve the grain quality through improved dryer design and through improved automatic dryer control.

4.2 Literature Review

This review will focus on the effect of artificial drying on maize quality, quality criteria of end-users, and the quality modeling in drying process.

(1) Effect of artificial drying on maize quality

MacMasters et al. (1959) conducted an extensive test on the wet-milling quality of maize dried under various conditions in five crop years. The maize was harvested at 30-20% moisture content, and dried at six air temperatures ranging from 49 to 93°C, and at relative humidity of 15 and 40%. The starch recovery rate was 82% of the maize dried at 49°C; it decreased to 74% when the drying temperature increased to 93°C. Maize reaching a temperature above 60°C during drying showed a definite decrease in viability. The initial moisture content of the maize and the relative humidity of the air were relatively unimportant with respect to the wet-milling quality.

Brekke et al. (1973) investigated the effects of the drying-air temperature on the dry-milling quality of maize. The tests were conducted with a fluidized-bed dryer at five air temperatures ranging from 32 to143°C; the maize was dried from approximately 25 to 15% w.b. in 0.5 to 7 hours. The yield of first-break grits (grits passing through a four mesh sieve and retained on a six mesh sieve) decreased from 45 to12% as the drying-air temperature was increased to 143°C. The percentage of stress cracked kernels was 56% at 32°C, and 84% at 143°C. The Steinlite breakage susceptibility changed from 7 to 35% as the drying-air temperature was increased from 32 to143°C.

Brown et al. (1979) studied the effect of three drying methods on the quality of maize dried from 20 to 15%: (1) high-temperature crossflow batch drying and cooling, (2)

crossflow batch drying followed by dryeration, and (3) low-temperature (ambient air) drying. The drying air temperature ranged from 45 to 80°C in the crossflow dryer; 60, 80 and 100°C were used in the high-temperature drying stage of dryeration. Viability was found to be the most sensitive quality factor; it was markedly reduced at temperatures above 60°C. Grain dried with a low-temperature drying system had a negligible amount of stress-cracks; dryeration also caused few stress-cracks (i.e. 3-30%); batch-dried grain contained the most stress-cracked kernels, between 45 to 79%. The combination of viability, test weight, and stress cracks correlated well with the steeping index as a measure of wet-milling quality.

Le Bras (1982) investigated the effects of the variety, maturity and drying conditions on the wet-milling quality of maize. The drying condition was the major factor in degrading the maize quality. A noticeable decrease occurred in starch yield when the drying-air temperature was raised to 90°C. Five drying methods were investigated: (1) one-pass drying, (2) two-passes drying with intermediate aeration, (3) dryeration, (4) two-stage drying, and (5) multi-stage drying processes. Dryeration resulted in the best quality, followed by drying in two passes with intermediate aeration; drying in one pass resulted in the worst quality grain.

Weller et al. (1987, 1988) investigated the effects of harvest moisture and drying-air temperature on starch recovery. The maize was harvested at high, medium, and low moisture contents of approximately 30, 24 and 18% w.b., and was dried to about 14% w.b. at 22 (ambient), 49, 71 and 93°C, at an airflow rate of 2 $m^3m^{-3}min^{-1}$. Starch recovery was not significantly different for four hybrids but decreased as both the harvest moisture and the drying-air temperature increased. The test weight decreased as the drying-air

temperature increased, and the germination increased from 89% at 22°C to 95% at 49°C. All samples showed greater than 80% stress cracking at drying air temperature above 49°C except the low moisture content samples. The stress cracks for the soft maize varieties ranged from 62 to 82% while those for the hard varieties ranged from 39 to 65%.

Maize samples were collected prior to and after drying in four commercial dryers (three crossflow and one concurrent-flow) by Chang et al. (1989), and their physical and chemical properties were investigated. The drying-air temperature ranged from 63 to 96°C, the initial moisture content from 18 to 28%, and final moistures from 14.3 to 18.0%. The percentage of stress-cracks increased from almost 0 % to a low of 3-34 % after drying. Before drying the individual kernel moistures ranged from 15 to 27%; after drying, the kernel moistures ranged from 6 to 20%; a wider variation in the individual kernel moisture content was indicative of a more severe drying treatment which led to reduced starch recovery.

Peplinski et al.(1989) investigated the physical and chemical characteristics of six maize hybrids dried at 25 (ambient) and 60°C, with a moisture removal from 20-24% to 10-13%. Increasing the drying-air temperature from 25 to 60°C had no apparent effect on the chemical composition but increased the percentage of stress-cracked kernels from 0-3 % to 23-74%, respectively, depending on the maize hybrid. The breakage susceptibility, as measured in the Stein breakage test, at 25 °C ranged from 1to 7 % and at 60°C from 3 to 9%; the grits yield decreased 1% at 25°C and 7% at 60°C.

Maize at 30% moisture was dried in a stationary bed at 25 to 100°C at a depth of 5.1 cm (Peplinski et al., 1994). Drying times to 12% final moisture ranged from 1 hr at 100°C to 38 hr at 25°C. The chemical composition of the maize dried at 100°C was

unaltered but the breakage susceptibility ranged from 27 to 67% and the stress-cracked kernels from were 78-84%. Germination decreased to 0% at air temperatures higher than 70°C. The amount of water-extractable protein (albumin solubility) remained constant in the maize dried at 25-55°C, but rapidly decreased as the drying temperature exceeded 60°C.

Zhang et al. (1991) investigated maize-quality variation in a commercial crossflow dryer. Samples from 15 points in the dryer were collected. Large variations in moisture content were observed across the dryer column. Maize at the air-inlet side of the grain column lost about twice as much moisture as the maize at the air-outlet side. A high percentage of stress cracked kernels (average of 20.5%) with high breakage-susceptibility values (20.5-36.8%) was measured in the samples at the inside layer of the grain column.

The effects of the drying parameters on the various qualities of maize were studied on a laboratory-size crossflow dryer by Beke et al. (1993). The drying-air temperature ranged from 60 to 160°C and the superficial air velocity ranged from 0.1 to 1.3 m/s. The drying-milling quality of maize was greatly affected when the drying-air temperature exceeded 110°C or the air velocity surpassed 0.9 m/s. The protein and starch content, and the feed value also decreased dramatically when the air-temperature exceeded 110°C. The maximum air temperature recommended for maize was 100°C for an initial moisture higher than 32% w.b., and 110°C for an initial moisture lower than 32% w.b..

(2) Quality criteria

The quality requirements are different for each end-use of maize, i.e. wet-milling, dry-milling, and animal feeding; different criteria are used to assess maize quality for each use. The criteria can be categorized into two types: (a) direct, and (b) indirect. Direct criteria are, for instance, the grits yield for dry-milling, the starch-recovery for wet-milling, and the viability for seed grain. An indirect criterion measures a physical or chemical property associated with grain quality, e.g. moisture content, moisture uniformity, test weight, stress-cracks, breakage susceptibility, BCFM (Broken Corn and Foreign Materials), soluble protein, starch viscosity, and sedimentation (Brooker et al., 1992; Freeman, 1973; Chang et al., 1989). No single indirect criterion adequately predicts the grain quality, in contrast to a direct criterion which is definitive, but (generally) cumbersome to determine.

In the U. S. grade standard for yellow maize, five factors are employed to determine the grade, i.e. maximum moisture, test weight, BCFM, heat damage and total damage (Brooker et al., 1992). However, the standard does not address the end-use quality of the grain, and is considered to be inadequate in some industries (Lowell, 1996). End-users generally use a private grade-description in addition to the general standard in order to assess grain quality.

The main objective of the dry-milling of maize is to obtain large grits for cereal food. Wichser (1961) proposed the "milling evaluation factor" (MEF) for rating the dry-milling quality; the MEF is based on the proportion of grits, meal and flour after the milling process. Emam et al. (1981) proposed a modified MEF based upon the yield of grits larger than 7-mesh and on the percentage of endosperm extraction; the factor is highly correlated (R=0.92) with flaking-grit yield (Kirleis et al., 1990).

Among the indirect maize-quality criteria, kernel density is the best single predictor of the MEF (Kirleis et al., 1990); floaters and test weight have the highest correlation with grits yield (Paulsen et al., 1985). No quantitative relationship between the dry-milling quality and the drying conditions has been established although Peplinski et al. (1989,1994) recommended (as a rule-of-thumb) a maximum kernel-temperature of 60°C for the drying of maize, regardless of the moisture content.

Direct measurement of the wet-milling quality of maize requires a 2-day laboratory-scale wet-milling procedure, and is therefore not suitable for examining a lot of maize on a routine basis (Freeman, 1973; Chang et al., 1989). Viability, test weight, and stress cracks do not separately predict wet-milling performance (Brown et al., 1979). Among the indirect criteria, starch content, test weight, and ethanol-soluble protein have the highest correlation with starch recovery (Weller et al., 1988). Le Bras (1982) recommended breakage susceptibility, water re-absorption, sedimentation and turbidity as rapid tests for the measurement of quality damage by artificial drying. Courtois et al. (1991) and Mourad et al. (1996) used the protein-soluble in saline-water as an indicator of the wet-milling quality of maize.

(3) Quality models and simulation

A germination model for dried seed grains was developed by Nellist (1981). At constant temperature and moisture content, seed death is shown to be normally distributed over time and can be quantified by use of the integral of the normal distribution. The germination percentage is represented as a probability, which, when transformed to equivalent values of the standardized normal deviate or 'probit', has a

linear death rate defined the reciprocal history of seed. A similar germination model was developed by Lescano et al. (1987) for maize based on thin-layer drying tests; the model was employed to predict the viability of maize dried in a concurrent-flow dryer.

Courtois et al. (1991) proposed an empirical model for the wet-milling quality of maize dried in mixed-flow dryers. Transmittance of light through a grain-saline solution was employed as the quality criterion. The error in the predicted transmittance of mixed-flow dried maize was generally less than 10%.

Bruce (1992) developed a model for the effect of the heated-air drying on the bread-baking quality of wheat. Two varieties of wheat at three initial moisture contents were dried in thin layers with air from 65 to 85°C for periods from 1 min to 4 hours. Two models were developed to describe the relationship between the loss of loaf volume and the moisture and temperature histories of the wheat kernels.

Zhang et al. (1992) developed a fuzzy model to predict the breakage susceptibility of dried maize. The model is based on data obtained from experiments with a laboratory crossflow dryer with maize of various initial moisture contents.

Mourad et al.(1996) developed a wet-milling maize quality model based on a number of fluidized-bed drying tests. Protein solubility and the separation index of starch and protein were the quality criteria. The relationship between the degradation rate of protein (i.e. the wet-milling quality) and the drying conditions was established.

The aim of this Chapter is to combine two maize-quality models with the stochastic grain drying model developed in Part I, Chapter 2, in order to simulate the change of grain quality in crossflow dryers, and to provide a tool for minimizing the quality damage of grain in a crossflow dryer.

4.3 Models and Simulation

4.3.1 Quality models

The transmittance model developed by Courtois et al. (1991) and the viability model of Lescano et al.(1987) were employed for the quality simulation of dried maize. The Courtois transmittance model is:

$$\frac{\partial A}{\partial t} = -K_A A^2 \tag{4.1}$$

where

$$K_A = K_{A\phi} \exp[-133.2 \times 10^3 / (8.314(\theta + 273.16))]$$
$$K_{A\phi} = 1.9561 \times 10^{16} + 5.4287 \times 10^{17} M + 6.8210 \times 10^{17} M^2$$

where A is the absorbance unit (dimensionless), θ the grain temperature (°C), and M the grain moisture content (dec. d.b.). The relationship between the absorbance unit A and the transmittance T (%) is:

$$A = -\log_{10}(T/100) \tag{4.2}$$

The percentage of protein denaturation DP (%) was calculated from (Chang et al., 1989):

$$DP = 100\frac{T_f - T_0}{100 - T_0} \tag{4.3}$$

where T_0 is the initial transmittance and T_f the final transmittance.

The viability model of Lescano et al. (1987) has the form:

$$G = \frac{1}{\sqrt{2\pi}} \int_X^{+\infty} \exp\left[-\frac{1}{2} X^2\right] dX \tag{4.4}$$

where: $$X = (t - \bar{t}) / \sigma \tag{4.5}$$

and G is the germination, X the standardized normal deviate, $\bar{t}$ the time for 0.5 viability, and σ the standard deviation of the seed viability loss, which is a function of the drying air temperature T_a and the seed moisture content M. For maize,

$$\ln \sigma = 4.20 - 0.27T_a - 33.20 \ln M \tag{4.6}$$

where T_a is expressed in °C and M in % (w.b.).

4.3.2 Quality simulation

A subroutine for grain quality simulation was added to the stochastic grain drying program developed in Part I, Chapter 2. The subroutine predicts the germination and the percentage of denatured protein of maize during the crossflow drying process.

In the stochastic crossflow grain-drying model, the grain column is divided into a number of equal-depth sub-columns in the direction of the airflow. Each sub-column is further divided into stacked grain beds from the inlet to the outlet of the dryer. It was established that if the grain moisture content is initially normally distributed, the moisture content keeps the normal distribution during the drying process in a sub-column, but with a changed average and standard deviation (see Chapter 2.3). The stochastic drying model predicts the average moisture content of the maize and its standard deviation at the outlet of each bed.

The quality models of Eqs (4.1) and (4.4) are both functions of the grain moisture content. With the grain moisture content initially normally distributed, the grain quality will also be stochastically distributed among the grain kernels (not necessarily as a normal distribution). In the quality simulation subroutine, 80 values of the moisture

content are selected evenly spread in the range of -4σ to $+4\sigma$ of the normal distribution; the grain quality is predicted for each value of the moisture content. The average grain quality at the outlet of each bed is subsequently calculated by:

$$Q = \sum_{i=1}^{80} f(M_i) Q_i \tag{4.7}$$

where Q is the average grain quality; Q_i is the predicted quality of the grain with the moisture content of M_i; and f is the probability density of the moisture distribution at M_i, i.e.:

$$f(M_i) = \frac{1}{\sqrt{2\pi\sigma^2}} e^{-\frac{1}{2}\left(\frac{M_i - \overline{M}}{\sigma}\right)^2} \tag{4.8}$$

where $\overline{M}$ is the average grain moisture content and σ is the standard deviation of the normal distribution.

For simulation of the denatured protein in a sub-column, the changes in the grain temperature and moisture content are negligible for the quality simulation. Thus, assuming constant temperature and moisture content, the solution of Eq. 4.1 is:

$$Q_i = \frac{1}{1/Q_{i-1} + K_Q \Delta\tau} \tag{4.9}$$

where Q_{i-1} is the absorbance unit of maize at the inlet of the bed and Q_i the predicted absorbance unit at the outlet of the bed; and $\Delta\tau$ is the residence time of the maize in the bed. Then, the percentage of protein denaturation *DP* (%) is calculated from the absorbance unit (Q) with Eqs. 4.2 and 4.3.

For simulation of the germination, the solution for germination model of Eq. 4.5 is:

$$X_i = X_{i-1} + \frac{\Delta t}{\sigma} \tag{4.10}$$

where X_{i-1} is the standardized normal deviate at the inlet of the bed, and X_i is the predicted standardized normal deviate at the outlet of the bed; σ is the standard deviation of the seed viability loss, and $\Delta\tau$ is the residence time of grain in the bed. The viability of the grain is converted from the standardized normal deviate (X) to germination (G) with Eq. 4.4.

The procedure of determining the grain quality in a crossflow dryer is: (1) use the stochastic drying model to predict the average and the standard deviation of the grain moisture content in each bed in a sub-column; (2) apply Eqs. 4.7-4.10 to each bed in sequence from the inlet of the dryer to the outlet; and (3) calculate the average of the values determined in step (2) to obtain the average quality of the dried grain.

4.3.3 Model validations

The experimental data collected from three commercial crossflow maize dryers by Chang et al. (1989) were used for validation of the wet-milling quality simulation. The dryers were a Redex R-RT-RX30, a Meyer-Morton 3000 and a Delux DG-1500; the specifications of the dryers are contained in the paper by Chang et al. (1989). The dryer capacity in a specific test was found by matching the experimental and simulated final moisture contents. A comparison of the experimental and predicted transmittance and denatured-protein percentages in maize is tabulated in Table 4.1.

The average difference between the experimental and predicted values of the transmittance is 3.0% (32 vs 35%), and of the denatured protein is 3.8% (15.2 vs 19.0%).

Table 4.1 Experimental and predicted transmittance and denaturation of protein after drying of maize in three commercial crossflow dryers.

Dryer model	Redex				Meyer-Morton				Delux			
Test Number	1	2	3	4	5	6	7	8	9	10	11	12
Drying air temp., °C	82	93	82	82	82	93	93	96	63	68	93	96
Initial M.C., % w.b.	22.5	20.1	21.4	21.0	28.0	21.4	23.0	18.0	22.4	20.8	20.6	24.1
Final M.C., % w.b.	15.0	14.3	14.5	14.7	17.5	16.1	17.4	15.0	15.1	14.6	16.5	15.2
Initial trans., %	22.5	20.3	24.5	21.3	20.3	25.3	23.1	17.6	24.3	25.6	21.9	25.0
Exp. Final trans., %	34.5	30.6	34.2	32.6	35.5	31.6	39.0	39.4	31.4	28.2	42.4	34.5
Predicted final trans., %	33.5	33.7	34.4	30.9	33.8	36.0	33.8	24.3	27.9	28.6	25.4	35.9
Exp. dena. of protein, %	15.5	12.9	12.8	14.4	19.1	8.4	20.7	26.5	9.4	3.5	26.2	12.7
Predicted dena. of protein, %	14.2	16.8	13.1	12.2	16.9	14.3	13.9	8.1	4.8	4.0	4.5	14.5

Table 4.2 Experimental and predicted germination of maize after two hours of drying in a batch dryer in drying maize to 15% MC.

Test no.	Drying air temp., °C	Initial M.C., % w.b	Final M. C., % w.b.	Initial germ., %	Final germ., %	Predicted final germ., %
1	93	31.0	14.9	90	11	24
2	93	30.5	14.4	92	5	25
3	93	27.0	13.4	97	3	27

Table 4.3 Drying conditions for the grain-quality simulation study in a crossflow dryer.

Drying air temp., °C	50	60	70	80	100	120
Airflow rate , cfm bu^{-1}*	40	60	80	100	120	
Initial M.C., % w.b.	17.5	20	25	30	35	
Initial transmittance, %	25					
Initial germination, %	95					
Standard deviation of initial M.C., % w.b.	3					

*1 cfm bu^{-1} = 0.804 $m^3m^{-3}min^{-1}$

[The experimental percentage of denatured protein in Tests 6 and 10 seems unreasonable low compared to the values in the similar conditions in the test.]

Experimental germination data of maize was collected by Gustafson (1981) on a laboratory batch dryer; the dryer has a 30.5 cm wide column, and an airflow rate of approximately 80 m^3 min^{-1} t^{-1}. The predicted germination was higher than the experimental results as shown in Table 4.2. Fig. 4.1 shows a comparison of the germination percentage at four positions within the grain column during a two-hour drying period. Considerable disagreements occurred at 2/3 and at the air-outlet side of the column, especially in the low germination range. A major reason could either be the inaccurate prediction of the grain-temperature distribution in the drying column (Sokhansanj, 1987) or the effect of maize hybrid (Lescano et al., 1987).

In general, it is the opinion of the author that the grain-quality/grain-dryer simulation models are acceptable for use in further analysis.

4.4 Gain-quality Analysis

A simulation study of the quality change of maize in a crossflow dryer was conducted. The thickness of the grain column was assumed to be 30.5 cm; the drying air (or grain stream) is reversed at the midpoint of the drying column. The cooling time is one-third of the drying time, and the ambient temperature and humidity are 15°C and 60%, respectively. For each drying condition, the drying time and cooling time were searched for so that the final moisture content would be 15% w.b.. The drying conditions are tabulated in Table 4.3. A total of 150 drying conditions were investigated. Tables 4.4a-4e show the results.

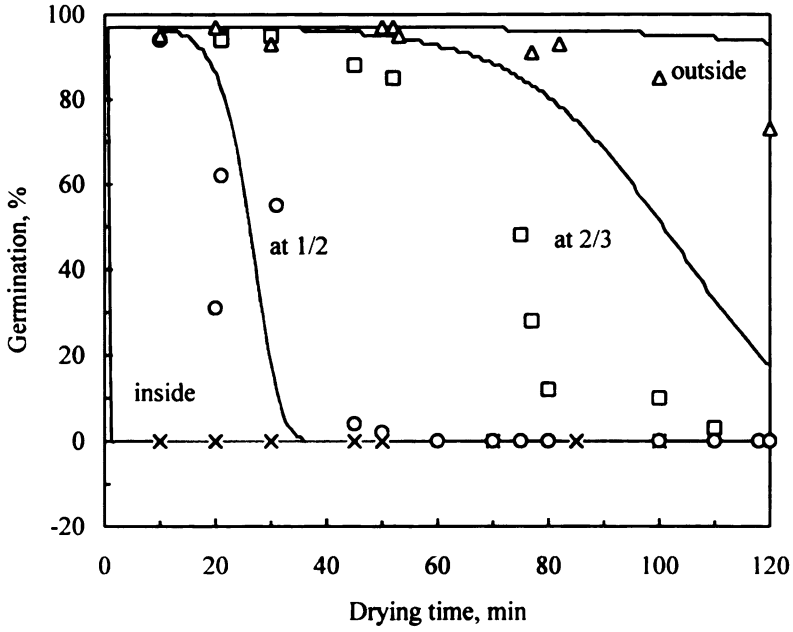

Fig. 4.1 Experimental (points) and predicted (lines) germination vs. time of maize at four locations (at the air inlet, at 1/2, 2/3 and air outlet) in the grain column.

Table 4.4a Predicted quality of maize after crossflow drying at an airflow rate of 40 cfm/bu (32 $m^3m^{-3}min^{-1}$)

Drying air temp., °C	Inlet M.C., % w.b.	Trans-mittance, %	Dena. protein, %	Germ., %
50	17.5	25.1	0.1	94.7
50	20	25.9	1.2	94.6
50	25	27.3	3.1	94.3
50	30	27.9	3.9	93.7
50	35	28.0	4.0	92.3
60	17.5	25.2	0.3	94.3
60	20	26.4	1.9	93.2
60	25	28.4	4.5	70.3
60	30	29.3	5.7	71.9
60	35	29.2	5.6	65.2
70	17.5	25.4	0.5	81.4
70	20	27.1	2.8	66.6
70	25	29.8	6.4	61.4
70	30	31.0	8.0	52.7
70	35	30.8	7.7	44.2
80	17.5	25.8	1.1	65.9
80	20	28.0	4.0	54.8
80	25	31.5	8.7	37.7
80	30	32.7	10.3	34.7
80	35	32.5	10.0	32.5
100	17.5	26.7	2.3	39.9
100	20	30.4	7.2	31.3
100	25	35.3	13.7	11.5
100	30	36.7	15.6	9.9
100	35	35.8	14.4	9.8
120	17.5	27.9	3.9	34.3
120	20	33.5	11.3	12.2
120	25	39.3	19.1	2.6
120	30	40.5	20.7	0.3
120	35	39.1	18.8	0.4

Table 4.4b Predicted quality of maize after crossflow drying at an airflow rate of 60 cfm/bu (48 $m^3m^{-3}min^{-1}$).

Drying air temp., °C	Inlet M.C., % w.b.	Trans-mittance, %	Dena. protein, %	Germ., %
50	17.5	25.1	0.1	94.7
50	20	26.0	1.3	94.6
50	25	27.6	3.5	94.3
50	30	28.3	4.4	93.8
50	35	28.3	4.4	92.9
60	17.5	25.3	0.4	94.3
60	20	26.7	2.3	93.4
60	25	28.9	5.2	88.8
60	30	30.0	6.7	76.9
60	35	29.8	6.4	65.6
70	17.5	25.7	0.9	85.0
70	20	27.7	3.6	67.6
70	25	30.8	7.7	58.0
70	30	32.0	9.3	46.3
70	35	31.6	8.8	39.9
80	17.5	26.0	1.3	64.4
80	20	28.7	4.9	46.1
80	25	32.9	10.5	32.4
80	30	34.0	12.0	24.7
80	35	33.4	11.2	21.5
100	17.5	26.9	2.5	38.0
100	20	31.8	9.1	12.4
100	25	37.5	16.7	2.3
100	30	38.8	18.4	0.3
100	35	37.6	16.8	0.3
120	17.5	28.3	4.4	13.6
120	20	35.3	13.7	1.0
120	25	42.5	23.3	0.0
120	30	43.3	24.4	0.0
120	35	41.6	22.1	0.0

Table 4.4c Predicted quality of maize after crossflow drying at an airflow rate of 80 cfm/bu (64 $m^3m^{-3}min^{-1}$).

Drying air temp., °C	Inlet M.C., % w.b.	Trans-mittance, %	Dena. protein, %	Germ., %
50	17.5	25.1	0.1	94.7
50	20	26.1	1.5	94.6
50	25	27.8	3.7	94.3
50	30	28.6	4.8	93.8
50	35	28.6	4.8	93.1
60	17.5	25.4	0.5	94.4
60	20	26.9	2.5	93.5
60	25	29.4	5.9	89.5
60	30	30.6	7.5	79.3
60	35	30.4	7.2	67.7
70	17.5	25.8	1.1	87.1
70	20	27.9	3.9	69.5
70	25	31.5	8.7	55.0
70	30	32.9	10.5	41.4
70	35	32.4	9.9	35.9
80	17.5	26.2	1.6	62.9
80	20	29.4	5.9	40.6
80	25	33.8	11.7	24.4
80	30	35.3	13.7	13.1
80	35	34.6	12.8	11.1
100	17.5	27.3	3.1	32.0
100	20	32.8	10.4	6.7
100	25	39.3	19.1	0.0
100	30	41.0	21.3	0.0
100	35	39.4	19.2	0.0
120	17.5	29.1	5.5	10.9
120	20	37.0	16.0	0.0
120	25	44.9	26.5	0.0
120	30	46.4	28.5	0.0
120	35	44.2	25.6	0.0

Table 4.4d Predicted quality of maize after crossflow drying at an airflow rate of 100 cfm/bu (80 $m^3m^{-3}min^{-1}$).

Drying air temp., °C	Inlet M.C., % w.b.	Trans-mittance, %	Dena. protein, %	Germ., %
50	17.5	25.2	0.3	94.7
50	20	26.2	1.6	94.6
50	25	28.0	4.0	94.3
50	30	28.9	5.2	93.9
50	35	28.9	5.2	93.2
60	17.5	25.5	0.7	94.4
60	20	27.1	2.8	93.6
60	25	29.8	6.4	89.9
60	30	31.1	8.1	80.6
60	35	30.9	7.9	69.2
70	17.5	25.9	1.2	82.2
70	20	28.4	4.5	71.2
70	25	32.2	9.6	52.5
70	30	33.5	11.3	37.6
70	35	33.1	10.8	33.3
80	17.5	26.5	2.0	61.3
80	20	30.0	6.7	37.0
80	25	34.8	13.1	15.8
80	30	36.4	15.2	6.6
80	35	35.7	14.3	5.4
100	17.5	27.6	3.5	23.4
100	20	33.9	11.9	0.0
100	25	40.8	21.1	0.0
100	30	42.7	23.6	0.0
100	35	41.1	21.5	0.0
120	17.5	30.0	6.7	2.8
120	20	38.6	18.1	1.0
120	25	47.5	30.0	0.0
120	30	48.9	31.9	0.0
120	35	46.6	28.8	0.0

Table 4.4e Predicted quality of maize after crossflow drying at an airflow rate of 120 cfm/bu (96 $m^3m^{-3}min^{-1}$).

Drying air temp., °C	Inlet M.C., % w.b.	Trans-mittance, %	Dena. protein, %	Germ., %
50	17.5	25.2	0.3	94.7
50	20	26.3	1.7	94.6
50	25	28.1	4.1	94.3
50	30	29.1	5.5	93.9
50	35	29.1	5.5	93.2
60	17.5	25.5	0.7	94.4
60	20	27.4	3.2	93.6
60	25	30.2	6.9	90.0
60	30	31.4	8.5	81.4
60	35	31.3	8.4	70.0
70	17.5	26.0	1.3	88.9
70	20	28.8	5.1	72.6
70	25	32.7	10.3	49.7
70	30	34.3	12.4	34.2
70	35	33.8	11.7	28.4
80	17.5	26.6	2.1	60.6
80	20	30.5	7.3	33.7
80	25	35.8	14.4	8.8
80	30	37.5	16.7	2.6
80	35	36.7	15.6	1.8
100	17.5	28.1	4.1	15.7
100	20	34.8	13.1	0.0
100	25	42.8	23.7	0.0
100	30	44.4	25.9	0.0
100	35	42.6	23.5	0.0
120	17.5	30.7	7.6	0.0
120	20	39.8	19.7	0.0
120	25	49.7	32.9	0.0
120	30	51.2	34.9	0.0
120	35	48.7	31.6	0.0

The highest transmittance (and thus the worst grain quality) obtained in the tests was 51.2%, corresponding to a denatured protein value of 34.9%; it occurs (obviously) with drying conditions of 120°C, 120 cfm/bu (96 m^3 m^{-3} min^{-1}) initial moisture (Table 4.4e). At a drying-air temperature of 50°C, the germination exceeded 92.3%, regardless of airflow. A significant change in the germination happened in the temperature range of 60-70°C; for instance, at initial moisture content of 20% (w.b.) the germination changed from 93% to about 70%. In general, higher drying- air temperatures, airflow rates and initial moisture contents resulted in higher denatured-protein values and lower germination rates. The drying air temperature appeared to be the most significant factor, especially for germination.

Figs. 4.2, 4.3, and 4.4 show the values of denatured protein at different drying air temperatures, airflow rates and inlet moisture contents. From Figs. 4.2 and 4.3 it is clear that the denatured protein percentage increases with increased drying-air temperatures and airflow rates; at temperatures above 80°C the rate increases. With an increase in the inlet moisture content, the denatured protein percentage increases rapidly at the lower moisture contents, and reaches a maximum value at about 28% w.b. moisture content (Fig. 4.4). The denatured protein percentage decreases at a rate dependent on the drying air temperature; it is not clear why the denatured protein percentage sharply decreases for inlet moisture contents above 28% w.b..

Fig. 4.5 demonstrates that the germination does not significantly change until the drying air temperature exceeds 60°C, except at a moisture of 35%w.b.. Fig. 4.6 shows

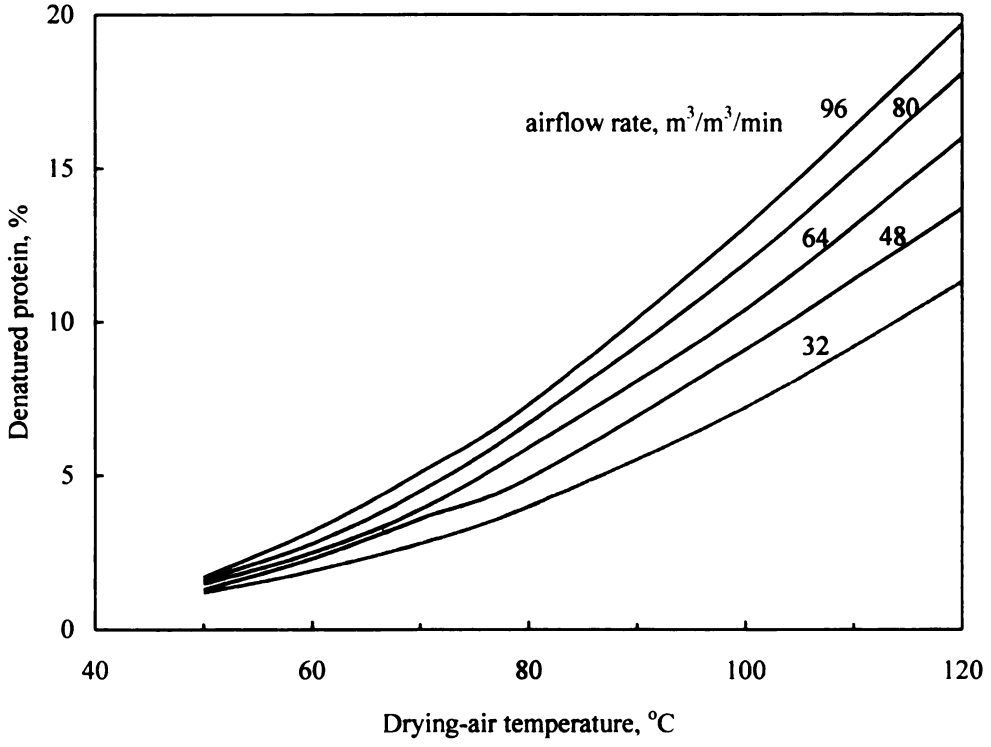

Fig. 4.2 Denatured protein vs. drying air temperature in maize dried in a crossflow dryer with an initial moisture content of 20% w. b. at airflow rates of 32, 48, 64, 80 and 96 $m^3m^{-3}min^{-1}$.

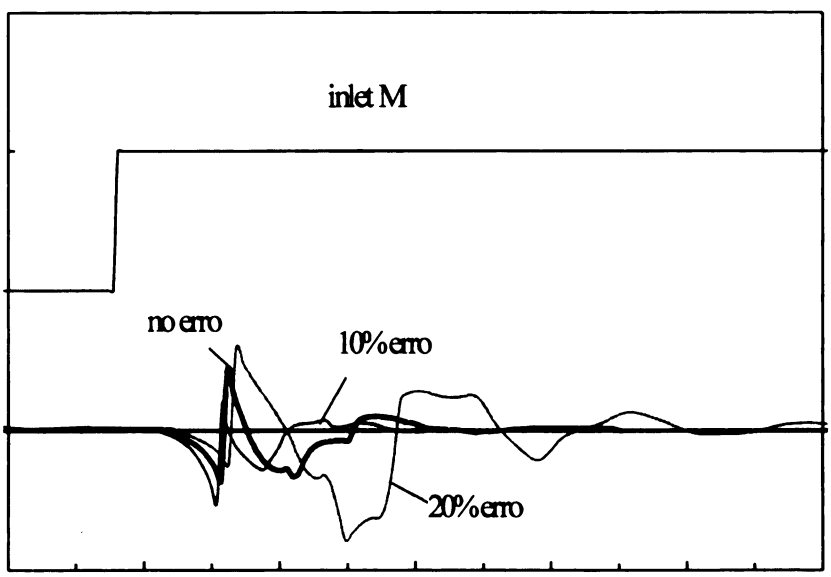

Fig. 4.3 Denatured protein vs. airflow rate in maize dried in a crossflow dryer with an initial moisture content of 20% w.b. and at drying air temperatures of 50, 60, 70, 80, 100 and 120°C.

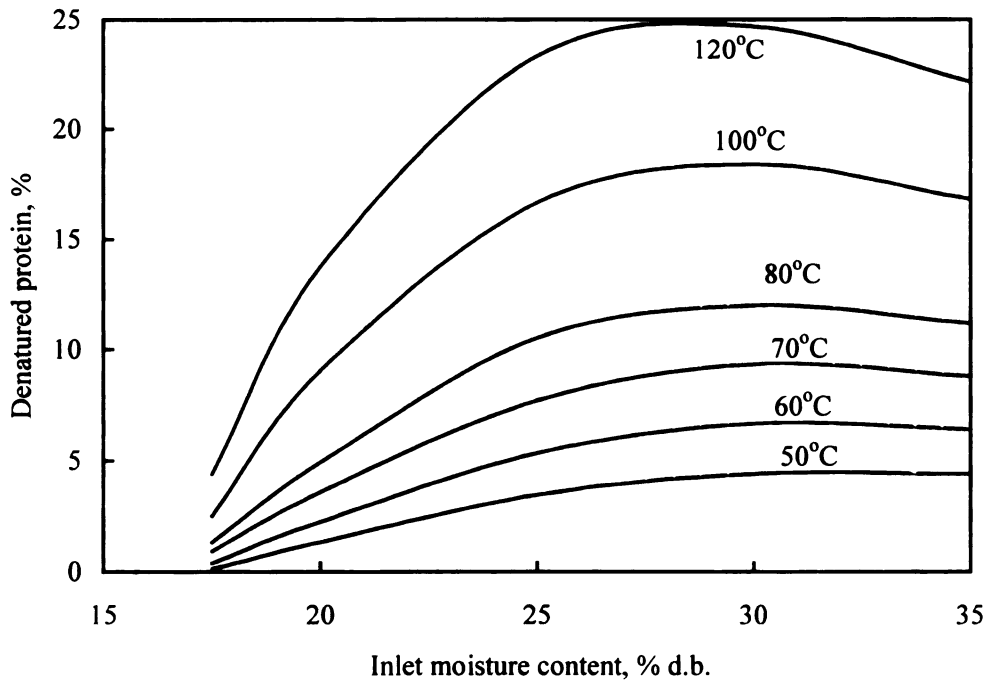

Fig. 4.4 Denatured protein vs. inlet moisture content in maize dried in a crossflow dryer at an airflow rate of 48 $m^3m^{-3}min^{-1}$ and at drying air temperatures of 50, 60, 70, 80, 100 and 120°C.

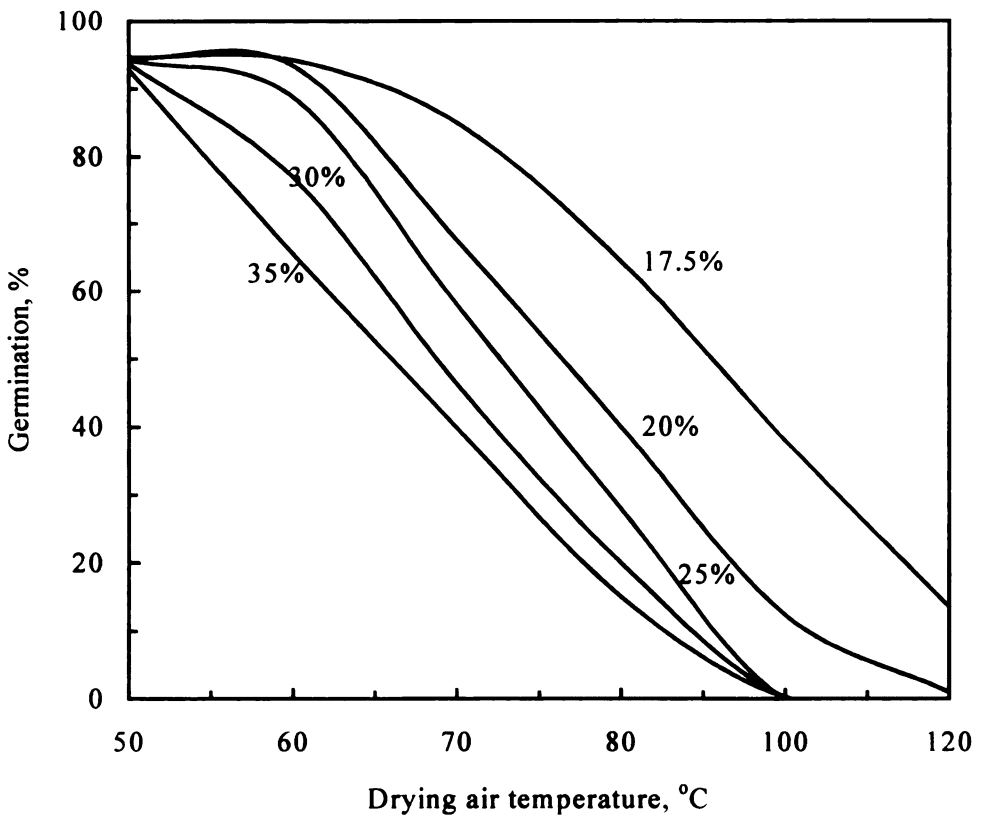

Fig. 4.5 Germination vs. drying air temperature in maize dried in a crossflow dryer at an airflow rate of 48 $m^3m^{-3}min^{-1}$ and with inlet moisture contents of 17.5, 20, 25, 30 and 35%w.b..

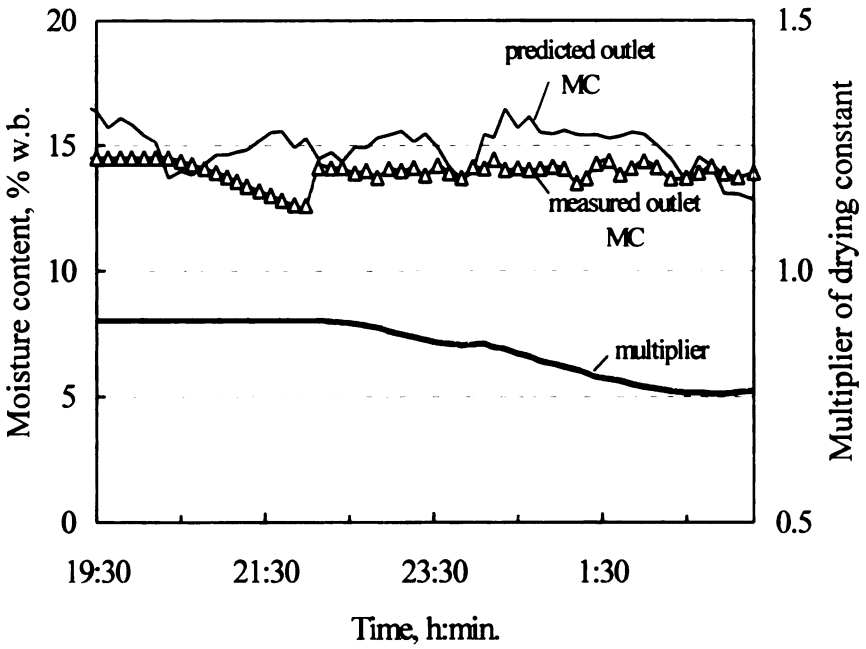

Fig. 4.6 Germination vs. airflow rate in maize dried in a crossflow dryer with an initial moisture content of 20% and at drying air temperatures of 50, 60, 70, 80, 100 and 120°C.

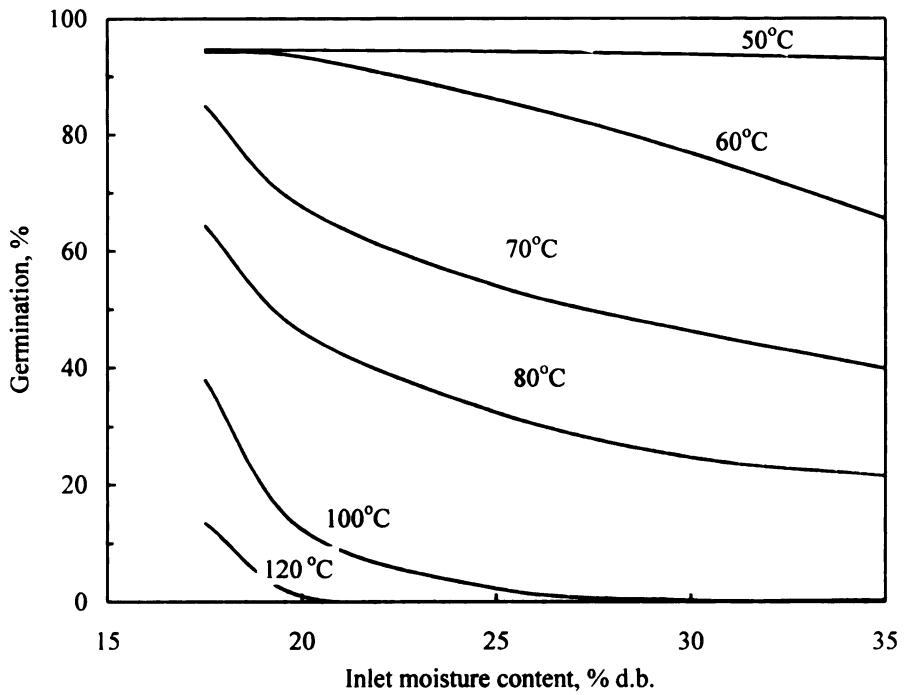

Fig. 4.7 Germination vs. inlet moisture content in maize dried in a crossflow dryer at an airflow rate of 48 $m^3m^{-3}min^{-1}$ and at drying air temperatures of 50, 60, 70, 80, 100 and 120°C.

that the airflow rate does not affect the germination significantly below 70°C. Higher initial moisture contents result in higher germination losses (Fig. 4.7).

Inverting the airflow or grain column at the midpoint along the drying column has been advocated as a means of alleviating the overdrying and underdrying of grain in a crossflow dryer, thus improving the grain quality. Table 4.5 compares the predicted final denatured protein and germination percentage with and without airflow inversion in a crossflow dryer. The denatured protein percentage is decreased slightly if the air flow is inverted, but additional germination damage occurs. This can be explained by considering Fig. 4.1; the germination of the maize at the air-inlet side of the column rapidly drops to zero. Inverting of the airflow causes the germination of the other side of the column to approach zero also. At a drying air temperature of 60°C, there is no significant difference in the quality of maize dried with and without an inversion.

Table 4.6 shows the effect of the standard deviation (SD) of the inlet moisture content on the final maize germination. The germination decreases slightly when the SD increases. No difference is found in the denatured protein percentage when the SD changes from 0 to 4% w.b..

Conclusions

(1) The changes in the denatured protein content and in the germination of maize after crossflow drying were successfully simulated by combining thin-layer drying-quality models with the MSU stochastic grain-drying model. Validation of the simulation models is satisfactory.

(1) The quality of maize dried at a wide range of crossflow-drying conditions was analyzed. The germination decreases rapidly when the drying air temperature exceeds 60°C. The denatured protein percentage increases almost linearly with the drying air temperature. Inverting the airflow midway through the drying process decreases the denatured protein percentage slightly, but increases the germination loss.

Table 4.5 Maize quality after crossflow drying with and without air inversion at the midpoint along the drying column with an airflow rate of 60 cfm/bu (48 $m^3m^{-3}min^{-1}$).

Inlet M. C., %	Airflow	Drying air temp., °C			Drying air temp., °C		
		60	70	80	60	70	80
		Denatured protein, %			Germination, %		
20	without inv.	2.5	4.1	6.0	93.5	78.4	63.8
20	with inv.	2.3	3.6	4.9	93.4	66.4	46.1
25	without inv.	5.7	8.5	11.5	89.5	69.4	52.3
25	With inv.	5.3	7.7	10.5	88.8	58	32.4

Table 4.6 Effect of the standard deviation (SD) of the inlet moisture content of maize on the final germination after crossflow drying (with an airflow rate of 60 cfm/bu or 48 $m^3m^{-3}min^{-1}$).

Air temp., °C	SD, % w.b.			
	0	2	3	4
	Germination, %			
60	93.4	93.4	93.4	93.1
70	67.6	67.4	66.7	65.9
80	46.2	45.7	44.6	42.8

References

Beke, J., A. Vas, A. Mujumdar.1993. Impact of process parameters on the nutritional value of convectively dried grains. Drying Technology 11(6):1415-1428.

Brekke, O. L., E. L. Griffin, Jr., G. C. Shove. 1993. Drying milling of corn artificially dried at various temperatures. Transactions of the ASAE 16 (4) :761-765.

Brooker, D. B., F. W. Bakker-Arkema, C. W. Hall. 1992. Drying and Storage of Grains and Oilseeds. Van Nostrand Reinhold, New York, NY.

Brown, R. B., G. N. Fulford, T. B. Daynard, A. G. Meiering, L. Otten. 1979. Effect of drying method on grain corn quality. Cereal Chemistry 56:529-532.

Bruce, D. M. 1992. A model of the effect of heated-air drying on the bread baking quality of wheat. J. of Agric. Eng. Res. 52:53-76.

Chang, C. H., M. R. Paulsen. 1989. Moisture distribution and starch recovery of commercially dried corn. Paper No. 89-6525. ASAE, St. Joseph, MI.

Courtois, F., A. Lebert, A. Duquenoy, J. C. Lasseran, J.J. Bimbenet. 1991. Modeling of drying in order to improve processing quality of maize. Drying Technology 9(4):927-945.

Emam, A., R. Stroshine, J. Tuite. 1981. Evaluating drying rate and grain quality parameters of corn inbreds/hybrids: methodology. Paper No. 81-3522. ASAE, St. Joseph, MI.

Freeman, J. E. 1973. Quality factors affecting the value of corn for wet milling. Transactions of the ASAE 16:671-678, 682.

Gustafson, R, R. V. Morey. 1981. Moisture and quality variations across the column of a crossflow grain dryer. Transactions of the ASAE 24(6):1621-1625.

Kirleis, A. W., R. L. Stroshine. 1990. Effects of hardness and drying air temperature on breakage susceptibility and dry-milling characteristics of yellow dent corn. Cereal Chemistry 67 (6):523-528.

Lasseran, J. C., A. Le Bras. 1988. Improvement of drying techniques to better grain quality for processing industries. Paper No. 88-323. Presented at the International Conference on Agricultural Engineering, Ag Eng 88, Paris, France. March 2-5, 1988.

Le Bras, A.1982. Maize drying and its resulting quality for wet-milling industry. In: Maize: Recent Progres in Chemistry and Technology. Academic Press, Inc., New York, NY.

Lescano, C. L., D. E.,Tyrrell. 1987. Change in viability of corn during high-temperature drying. Drying Technology 5(4):497-510.

Lowell, D. H. 1996. Quality of U. S. Agricultural Products. CAST Report, West Lincoln, LA.

MacMasters, M. M., M. D. Finkner, M. M. Holzaptel, J. H. Ranser, G. H. Dungan. 1959. Study of the effect of drying condition upon the composition and suitability for the wet milling of artificial dried corn. Cereal Chemistry 36(3):247-260.

Mourad, M., M. Hemati, C. Laguerie. 1996. Kinetic study and modeling of the degradation of the maize kernels quality during drying in fluidized bed. Drying Technology 14(10):2307-2337.

Nellist, M. E. 1981. Predicting the viability of seeds dried with heated air. Seed Science and Technology 9:439-455.

Peplinski, A. J., M. R. Paulsen, R. A. Anderson, W. F. Kwolek. 1989. Physical, chemical, and dry-milling characteristics of corn hybrids from various genotypes. Cereal Chemistry 66(2):117-120.

Peplinski, A. J., J. W. Paulis, J A. Bietz, R. C. Pratt. 1994. Drying of high-moisture corn: change in properties and physical quality. Cereal Chemistry 71(2):129-133.

Weller, C. L., M. P. Paulsen, M. P. Steinberg. 1987. Viability, harvest moisture and drying air temperature effects on quality factors affecting corn wet milling. Paper No. 87-6046. Am. Soc. Agric. Eng., St. Joseph, MI.

Weller, C. L., M. P. Paulsen, M. P. Steinberg. 1988. Correlation of starch recovery with assorted quality factors of four corn hybrids. Cereal Chemistry 65(5):392-397.

Wicher, W R. 1961. Problems of the dry corn processor. Paper presented at the January 10, 1961 meeting of the Midwest Section of the American Association of Cereal Chemists, Chicago, Illinois.

Zhang, Q., J. B. Litchfield. 1991. Corn quality distribution within a continuous crossflow dryer. Transactions of the ASAE 36(6) :2516-2520.

Zhang, Q., J. B. Litchfield, J. Bentsman. 1992. Fuzzy prediction of maize breakage. Journal of Agricultural Engineering Research 52:77-90.

CHAPTER 5. DISTRIBUTED-PARAMETER PROCESS MODEL FOR GRAIN DRYING

Abstract

A process model is essential for the design of a control system. General-purpose simulation models can not be directly used in a controller because of the large computation requirement. A lump-parameter process model is simple, but has several limitations in representing the grain-drying process. A distributed-parameter process model of crossflow drying is developed in this Chapter. The model is more flexible and accurate than a lumped-parameter model, and is of adequate simplicity for use in a dryer-control system.

5.1 Introduction

The moisture content of grain at harvest varies randomly. A variation of 3-5 % w.b. in the moisture content of maize entering a dryer is common. The discharge rate of a grain dryer (i.e. the retention time of grain in the dryer) is controlled manually or automatically in order for the outlet grain moisture content of the dryer to reach the set-point. Automatic control should outperform manual control, and result in better grain quality, higher energy efficiency and less manpower.

The grain drying process is difficult to control because of its non-linearity and long delay. Much research has been conducted on the development of automatic controllers but only few are in use on commercial dryers. There still exists a need to improve the quality of control on grain dryers, especially with respect to the robustness of the controller (i.e. working successfully over a wide range of operating conditions).

Grain quality is rapidly becoming of greater importance to the grain market. High-temperature grain drying is a main factor in degrading the grain quality (Le Bras, 1982). In practice, the drying-air temperature is determined by rule-of -thumb, and is seldom changed during dryer operation. The quality of dried grain is uncertain since it fluctuates with residence time of grain in the dryer. With the advancement in grain quality modeling, it is possible to establish the optimum drying-air temperature based on the quality requirement of the dried grain (Liu et al., 1997).

Automatic quality control is a promising method to alleviate grain-quality damage during drying. However, quality control requires frequent change of the drying-air temperature, thereby introducing an extra disturbance to the controller. The moisture

controller must be robust to any change in the drying-air temperature to be able to control a dryer adequately.

The main objective of this series of three Chapters is to design a model-predictive moisture controller for crossflow grain dryers. Special attention is paid to the robustness of the controller, and its ability to work in concert with a grain-quality controller. A distributed-parameter grain drying model is developed in this Chapter, the control algorithm in Chapter 6, and the results of field tests of the controller in Chapter 6.

5.2 Review of Grain Drying Models

A process model is indispensable for process control. The dynamic characteristics of a system can be explored with a process model, and subsequently the proper control strategy can be selected. A process model is also essential in the design of the control parameters, and in the preliminary testing and fine-tuning of a controller.

A number of general-purpose grain-drying models have been developed (Cenkowski et al., 1993; Parry, 1985; Sharp, 1982); the authors' main objectives were to optimize dryer design. The best known general-purpose grain drying models are probably the Michigan State University (MSU) (Bakker-Arkema et al., 1974) and the Thompson (Thompson, 1968) models. The MSU model is based on the fundamental laws of simultaneous heat and mass transfer, and results in four partial differential equations (p.d.e.); it has been successfully used for the simulation of high-temperature grain dryers, i.e. crossflow, concurrent-flow and counter-flow grain dryers (Brooker et al., 1992). The Thompson model consists of a set of integral heat and mass balance equations and an empirical thin-layer drying equation. Because of the assumption of temperature

equilibrium between the grain and air, the Thompson model is more suitable for low-temperature drying simulation. The general-purpose grain drying models have most recently been reviewed by Cenkowski et al. (1993).

The general-purpose drying models are rarely used directly in dryer control because of the computation requirements. However, they are employed for developing process models for drying.

Process models for grain drying can be categorized into: (1) lumped-parameter (LP) models, and (2) distributed-parameter (DP) models. Lumped-parameter models relate the outlet moisture content of the dryer to the inlet moisture content and the drying time; the other factors, i.e. the drying air temperature, airflow rate, dryer dimensions and ambient conditions are lumped into one or two coefficients, and are quantified by computer simulation, field testing or on-line estimation (Moreira et al., 1990). A LP model can be linear (Holtman and Zachariah, 1969; Eltigani, 1987), exponential (Forbes et al., 1984; Marchant, 1985; Whitfield, 1988a) or non-linear (Olesen, 1987). LP models do not predict the moisture profile in the dryer.

Due to their simplicity, LP models are currently employed in some commercial grain-dryer controllers (see Chapter 6). However, LP models have disadvantages: (1) LP models are not self-contained (i.e. the values of the lumped parameters have to be determined, and thus it is inconvenient to transfer a LP control model from one dryer model to another); (2) LP models simplify a spatially-distributed process to a lumped point, and thus do not represent the characteristics of the process very precisely, especially not of a drying process with variable drying-air temperatures and airflow rates;

and, (3) LP models can not predict the spatial distribution of the moisture content of grain in the dryer (note: knowledge which is necessary for grain quality).

Only Gui et al. (1988) used a distributed-parameter model to minimize overdrying and/or underdrying and to optimize grain quality. The model is based on the p.d.e. model but was not validated.

The objective of this Chapter is to develop a control-oriented, distributed-parameter (c.o.d.) grain drying model for crossflow dryers.

5.3 Model Development

5.3.1 Elemental drying models (EDM)

In a crossflow dryer, drying-air traverses the grain column perpendicular to the downward flow of the grain. The grain column can be viewed as a stack of rectangular elements (Fig. 5.1). The thickness (Δx) of the elements is the same as the thickness of the grain column, but the height (Δy) is so small that the differences of the air temperature and humidity in the y direction are assumed to be negligible. The element drying model (EDM) describes the drying process within one element; it can be extended to model the full-size crossflow dryer.

(1) Assumptions and preliminaries

Assume the dryer is operated under standard environmental conditions, i.e. at ambient temperature of 20°C and humidity ratio of 0.0087 kg kg^{-1} (i.e. 60%). Further assume that the air is heated by direct combustion of natural gas or liquefied petroleum,

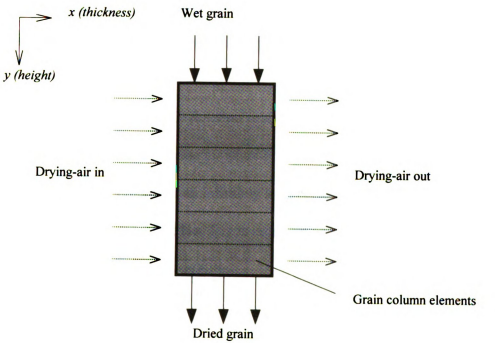

Fig. 5.1 Schematic of crossflow drying.

and reaches a humidity ratio of 0.0125 kg kg^{-1}, regardless of the temperature increase of the air.

When the drying-air passes through the grain column, the air temperature decreases and humidity increases, following the process curve 1-2 shown on the psychrometric chart in Fig. 5.2. If the energy used for the heating of the grain is negligible, the curve lies on the iso-enthalpy line (i.e. 1-2') and the process is defined as an ideal process. The drying process is assumed to be ideal in this Chapter.

(2) Equilibrium moisture content (EMC) function in an ideal drying process

The EMC of grain is defined as the moisture content after the grain has been exposed to a particular environment for an infinitely long period of time. For maize the EMC can be described by the modified Henderson equation (ASAE, 1991a):

$$M_e = [\frac{\ln(1 - RH)}{-A(T + B)}]^{\frac{1}{C}} \tag{5.1}$$

where M_e = EMC, % d.b.

T = drying-air temperature, °C

RH = relative humidity, decimal

A=8.6541x10^{-5}, B=1.8634 and C=49.81 for maize.

In the ideal drying process 1-2' illustrated in Fig. 5.2, the drying-air temperature and humidity change from the inlet status at point 1 to the outlet status at point 2', as does the EMC of the grain. If the drying-air temperature in the ideal drying process is known, the humidity of the air can be determined on the psychrometric chart or by the use

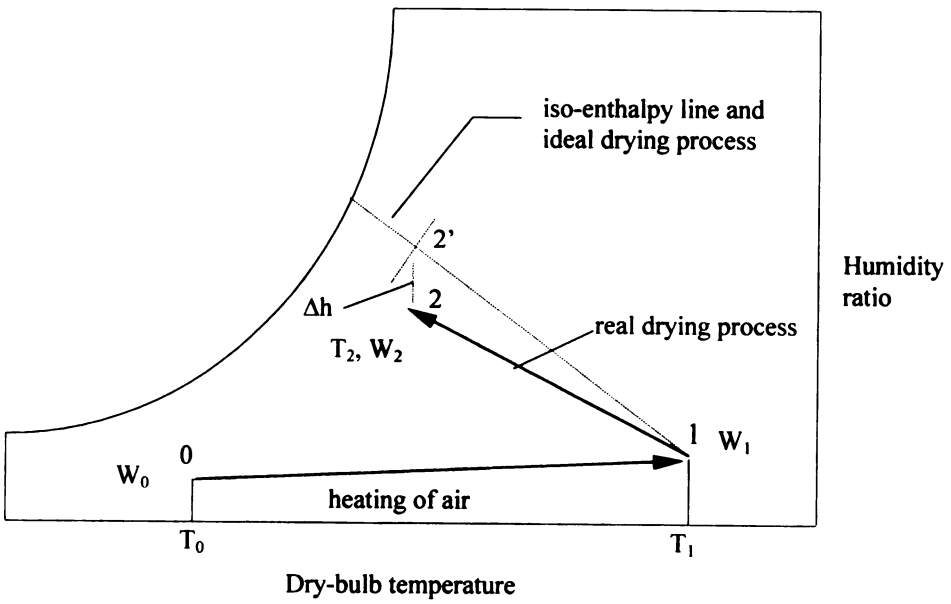

Fig. 5.2 Drying processes on a psychrometric chart.

of a psychrometric model (ASAE, 1991b). Therefore, the EMC in the drying process can be expressed as a single-variable function of the drying-air temperature.

The following procedure was used to obtain the EMC for an ideal drying process at an inlet drying-air temperature of T_I and inlet humidity ratio of 0.0125 kg kg^{-1}. First, starting from point 1 determined by the inlet drying-air temperature and humidity ratio, move along the ideal drying process line, and find the corresponding humidity values at several points. Second, use Eq. 5.1 to determine the EMCs at those points.

The empirical EMC function of the drying-air temperature in the ideal drying process, obtained by regression analysis, has the form:

$$M_e = e^{a+b/T_R} \tag{5.2}$$

where M_e = EMC, % d.b.

T_R= drying-air temperature, (1.8*(T+273.16)), °R

T = drying-air temperature, °C

a, b =coefficients

Empirical equations of the form of Eq. 5.2 were obtained for maize for nine inlet drying-air temperatures ranging from 40 to120°C. The correlation coefficients R are all higher than 0.99. The values for maize of a and b as functions of the inlet air temperature (T_1) were found to be:

$$\begin{aligned} a &= -20.39 + 0.075T_1 \\ b &= 12522.27 - 37.32T_1 \end{aligned} \tag{5.3}$$

Note that Eq. 5.2 is valid for determining the EMC along the ideal drying process line originating at the dry-bulb temperature range of 40-120°C, and for the absolute humidity of 0.0125 kg kg^{-1}.

(3) Derivation of the elemental drying models

The thin-layer drying rate of grain can be described by the following empirical equation (Brooker et al., 1992):

$$\frac{dM}{d\tau} = -k(M - M_e) \tag{5.4}$$

where M = grain moisture content, dec., d.b.

M_e = EMC, dec., d.b.

τ = drying time, h

k = drying constant, h^{-1}

The drying constant (k) is a function of the drying-air temperature, the EMC of the temperature and the humidity. As the drying-air traverses a grain column, its temperature and humidity change, and therefore, the drying rate and EMC of the grain also change across the grain column. In control problems, only the average moisture content across the column is of concern. By integrating Eq. 5.4 across the grain column, the average drying rate is obtained:

$$\frac{d\overline{M}}{d\tau} = \frac{1}{H}\int_0^H -k(\overline{M} - M_e)dx \tag{5.5}$$

where

$\overline{M} = \frac{1}{H}\int_0^H Mdx$, the average moisture content across the grain column, dec., d.b.

H = thickness of the grain column, m

Note that the grain moisture content M in the integrand is substituted by $\overline{M}$, the average moisture content across the grain column, in order to simplify the model. Physically, this can be interpreted as the grain being uniformly mixed in the x-direction of the column.

The drying constant k is a function of the drying-air conditions (Pabis and Handerson, 1961):

$$k = ce^{-r/T_R} \tag{5.6}$$

where for maize $c = 1941$, $r = 5032$.

An energy balance between the air and grain in a differential volume ($dx\ dy\ 1$) gives:

$$c_a G_a (1 \cdot dy) dT = h_{fg} G_g (1 \cdot dx) d\overline{M} \tag{5.7}$$

where

dT = air temperature increment in the differential volume, °C

$d\overline{M}$ = moisture content change of the grain in the differential volume, dec. d.b.

c_a = specific heat of dry air, J kg^{-1} $°C^{-1}$

G_a = dry airflow rate, kg h^{-1} m^{-2}

G_g = dry grainflow rate, kg dry product h^{-1} m^{-2}

h_{fg} = heat of moisture vaporization, J kg^{-1}

The left-hand side of Eq. 5.7 represents the energy transferred from the air to the grain, while the right-hand side is equal to the energy required to evaporate the moisture. [Note: the change of grain temperature is neglected.]

Solving Eq. 5.7 for $T=T_1$ at the air-inlet (i.e. x=0), yields:

$$\Delta T = \frac{h_{fg} G_g}{c_a G_a} \frac{d\overline{M}}{dy} x \tag{5.8}$$

where $\Delta T=T-T_1$.

The residence time $d\tau$ in a differential element with a height of dy is obtained from a mass balance. Thus:

$$d\tau = \frac{\rho_g}{G_g} dy \tag{5.9}$$

where ρ_g = grain density, kg (dry product) m^{-3}.

Substituting Eqs. 5.2, 6, 8 and 9 into Eq. 5.5, and integrating the right-hand side of Eq. 5.5 (see Appendix 5.1), results in the one-dimensional crossflow drying model which expresses the change in the average grain moisture content in the grain column (Eq. 5A.5).

If the average inlet moisture content of a bed element is $\overline{M}_i$, the height of the element is ΔY, the inlet air-temperature is T_{RI} and the EMC at air inlet is M_{e1},and assuming $\overline{M} - M_{e1} \approx \overline{M}_i - M_{e1}$ within the element, integrating of Eq. 5A.5 results in the following expression for the outlet moisture content ($\overline{M}_f$) of the element:

$$\overline{M}_f = \overline{M}_i - \frac{k_1(\overline{M}_i - M_{e1})\Delta Y}{G_g(1/\rho_g + k_1 c_1 q\overline{M}_i - k_1 c_2 q M_{e1})} \tag{5.10}$$

5.3.2 Full-size dryer model

(1) Drying model

Consider the grain column as a stack of elements (see Fig. 5.1). The outlet moisture content of the top element is found by applying the elemental drying model of Eq. 5.10 by setting $\overline{M}_i$ equal to the inlet moisture content of the dryer; the calculation is

repeated for the next element, using the outlet moisture content of the element above it as the inlet moisture content of the repeated element. After applying Eq. 5.10 to all the elements in the grain column, the spatial moisture distribution in the column is obtained. The model can also be applied to the cooling section (the overall moisture removal in the cooling section is minor (i.e. 0.5-0.8%)).

(2) Inverse drying model

Implementing a control action, an inverse drying model is needed to find the appropriate grain discharge rate such that the grain is dried to the set-point at the outlet of the dryer. If the moisture content of the grain is $\overline{M}_{yl}$ at a distance Y from the outlet of the drying section, the grain discharge rate (i.e. dryer capacity) for the grain to be dried to the set point (i.e. M_t) can be predicted by Eq. 5A.7 (see Appendix 5.1), or:

$$G_g = \frac{-k_1 \rho_g Y}{c_3 \ln \frac{\overline{M}_t - M_{el}}{\overline{M}_{yl} - M_{el}} + c_4 (\overline{M}_t - \overline{M}_{yl})} \tag{5.11}$$

5.4 Validation of the models

The Zimmerman VT1210 and VT4036 grain dryers manufactured by the ffi Co., Indianapolis, Indiana, were chosen as reference dryers. Both dryers are crossflow, cylindrically shaped dryers with grain turn-flow device midway in the drying sections. The specifications of the dryer are listed in Table 5.1

The outlet MC of both dryers was modeled using the c.o.d. model of Eq. 5.10,

Table 5.1 The specifications of the Zimmerman VT1210 and VT4036 dryers.

Dryer model	VT1210	VT4036
Overall height, m	17.07	22.89
Outside dryer diameter, m	3.56	5.18
Columns widths, m	0.32	0.32
Column cross-sectional area, m^2	3.25	4.89
Drying section		
length, m	8.76	17.22
airflow rate, m^3/h	97,222	291,134
Cooling section		
length, m	3.04	5.76
airflow rate, m^3/h	33,685	97,560
Drying-air temperature, °C	93.3	98.9
Rated capacity (at the outlet, moisture removal from 20% to 15%), kg/h	$27x10^3$	$90x10^3$

following the procedure described in section 5.3.2. The values of the physical property parameters for maize are: ρ_g = 560 (dry matter) $kg^{-1}m^3$, c_a = 1.007 kJ $kg^{-1}k^{-1}$, c_g = 2.17 kJ $kg^{-1}k^{-1}$ (Brooker et al. 1992). The heat loss due to the heating of the grain was accounted for in the calculations of the heat of vaporization, i.e.:

$$h_{fg} = 2427 + 2.17 \times 35/(M_i - 0.183) \text{ kJ kg}^{-1} \quad (5\text{-}12)$$

where the temperature increase of the grain in the drying section was assumed to be 35°C, with moisture removal from M_i to 0.183 kg kg^{-1} d.b. (i.e. 15.5% w.b.).

The moisture removal in the cooling section of the dryer was assumed to be 0.5%, and was not simulated. The ambient conditions were assumed to be 20°C, 60% relative humidity, with an initial grain temperature of 20°C.

Tables 5.2 and 3 show the c.o.d. model data and the values calculated with the p.d.e. grain drying simulation model. [Note: the thin-layer drying model of Li et al. (1984) was employed to predict the drying rate of maize in the p.d.e. model.]

Table 5.2 Predicted capacity of Zimmerman VT1210 maize dryer using the c.o.d. model and p.e.d. model.

Drying air temp., °C	85			95			105		
Inlet M.C., % w.b.	20	25	30	20	25	30	20	25	30
Capacity by c.o.d. model, 10^3 kg/h	22.69	11.96	8.32	26.87	14.53	10.07	32.27	17.33	11.99
Capacity by p.d.e. model, 10^3 kg/h	22.46	11.94	8.17	26.32	14.17	9.69	30.04	16.38	11.26
Relative difference, %	-1.6	1.7	1.8	2.1	2.5	3.9	7.4	5.8	6.3

Table 5.3 Predicted capacity of the Zimmerman VT4036 maize dryer using the c.o.d. model and p.d.e. model.

Drying air temp., °C	85			95			105		
Inlet M.C., % w.b.	20	25	30	20	25	30	20	25	30
Capacity by c.o.d. model, 10^3 kg/h	60.78	33.82	23.31	74.23	41.12	28.23	88.83	49.15	33.68
Capacity by p.d.e. model, 10^3 kg/h	67.43	35.99	24.72	76.16	42.84	29.34	91.55	49.87	34.04
Relative difference, %	-9.9	-6.0	-5.7	-2.5	-4.0	-3.8	-3.0	-1.4	-1.1

Table 5.2 shows that the c.o.d.-predicted capacities of the VT1210 dryer at 85 to105°C and inlet moisture contents from 20 to 25% w.b. are slightly higher than those predicted by p.d.e. model. The maximum difference is 7.4%. The results for the VT4036

are listed in Table 5.3; the maximum difference between the c.o.d. and p.d.e. calculated capacities is -9.9%.

5.5 Discussion and Conclusions

The agreement between the c.o.d. model and p.d.e. model is remarkable considering the fundamental difference between the two models. The c.o.d. model can be viewed as the averaging form of the p.d.e. model across the grain column, changing the two-dimensional p.d.e. model to an one-dimensional model. The reduction in complexity of the c.o.d. model is reflected in the number of Fortran-code lines required for the VT1210 dryer, i.e. 67 lines for the c.o.d. model and 1750 lines for the p.d.e. model.

The agreement between the results of the c.o.d. model and the p.d.e. model implies that although the c.o.d. model is simple, it represents the characteristics of the crossflow drying process well. The c.o.d. model retains the advantages of a general-purpose model, i.e. it is self-contained, provides spatial moisture information on the grain column, and is flexible for modeling various drying processes.

In conclusion, the c.o.d. drying model has adequate precision, simplicity and flexibility for implementation on a dryer controller.

Appendix 5A: One-dimensional Crossflow Drying Model

Substituting Eqs. 5.2 and 5.6 into Eq. 5.5 yields:

$$\frac{d\overline{M}}{d\tau} = \frac{1}{H}\int_0^H -(\overline{M}ce^{-r/T_R} - 0.01ce^{a-(r-b)/T_R})dx \qquad (5A.1)$$

The exponential terms in the integrand make it impossible to integrate analytically. Linear approximation of the exponential terms results in:

$$e^{-r/T_R} \approx e^{-r/T_{R1}}[1 + \frac{1-\exp(r/T_{R1} - r/618)}{T_{R1} - 618}\Delta T_R] \qquad (5A.2)$$

and

$$e^{-(r-b)/T_R} \approx e^{-(r-b)/T_{R1}}[1 + \frac{1-\exp[(r-b)/T_{R1} - (r-b)/618)]}{T_{R1} - 618}\Delta T_R] \qquad (5A.3)$$

where $\Delta T_R = T_R - T_{R1}$.

As shown in Fig. 5A.1, the linear approximation of Eq. 5A.2 is a line passing through two points on the curve of $exp(-r/T_R)$, namely at inlet air temperature T_{R1} (i.e. 100°C) and the intermittent temperature of 618°R (i.e. 70°C). A similar explanation can be given for Eq. 5A.3.

Substituting Eqs. 5A.2 and 5A.3 into 5A.1 yields:

$$\frac{d\overline{M}}{dt} = \frac{1}{H}\int_0^H -[k_1\overline{M}e^{-r/T_{R1}}(1 + c_1\Delta T_R) - k_1 M_{e1}(1 + c_2\Delta T_R)]dx \qquad (5A.4)$$

From Eqs. 5.8, 9, and since $\Delta T_R = 1.8\ \Delta T$, integration of Eq. 5A.4 across the grain column yields the one-dimensional crossflow drying model:

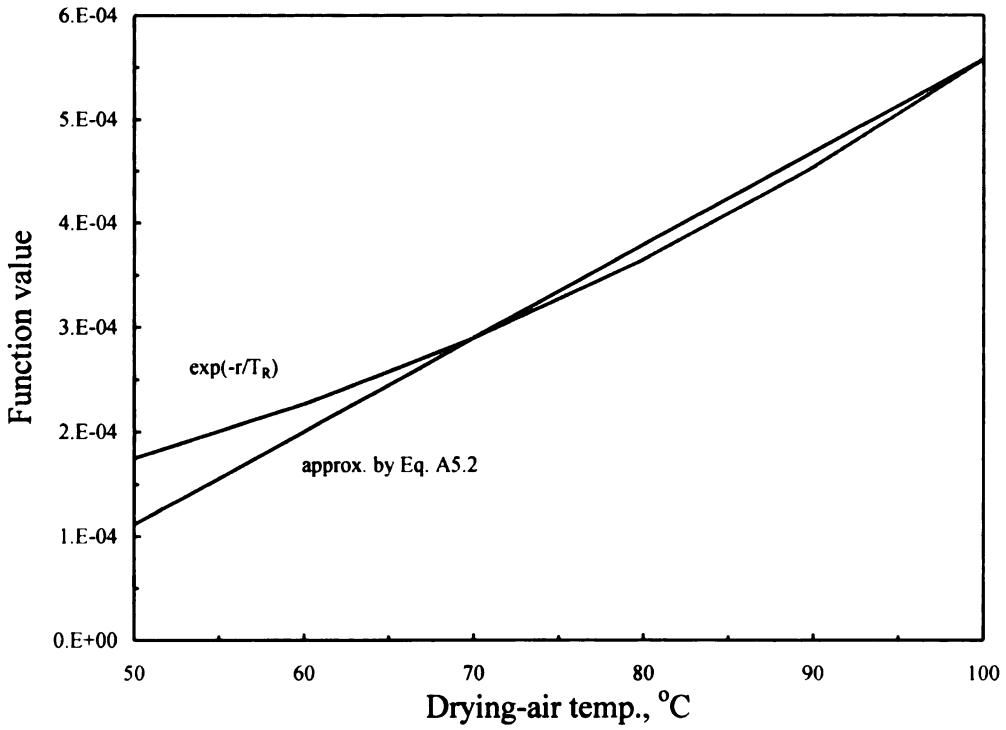

Fig. 5A.1 Linear approximation of Eq. 5A.2 at inlet drying-air temperature of 100°C (or 672°R).

$$G_g\left(\frac{1}{\rho_g} - k_1 c_1 q\overline{M} + k_1 c_2 q M_{e1}\right)\frac{d\overline{M}}{dy} = -k_1(\overline{M} - M_{e1}) \tag{5A.5}$$

where

$$c_1 = \frac{1 - \exp(r / T_{R1} - r / 618)}{T_{R1} - 618}$$

$$c_2 = \frac{1 - \exp[(r-b) / T_{R1} - (r-b) / 618)}{T_{R1} - 618}$$

$$q = \frac{h_{fg}(0.9H)}{c_a G_a}$$

$$k_1 = ce^{-r/T_{R1}}$$

$$M_{e1} = 0.01e^{a+b/T_{R1}}$$

If the height of a drying section in a dryer is Y, the solution of Eq. 5A.5 for the drying section is:

$$c_3 \ln\left(\frac{\overline{M}_f - \overline{M}_{e1}}{\overline{M}_i - \overline{M}_{e1}}\right) + c_4(\overline{M}_f - \overline{M}_i) = -k_1\frac{\rho_g Y}{G_g} = -k_1\tau \tag{5A.6}$$

or

$$G_g = \frac{-k_1\rho_g Y}{c_3 \ln\left(\frac{\overline{M}_f - \overline{M}_{e1}}{\overline{M}_i - \overline{M}_{e1}}\right) + c_4(\overline{M}_f - \overline{M}_i)} \tag{5A.7}$$

where

$$c_3 = 1 + k_1(c_1 - c_2)\rho_g q M_{e1}$$

$$c_4 = k_1 c_1 \rho_g q$$

Symbols

a, b = coefficients of Eq. 5.2, defined in Eq. 5.3
c = coefficient for drying constant in Eq. 5.6, 1941 for maize
c_1, c_2 = constants in Eq. 5A.5
c_1, c_2 = constants in Eq. 5A.7
c_a = specific heat of dry air, J kg^{-1} $°C^{-1}$
G = flow rate, kg (dry matter) h^{-1} m^{-2}
H = thickness of the grain column, m
h_{fg} = heat of vaporization, J kg^{-1}
k = drying constant, h^{-1}
k_1 = drying constant at air inlet, h^{-1}
M = grain moisture content, dec., d.b.
$\overline{M}$ = average grain moisture content across the grain column, dec., d.b.
M_e = EMC, dec., d.b.
M_{e1} = EMC at air inlet, dec., d.b.
q = constant in Eq. 5A.5
r = coefficient for drying constant in Eq. 5.6, 5032 for maize
RH = relative humidity, decimal
T = drying-air temperature, °C
T_1 = inlet air temperature, °C
T_R = drying-air temperature, °R
T_{R1} = inlet air temperature, °R
x, y = coordinates, m
Y = height of the drying section, m
ΔY = height of the grain element, m
τ = drying time, h
ρ_g = grain density, kg (dry product) m^{-3}

Subscripts:
1 = air inlet
a = air
e = equilibrium
f = final, outlet
g = grain
i,o = initial
R = temperature, °R
t = target value

Abbreviations

c.o.d. = control-oriented distributed-parameter

DP = distributed parameter

EMC = equilibrium moisture content

LP = lumped parameter

p.d.e. = partial differential equation

References

ASAE Standards, 38th Ed. 1991a. D245.4-Moisture relations of grains. Am. Soc. Agr. Eng., St. Joseph, MI.

ASAE Standards, 38th Ed. 1991b. D271.2-Psychrometric Data. Am. Soc. Agr. Eng., St. Joseph, MI.

Bakker-Arkema, F.W., L. E. Lerew, S. F. DeBoer, M. G. Roth. 1974. Grain drying simulation. Research report 224. Agr. Exp. Sta., Michigan State University, East Lansing, MI.

Brooker, D. B., F. W. Bakker-Arkema, C. W. Hall. 1992. Drying and Storage of Grains and Oilseeds. Van Nostrand Reinhold, New York, NY.

Cenkowski S., D. S. Jayas, S. Pabis. 1993. Deep-bed grain Drying - A review of particular theories. Drying Technology 11(7):1553-1581.

Eltigani, A. Y. 1987. Automatic control of commercial crossflow grain dryers. Ph. D. Dissertation, Michigan State University, E. Lansing, MI.

Forbes, J. F., B. A. Jacobson, E. Rhodes, G. R. Sullivan. 1984. Model based control strategies for commercial grain drying systems. Canadian Journal of Chemical Engineering 62:773-779.

Gui, X. Q., J. Bentsman, J. B. Litchfield. 1988. Control of grain drying: State of the art and open problems. ASAE Paper No. 88-3502. Am. Soc. Agr. Eng., St. Joseph, MI.

Holtman, R. D., G. L. Zachariah. 1969. Computer control for grain dryers. Transactions of the ASAE 12:433-437.

Le Bras, A.1982. Maize drying and its resulting quality for wet-milling industry. In: Maize: Recent Progressing Chemistry and Technology, ed. by G. E. Inglett. Academic Press, Inc., New York, NY.

Li, H. Z., R. V. Morey. 1984. Thin-layer drying of yellow dent corn. Transactions of the ASAE 27(2):581-585.

Liu, Q., F. W. Bakker-Arkema. 1997. Stochastic modelling and control of grain quality in crossflow dryers. ASAE Paper No. 97-6030. Am. Soc. Agr. Eng., St. Joseph, MI.

Marchant, J. A. 1985. Control of high temperature continuous flow grain dryers. Agricultural Engineer 40(4):145-149.

Moreira, R. G., F. W. Bakker-Arkema. 1990. A feedforward/feedback adaptive controller for commercial cross-flow grain dryers. J. agric. Eng. Res.: 107-116.

Olesen, H. T. 1987. Controlling drying percentage. Chapter 3, Appendix E, in *Grain Drying.* Innovation Development Engineering APS, Thisted, Denmark.

Pabis, S., Henderson S. M. 1961 Grain drying theory: II. A critical analysis of the drying curve of shelled maize. J. agric. Eng. Res. 6:272-277.

Parry, J. C. 1985. Mathematical modeling and computer simulation of heat and mass transfer in agricultural grain drying: a review. J. agric. Eng. Res. 32(1):1-29.

Sharp, J. R. 1982. A review of low temperature drying simulation models. J. agric. Eng. Res. 27(3):169-190.

Thompson, T. L., R. M. Peart, G. H. Foster. 1968. Mathematical simulation of corn drying - A new model. Transactions of the ASAE 11(4):582-586.

Whitfield R D. 1986. An unsteady-state simulation to study the control of concurrent and counter-flow dryers. J. agric. Eng. Res. 32:171-178.

Whitfield R. D. 1988a. Control of a mixed-flow drier. Part 1: Design of the control algorithm. J. agric. Eng. Res. 41:275-287.

Whitfield R. D. 1988b. Control of a mixed-flow drier. Part 2: Test of the control algorithm. J. agric. Eng. Res. 41:289-299.

CHAPTER 6: DESIGN OF CONTROL ALGORITHM

Abstract

The grain drying process features non-linearity, long delays and large disturbances. Model-based control can successful at controlling processes with those features. In this Chapter, a model-predictive control system is developed for crossflow drying of maize. The control system has a feedforward loop (i.e. the predictive model and the optimizer for the control actions) and an indirect feedback loop (i.e. the parameter estimator and modifier). Two algorithms are proposed for the optimizer. Simulation tests show that the controller performs well over a wide range of drying conditions, and with disturbances from the inlet moisture content of the grain, the drying-air temperature and the sensors.

6.1 Introduction

The fundamental requirements of a grain dryer controller are no different from those of other control systems, i.e.: *stable*-the system must not oscillate wildly; *accurate* - the output moisture content must be close to the desired value; and, *robust* - it must perform successfully over a wide range of conditions.

A special strategy has to be found to meet the above requirements because grain drying is unique: (1) the drying process takes hours, the output of the process (i.e. the moisture content and quality of the grain at the outlet of the dryer) is determined collectively by the control actions taken during the drying process; (2) the major disturbance (i.e. variation in the inlet grain moisture content) enters the system at the inlet of the dryer, its effect will not be detected at the outlet of the dryer until the grain exits the dryer; and (3) the drying process is subject to disturbances from ambient conditions, and from the possible change in genotype and physical properties of the grain.

For a sophisticated process such as grain drying, only a control algorithm which addresses the dynamic characteristics of the process has a chance for success. The control-oriented, distributed-parameter (c.o.d.) model developed in Chapter 5 is able to provide this type of information of the system to the controller.

In this Chapter, a model-predictive control algorithm for crossflow grain dryer is developed. The performance of the controller is extensively investigated using simulation. Special attention is paid to the robustness of the controller and its ability to work in concert with a grain-quality controller.

6.2 Process Characteristics and Review of the Control Strategies

In continuous-flow dryers, grain loses most of the moisture when moving through the drying section; and is usually cooled in the cooling section by ambient air before leaving the dryer. The moisture content of grain entering a dryer may vary with time, and thus the required retention time in the dryer changes. *It is impossible to control the dryer such that all of the grain is dried to the set point*; when grain with a high initial moisture is dried to the set point, the grain with a lower initial moisture content has probably been overdried. The objective of a moisture controller is to minimize the deviation of the outlet grain moisture content from the set point. Although under-/over-drying is inevitable, it is desirable to have the same amount of grain overdried as underdried.

The residence time of grain in a high-temperature dryer ranges from one half hour to several hours, depending on the initial grain moisture content and on the dryer parameters. As the moisture removal in the cooling section is small, the retention of grain in the cooling section is considered as the dead-time of the process. The response of the system to a control action (i.e. a change in grain discharge rate or drying-air temperature) will not be observed at the outlet of the dryer until one dead-time later; the transition period will continue as long as the grain presently in the dryer has not been replaced. Thus, the outlet grain moisture content is dependent upon the accumulated effects of the control actions during the retention of the grain in the dryer.

The relationship between the controlled variable (i.e. the grain moisture content decrease in the dryer) and the manipulated variable (i.e. the grain discharge rate and/or the drying-air temperature) is non-linear. The non-linearity stems from the fact that grain dries faster in the high moisture range than in the low moisture range.

The long time delay and non-linearity make the grain drying process difficult to control. The time delay severely limits the performance of conventional feedback control systems (Perry, 1997; Shinskey, 1994).

Marchant (1985) examined classical proportional and integral (PI) feedback control of continuous-flow grain dryers and showed that the stability and response speed of the controller are unacceptable. Whitfield (1986) tested PI control on concurrent-flow dryers by simulation and concluded that the control parameters require tuning for different inlet moisture contents because of the non-linearity of the system; by linearnizing the system, the stability of the control was much improved, but the response remained slow.

To speed up the response, McFarlane et al (1991) added a first-order lag feedforward term to the Whitfield controller. The peak error in the outlet MC of a mixed-flow dryer was approximately half of that occurring with the feedback-only control system. The oscillating behavior of the original feedback controller was prevented by varying the sampling period in inverse proportion to the discharge rate. The resulting dependency on the drying-air temperature required changing the controller gain to compensate for the temperature changes.

Bruce et al. (1993) improved the McFarlane control system performance for step changes in the drying-air temperature. Both feedforward and feedback gains were expressed as functions of temperature in order to adjust the discharge rate of the grain whenever a change occurred in the drying air temperature. The control strategy during the start-up period of grain dryer was also addressed. The procedure of applying the Bruce

algorithm to dryers other than for which the control algorithm was designed, was described.

Platt et al. (1992) studied a feedforward-feedback control for crossflow dryers. The feedforward control was based on a mass balance on the water vapor in the air. The PI with scheduled gain control was used for feedback. The disadvantage of this control type is that the absolute humidity values of the inlet and outlet drying air have to be measured intermittently.

Courtois (1995) investigated various control strategies theoretically and experimentally for a mixed-flow dryer, with an inlet moisture content of maize as high as 45% w.b., and residence time as long as 2-5 hours. Classical PID controllers showed poor stability. The non-linear PI feedforward plus feedback control performed best.

Zhang (1993) implemented fuzzy control on a laboratory grain dryer with the objective of both controlling the outlet moisture content and the breakage susceptibility of the maize through manipulation of the drying-air temperature and the discharge-auger rpm. He concluded that fuzzy logic control may be superior to conventional control for controlling grain quality.

Model-based control (MBC) has been a significant development in process control in last two decades. It is especially effective for deadtime-dominant and nonlinear processes. Forbes et al. (1984) and Eltigani et al. (1989) developed model-based controllers for grain dryers. In both, the control action is based upon a process model and the so-called "pseudo" inlet grain moisture content. A model parameter is updated on-line according to the difference between the predicted and measured outlet moisture contents. This type of process model intrinsically compensates for the space time (i.e. in the drying

section) and pure dead-time (i.e. in the cooling section) provided the residence time of the grain in the dryer is accurately estimated. Forbes et al. (1984) established that the model-based controller is superior to three other control algorithms investigated.

The current control algorithms used in commercial grain-dryer controllers can be classified as: (1) feedforward plus feedback (FF/FB) (McFarlane, 1991; Oleson, 1987), and (2) model-based control (MBC) (Forbes et al.,1984, Eltigani et al. 1989). Both types have feedforward and feedback loops, and require an inlet and an outlet moisture sensors.

The following conclusions can be drawn from the literature review: (1) classical feedback control is not adequate to control the grain-drying process; (2) an inlet moisture sensor and a feedforward loop are necessary for adequate response of the controller; and, (3) the MBC and FF/FB algorithms are effective in controlling the grain moisture of commercial dryers.

Lumped-parameter drying models are employed in the control algorithms reviewed above. However, the limitations of lumped-parameter models (see Chapter 5) negatively affect their performance. With the successful development of the c.o.d. (control-oriented and distributed-parameter) process model in Chapter 5, new control algorithms should be investigated. This is done in this Chapter.

6.3 Model-predictive Control Strategy

Model-predictive control or MPC was first employed in the oil refinery industry in the late seventies. Since then successful commercial applications have been reported in a variety of industrial processes (Bosley et al., 1991; Perry, 1997). A comprehensive survey

of the history and theoretical derivation of model-based predictive control methods can be found in Camacho et al. (1995) and Garcia et al (1989).

In MPC, a dynamic model of the process is used to predict the outputs over the next *n* sampling periods (prediction horizons); an optimizer is employed to determine the control action. The optimization is repeated each sampling period with up-to-data information about the process. The main advantages of MPC are: (1) the control strategy is especially suitable for processes with long-delay times or dead-times, and for non-linear systems, or for systems with inequality constraints; (2) the performance is optimized by an on-line optimizer; and (3) the process model and control strategy can be updated on-line to compensate for changes in the process conditions or constraints. Thus, MPC is a perfect candidate for grain dryer control. The disadvantage of MPC is the large computation requirements for process modeling and control optimization (this is hardly relevant anymore since the microprocessor costs are rapidly decreasing).

The concept of MPC for grain dryers is shown on Fig. 6.1. The "Drying Model", "Inverse Drying Model" and "Optimizer" form a feedforward loop. The inlet grain moisture content and the drying-air temperature are measured for each sampling time; the moisture distribution in the dryer, including at the outlet of the dryer, is predicted by the "Drying Model". Based on this information, the "Inverse Drying Model" predicts the necessary flowrate for the grain currently in the dryer. The actual grain discharge rate for control of the dryer during a sampling period is the optimized rate, taking into account the flowrate of each bed, thereby minimizing the control error during the prediction horizon.

The "Parameter Estimator and Modifier" constitutes an indirect feedback loop; the outlet moisture content predicted by the "Drying Model" is compared with the moisture

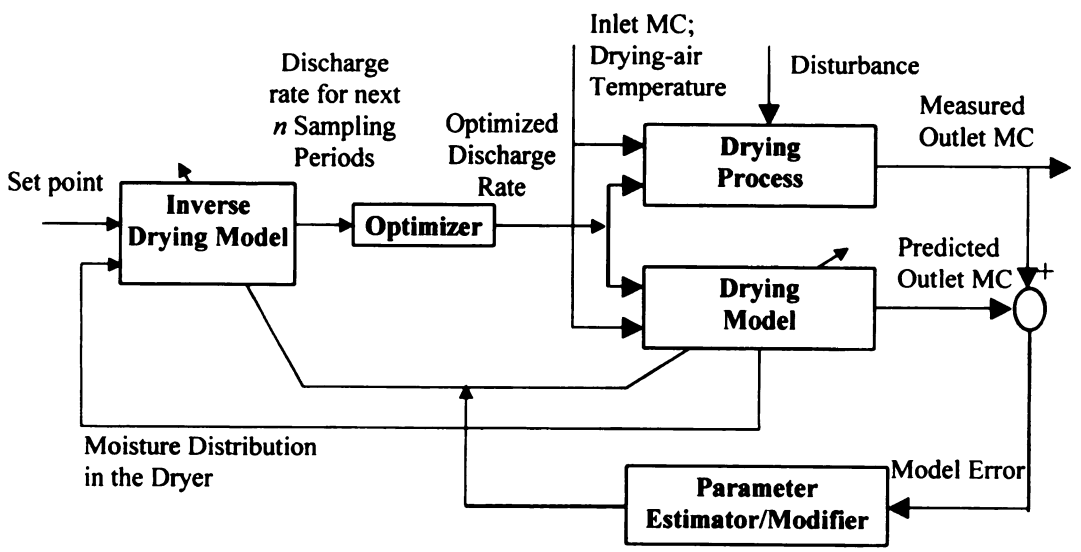

Fig. 6.1 Model-predictive control of grain dryers.

content to establish the model error; if not zero, the model parameters in the "Drying Model" and the "Inverse Drying Model" are adaptively modified by the "Parameter Estimator and Modifier" according to the size of the model error.

Each component of the controller is described in the following sections.

6.3.1 Feedforward loop

The grain column in a crossflow dryer is conceptually divided into stacked beds of identical dimensions. The sampling period equals the residence of the grain in a bed. It is supposed that there are *n* beds in the drying section and *m* beds in the cooling section.

(1) Drying model

Eq. 5.10 and the procedure described in section 5.3.2 in Chapter 5 are employed to predict the moisture distribution in the dryer during each sampling period. The inlet moisture content of the dryer (i.e. the inlet moisture content at the top of the bed) is measured by the moisture sensor, and its value is updated every sampling period. It is assumed that a total of 0.5% of moisture is removed in the *m* beds in the cooling section.

(2) Inverse Drying Model

Eq 5.11 in Chapter 5 is applied to calculate the discharge rate for each bed. M_{yi} is the inlet moisture content of bed *i*, and Y is the distance from the top of bed *i* to the end of the drying section.

(3) Optimizer

For each bed element, the calculated grain discharge rate is usually different. The grain discharge rate during the next sampling period is calculated by the "Optimizer". Two optimizing strategies were investigated: (a) zero average error (ZAE), and (b) least square error (LSE).

(a) Zero Average Error (ZAE)

The objective of the ZAE optimization is for the average control error during the next *n* sampling periods to be equal to zero, or the same amount of grain to be overdried and underdried.

If the inlet moisture content of grain in bed *i* is M_i, and the actual discharge rate of the dryer is *G* for the next *i* sampling periods, the final MC at the end of the drying section of the grain currently in bed *i* can be estimated by:

$$M_{fi} = M_i - \alpha \frac{\rho_g (i\Delta Y)}{G} \tag{6.1}$$

where

M_{fi} = final moisture content after *i* sampling periods of grain currently in bed *i*, where $i = 1,2, \ldots, n$ is the index of the bed numbered from the outlet to the inlet of the drying section, dec., d.b.

M_i = inlet moisture content of grain in bed *i*, dec., d.b.

ρ_g = grain density, kg (dry matter) m^{-3}

ΔY = height of one bed, m

$\rho_g (i\Delta Y) / G$ = time for grain moving down from bed *i* to the end of drying section, h

α = constant of the dryer depending upon dryer model and operating conditions, dec., d.b. h^{-1}

Given the target moisture content, M_t, the necessary discharge rate, G_i, i.e. the discharge rate for the grain currently in bed *i* (being dried to the target value at the end of the drying section) is defined by:

$$M_t = M_i - \alpha \frac{\rho_g (i\Delta Y)}{G_i} \tag{6.2}$$

If the actual discharge rate of the dryer G is not equal to the required discharge rate G_i during the next i sampling periods, the offset (error) of the final moisture content of the grain currently in bed i will be:

$$e_i = M_t - M_{fi} = \rho_g \alpha \Delta Y (\frac{i}{G_i} - \frac{i}{G}) \tag{6.3}$$

The actual error caused by using G instead of G_i for grain in bed *i* is one *i*th of e_i because G is applied for only one sampling period, and is updated every sampling period. The average error caused by using G during the next sampling period for the grain in all beds is:

$$e = \frac{1}{n}\sum_{i=1}^{n} e_i / i = \frac{\rho_g \alpha \Delta Y}{n}\sum_{i=1}^{n}(\frac{1}{G_i} - \frac{1}{G}) \tag{6.4}$$

By setting $e = 0$, the optimum grain flowrate is:

$$G = \frac{n}{\sum_{i=1}^{n} \frac{1}{G_i}} \tag{6.5}$$

(b) Least Square Error (LSE)

The average square error resulting by using G in the next sampling period for grain in all the beds is :

$$e = \frac{1}{n}\sum_{i=1}^{n}(e_i)^2 / i = \frac{(\rho_g \alpha \Delta Y)^2}{n}\sum_{i=1}^{n}\frac{1}{i}(\frac{i}{G_i} - \frac{i}{G})^2 \tag{6.6}$$

The grain flowrate G is optimized by minimizing e, or

$$\frac{de}{dG} = 0 \tag{6.7}$$

which yields:

$$G = \frac{\sum_{i=1}^{n} i}{\sum_{i=1}^{n} \frac{i}{G_i}} \tag{6.8}$$

Comparing Eqs 6.5 and 6.8, it is clear that the LSE algorithm assigns higher weights to the discharge rates of the grain beds closest to the inlet of the dryer (i.e. in sequence of $n, ..., i, i-1, ..., 1$ from inlet to outlet), whereas the ZAE algorithm assigns the same weight to each bed.

6.3.2 Feedback loop (Parameter Estimator/Modifier)

The model error is defined as the difference between the measured and the predicted outlet moisture contents of the dryer. If the model error is not equal to zero (which is most frequently the case), the drying constant k_1 in the drying model (Eqs. 5.10 or 5.11) is modified by multiplying by a multiplier γ , i.e.:

$$k_1^m = \gamma k_1 \tag{6-9}$$

where k_1^m = modified drying constant, h^{-1}

$k_1 = ce^{-r/T_{R1}}$, theoretical drying constant, h^{-1} (for maize c = 1941 and r = 5032, Pabis and Handerson, 1961)

T_{R1} = inlet air temperature, °R

γ = multiplier of the drying constant

If the initial moisture content of the grain at the inlet of the dryer is called M_i, the measured outlet moisture content M_f, and the total residence time of the grain in the drying section (not including the cooling section) τ, the estimated drying constant (see Eq. 5A.6 in Chapter 5) is:

$$k_1^e = \frac{-M_r}{(c_1 - c_2)\rho_g q M_{e1} M_r + c_1 \rho_g q (M_f - M_i) + \tau} \tag{6.10}$$

where

$$M_r = \ln \frac{M_f - M_{e1}}{M_i - M_{e1}}$$

$$c_1 = \frac{1 - \exp(r / T_{R1} - r / 618)}{T_{R1} - 618}$$

$$c_2 = \frac{1 - \exp[(r - b) / T_{R1} - (r - b) / 618)}{T_{R1} - 618}$$

$$q = \frac{h_{fg}(0.9H)}{c_a G_a}$$

$$k_1 = ce^{-r/T_{R1}}$$

$$M_{e1} = 0.01 e^{a + b/T_{R1}}$$

The average of the drying-air temperature during the residence of the grain in the drying section should be used in the calculation of the coefficients c_1, c_2 and M_{e1} in Eq. 6.10 if the drying-air temperature changes during that period.

The estimated multiplier γ is:

$$\gamma^e = \frac{k_1^e}{k_1} \tag{6.11}$$

The predicted multiplier is recursively modified by:

$$\gamma = \gamma' + \beta(\gamma^e - \gamma') \tag{6.12}$$

where γ = predicted multiplier for current sampling period

γ' = multiplier used in last sampling period

γ^e = estimated multiplier from Eq. 6.11

β = filter factor

The filter factor β is determined by tuning of the controller, and is discussed in the next section.

6.4 Simulation Tests and Tuning of the Controller

6.4.1 Virtual grain dryer and controller

A virtual grain dryer was programmed in LabVIEW (Johnson, 1997) based on the p.d.e. drying model. Fig. 6.2 shows the control panel of the virtual dryer. An arbitrary inlet grain moisture pattern can be introduced to the dryer at the MC_{in} entry. The drying-air temperature and the dryer capacity (i.e. grain discharge rate) can be controlled manually or by a controller. The inlet/outlet moisture contents and other controlled variables are traced and printed in real time. The virtual dryer was used as a test bench in the design of the controller.

Two control algorithms, i.e. ZAE and LSE, were implemented in LabVIEW to control a virtual Zimmerman VT1210 dryer. The VT1210 has been described in Chapter

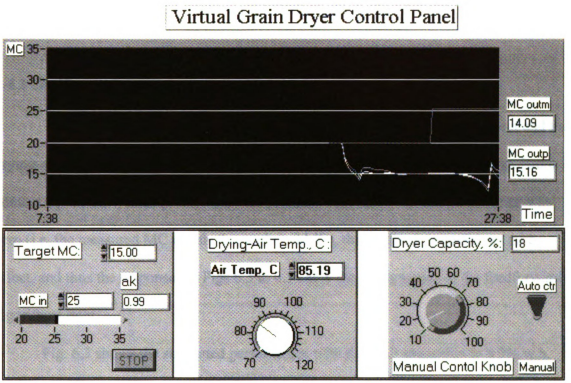

Fig. 6.2 Control panel of the virtual grain dryer for control test.

5; and its specifications are listed in Table 5.1.

To implement the control algorithms, the grain column in the dryer was conceptually divided into 20 identical beds, 12 in the drying section and 8 in the cooling section. The sampling time of the controller was set equal to the residence time of the grain in one bed, i.e. 5-10 min, depending on the discharge rate.

6.4.2 Feedforward control

The response of the controller to step changes in the inlet moisture content and the drying-air temperature was tested by simulation, assuming the measured outlet moisture content equaled the value predicted by the process model. Because the model error was zero (i.e. the measured MC equals the predicted MC), the feedback loop did not take effect, and thus the responses in Figs 6.3 to 6.5 show the performance of the feedforward algorithms only.

Fig. 6.3 shows the simulated performance with the ZAE algorithm to a 5% w.b. step change in the inlet grain moisture content. Responding to a step-up of the inlet moisture content, the outlet moisture content started to decrease after 8 sampling periods (i.e. the residence time of grain in the cooling section); when the step change effect reached the outlet of the dryer, the outlet moisture content responded with a step increase, changing from overdrying to underdrying; finally the outlet moisture content came back to the set point. The total transition period lasted approximately one residence time of the grain in the drying section. About the same amount of grain was overdried and underdried, i.e. the average control error is close to zero (which is the intention of the ZAE algorithm).

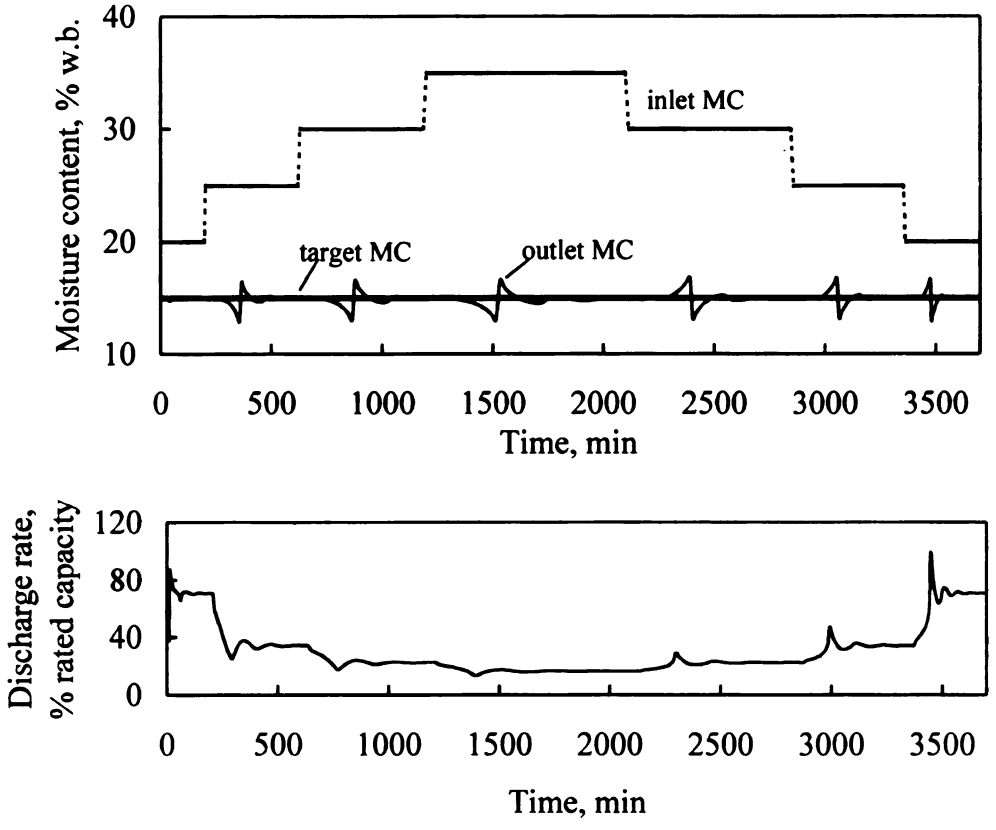

Fig. 6.3 Simulated response of the feedforward control to step changes in the inlet moisture content with ZAE optimization (drying-air temperature = 85 °C).

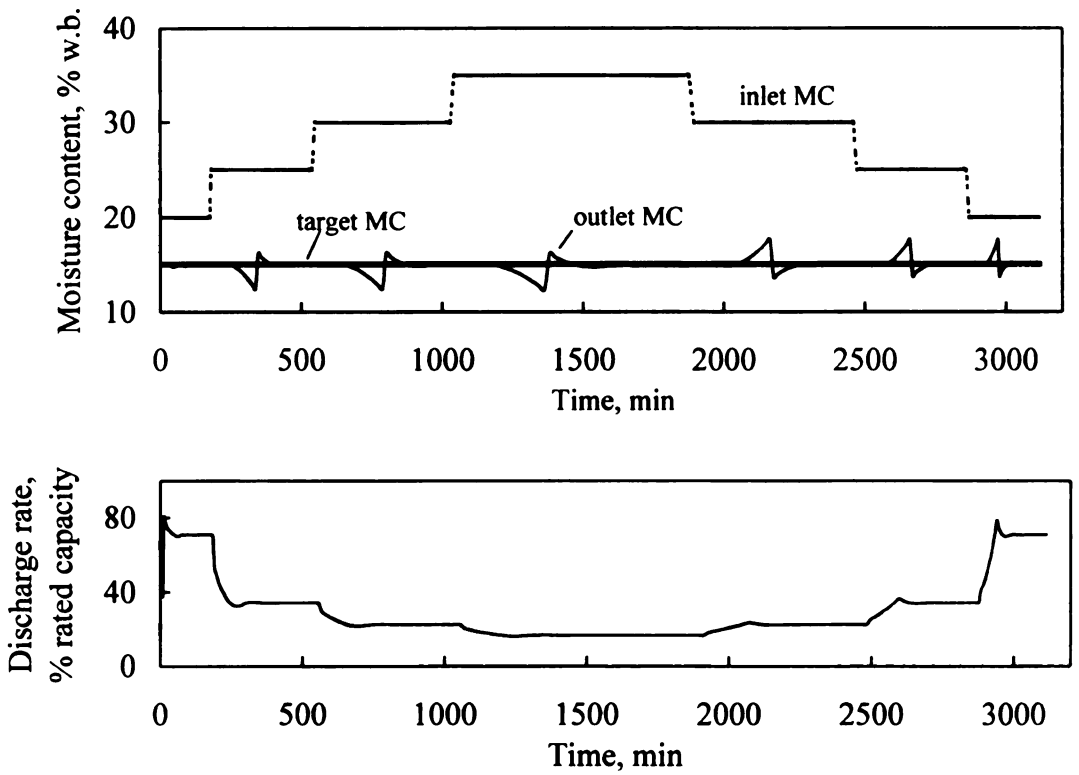

Fig. 6.4 Simulated response of the feedforward control to step changes in the inlet moisture content with LSE optimization (drying-air temperature = 85°C).

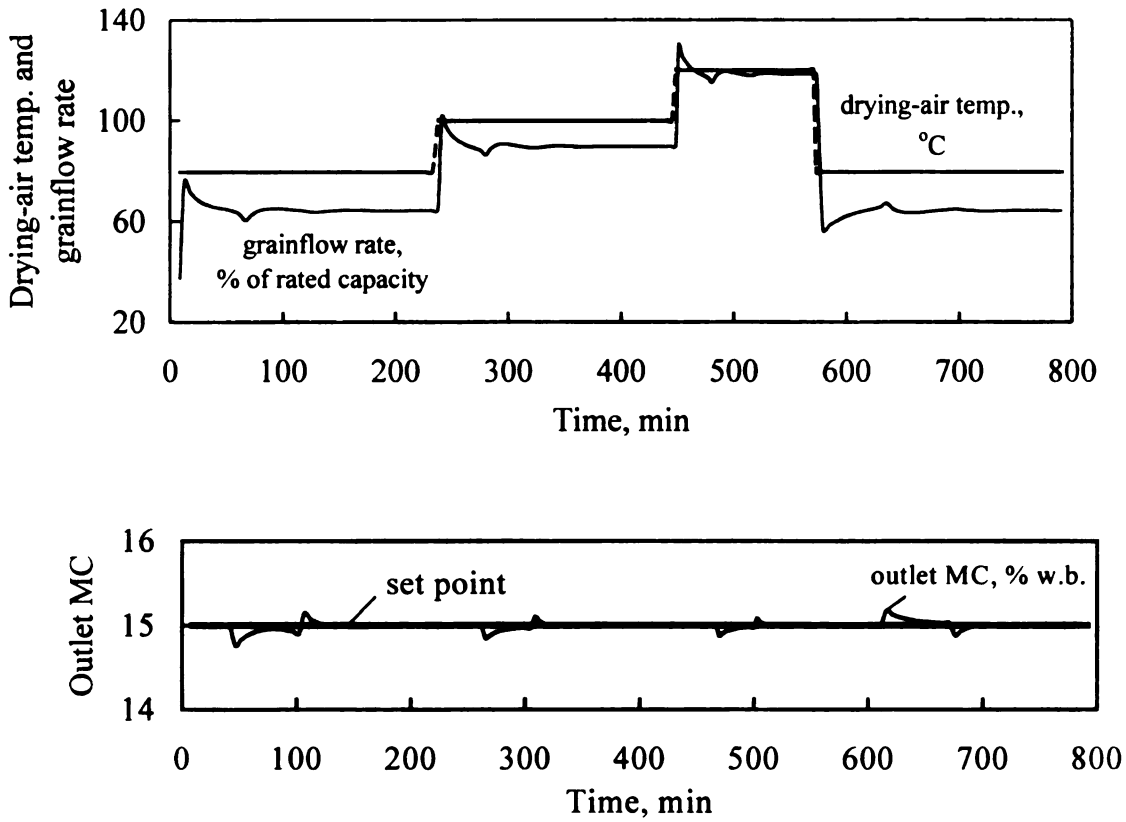

Fig. 6.5 Simulated response of the feedforward control to step changes in the drying-air temperature with ZAE optimization (inlet grain moisture content = 20% w.b.)

A similar (but flipped) response pattern was found for a step-down of the inlet moisture content. The moisture distribution during the transition periods was (again) symmetric around the set point.

No significant differences were found in the response patterns to the 5% step changes at different levels of the inlet moisture content, except that the transition periods lasted longer in the higher inlet moisture range than in the lower range because the residence times of the grain in the dryer were different. This implied that the controller performed well over a large range of inlet moisture contents.

The discharge rate (i.e. the manipulated variable) of the dryer is also shown in Fig. 6.3. At each step change in the inlet moisture content, a sharp response in the discharge rate occurred.

The response of the controller with LSE optimization to a step change in the inlet moisture content is illustrated in Fig. 6.4. Although the overall pattern is similar to that in Fig. 6.3, the following differences were found: (1) the response pattern of LSE algorithm is not as symmetric as that of the ZAE algorithm, i.e. more grain is overdried due to a step up in the inlet moisture content, and more is underdried due to a step down; (2) the curve of the outlet moisture content in Fig. 6.4 is straighter than in Fig. 6.3 (which curves in to the set point); the total area between the response curves and the line of the set point are smaller in Fig. 6.3 than in 6.4; and thus the ZAE controller is better than LSE type in terms of the control error; (3) the reaction of the control variable (i.e. the grain discharge rate) is smoother for the LSE algorithm than for the ZAE algorithm (which, however, is more favorable in practice because there will be less chance to reach the lower or upper limits of the unloading system).

Fig. 6.5 shows the response of ZAE optimization to step changes in the drying air temperature. There was an immediate response in the discharge rate to each step change in the drying temperature. The disturbance in the outlet moisture content is hardly noticeable (i.e. less than 0.3% w.b. offset to a 20°C step change in the drying-air temperature) in the temperature range of 80-120° C. This implies that the temperature compensation in the drying model was effective.

6.4.3 Feedback control

The p.d.e. drying model employed in the virtual dryer is different from the c.o.d. process model implemented in the controller (see Chapter 5). Fig. 6.6 compares the outlet moisture contents predicted by the p.d.e. model and the process model without parameter modification. The difference between the outlet moisture contents is the model error of the process model, i.e. -0.71% w.b. at the inlet moisture content of 20% w.b., -0.46% w.b. at 25% w.b. and 0.2% at 30%w.b..

The filter factor β (in Eq. 6.12) is found by controller tuning. Fig. 6.7 shows the responses of the system for filter factors (β) ranging from 0 to 1.0. When β was initially set to zero, the control error was 0.71%w.b. A value between 0-1 was assigned to β after 320 min of drying; the response of the outlet moisture content is shown in Fig. 6.7a, and of the multiplier in Fig. 6.7b. For small values of β the outlet moisture content slowly approached the set point without overshooting. A faster response occurred for β values larger than 0.1 (although some overshooting and oscillating occurred). The differences in rise time and overshoot did not change significantly for

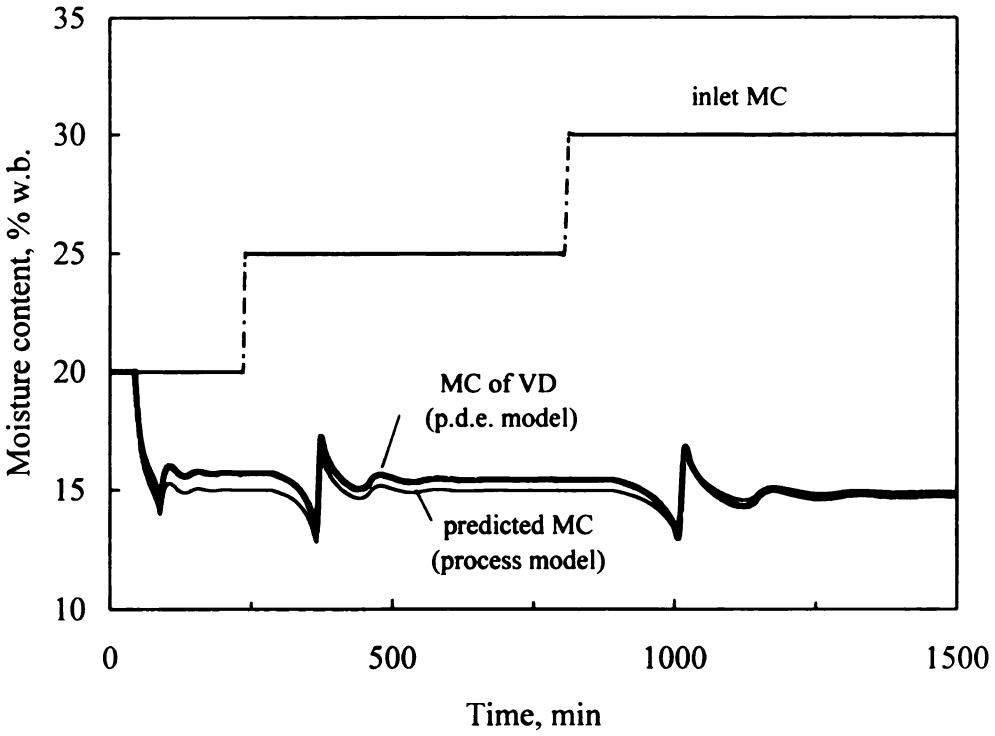

Fig. 6.6 Comparison of the outlet moisture contents output from the virtual dryer (VD) and predicted by the process model without parameter modification (drying-air temperature = 85°C).

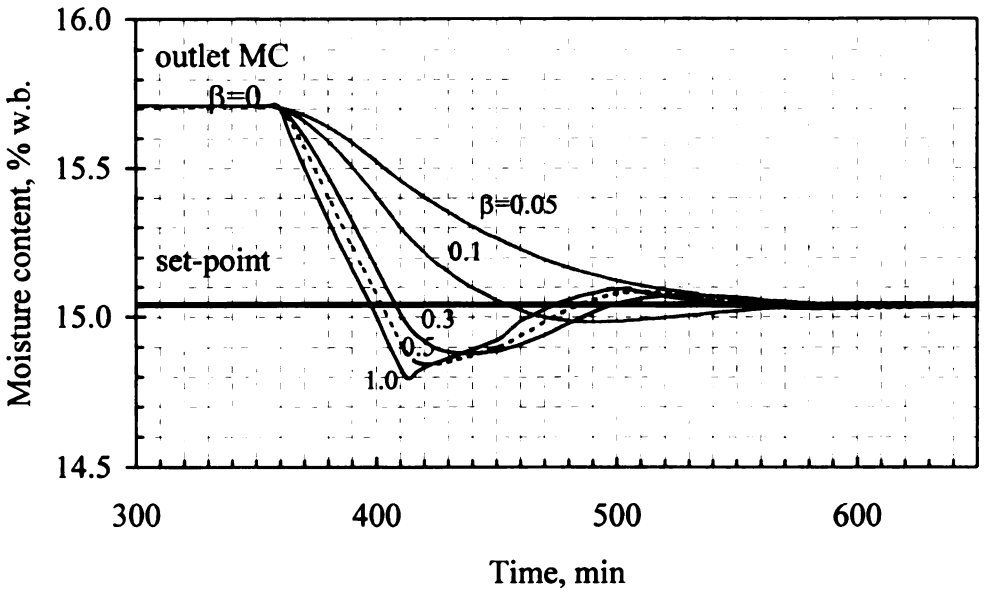

(a)

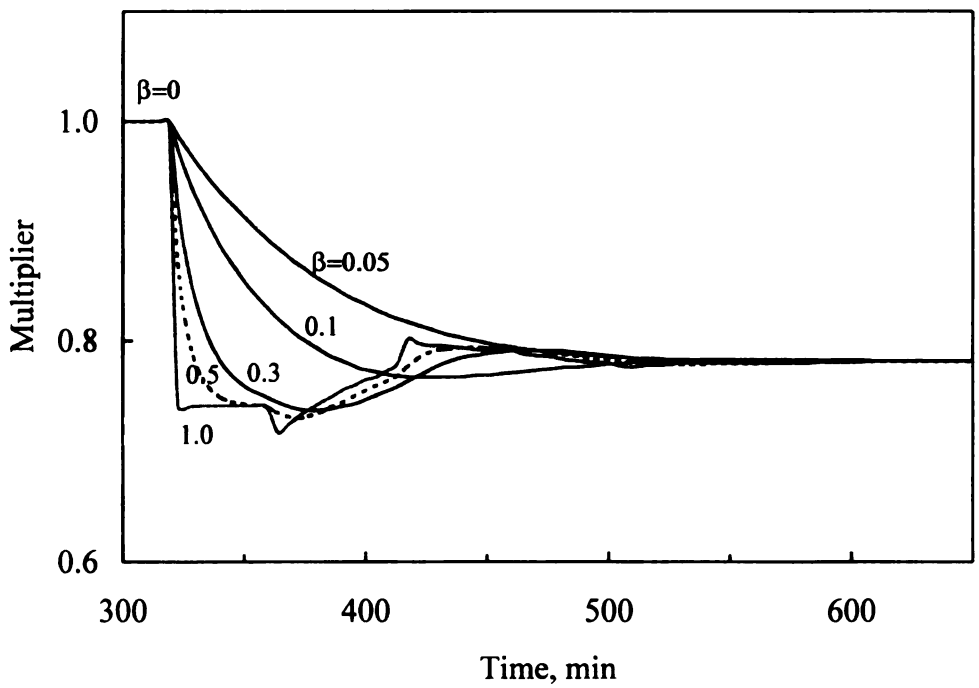

(b)

Fig. 6.7 Response of the system to parameter modification with different values of the filter factor (β): (a) outlet grain moisture content of the virtual dryer, (b) multiplier (γ) of the drying constant.

values of β in the 0.3 to1.0 range. Table 6.1 lists the rise time and percentage of overshoot of the moisture response at different β values.

Table 6.1 Response characteristics of the outlet moisture content to the modification of the drying constant for different values of the filter factor.

Filter factor β	0.05	0.1	0.3	0.5	1.0
Rise time, min	130	70	40	35	30
Overshoot, %	0	12	22	30	34

Choosing β is a compromise between rise time and overshoot. A range of 0.3-0.7 is recommended for the controller to achieve a fast response; this will result in 20-32% overshoot which is 0.4-0.7% w.b. offset from the set point (if the model error in MC is within 2% w.b.).

6.4.4 Robustness of the controller

A grain dryer operates over a wide range of the moisture contents and drying air temperatures. Besides, random disturbances occur in the ambient conditions and the sensor noise. Still, a controller should perform relatively uniformly over the full range of operating conditions, and should display adequate disturbance-rejection ability. Therefore, the robustness of the controller was tested on the virtual dryer by mimicing various drying conditions.

The conditions shown in Figs. 6.3 and 6.5 were rerun in Figs. 6.8 and 6.9, respectively, for the case that the model error was not zero and the feedback loop was on. The transition period of the outlet moisture content lasted longer in Fig. 6.8 than in 6.3, and the disturbance to the outlet moisture content from the drying-air temperature was

larger in Fig. 6.9 than in 6.5. The parameter modification for compensation of the model error took time and delayed the response of the controller.

Due to shrinkage of grain during the drying process, the residence time of the grain in a dryer can not be precisely estimated. A large error in the calculated residence time may cause wild oscillations of a system with a delay (Shinskey, 1994) because the predicted outlet moisture content is not of the grain currently at the outlet of the dryer. The mismatch causes a mistaken modification of the drying parameter. Fig. 6.10 shows the response of the system to a step increase in the inlet moisture content under different estimation errors of the grain residence time in the dryer. If the error is less than 10%, the response is not significantly effected; but at a 20% error, severe over-/under-drying and large oscillation occurs.

Decreasing the filter factor β can alleviate the effect of incorrectly estimating the residence time (see Fig. 6.11). When the residence-time error is 20%, decreasing β from 0.5 to 0.1 or less, results in a much improved response pattern. The trade-off is that it takes longer to compensate the model error with a smaller filter factor.

Both the moisture sensor and the drying-air temperature sensor may be inaccurate. To test the robustness of the controller regarding these sensors, a $\pm 2\%$ w.b. drift was introduced in the inlet moisture measurement (Fig. 6.12), and a $\pm 10^{o}C$ drift in the drying-air temperature (Fig. 6.13). The system was able to recover from the disturbances of both sensors with only short offsets in the outlet moisture content.

A grain dryer has a start-up period before reaching normal operation condition. At the first run of a dryer each drying season, all the grain in the dryer is initially wet. It takes

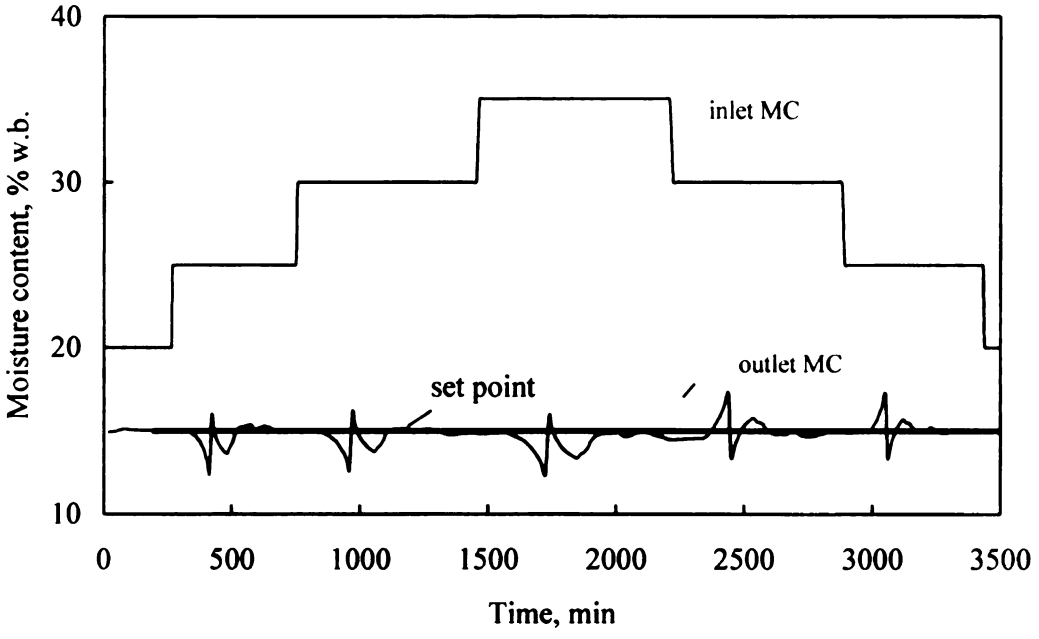

Fig. 6.8 Simulated response of the feedforward/feedback controller to step changes in the inlet moisture content with ZAE optimization (drying-air temperature = 85 °C, filter factor β=0.5).

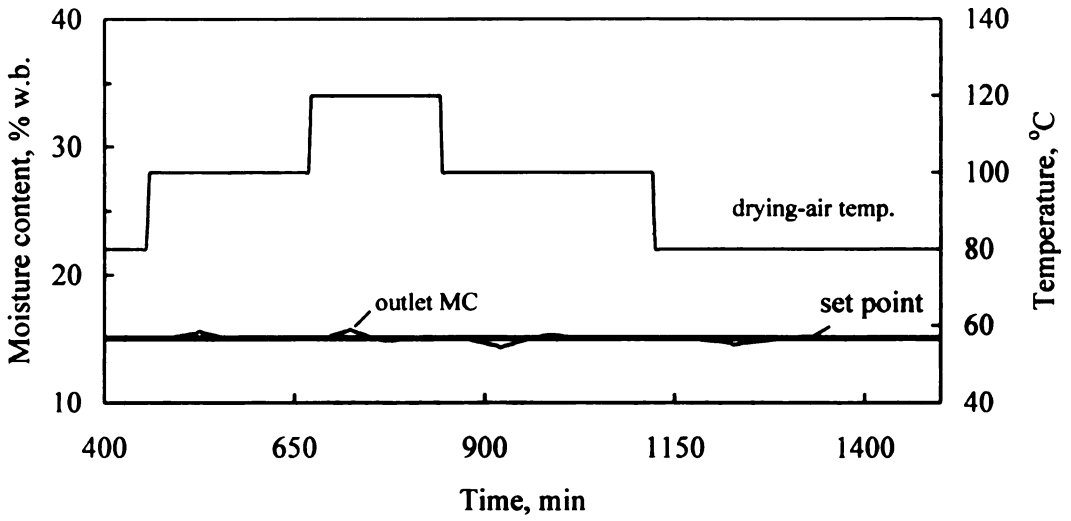

Fig. 6.9 Simulated response of the feedforward/feedback controller to step changes in the drying-air temperature with ZAE optimization (inlet grain moisture content = 20% w.b., filter factor β=0.5)

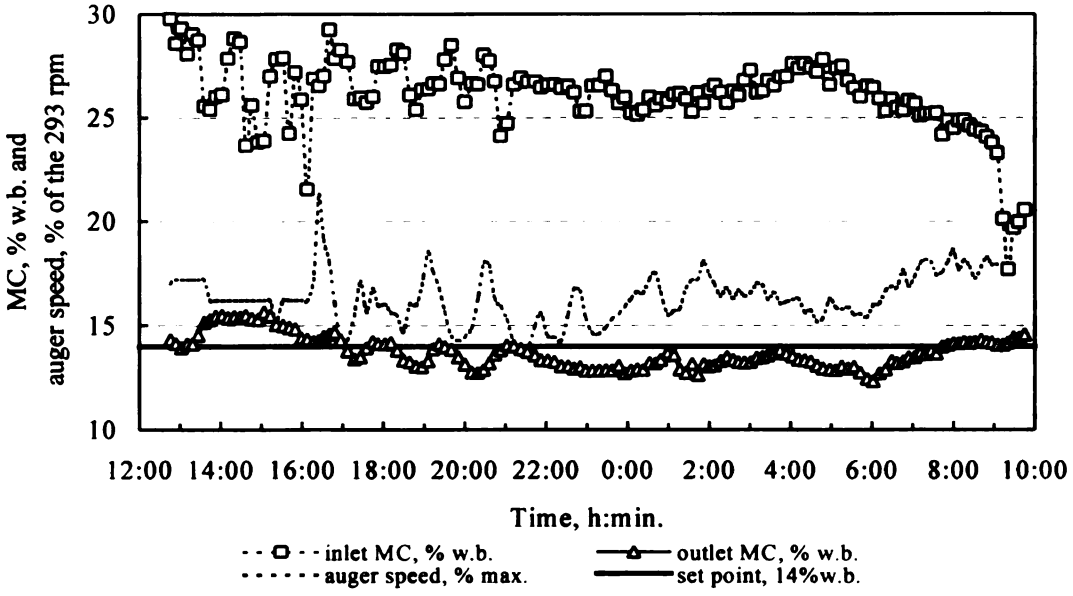

Fig. 6.10 Simulated control responses to a step change in the inlet moisture content at different estimation errors of the residence time of grain in the dryer (drying-air temperature = 85°C, filter factor β=0.5).

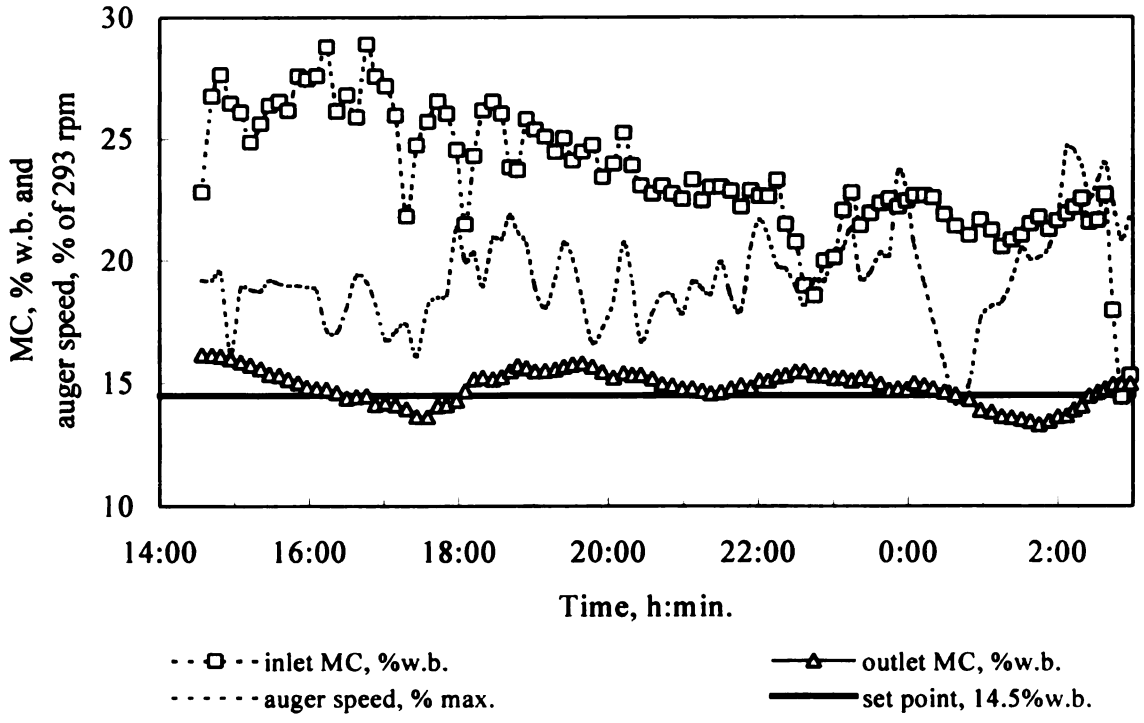

Fig. 6.11 Simulated control responses to a step change in the inlet moisture content at different values of the filter factor (β) (estimation error of residence time = 20%, drying-air temperature = 85°C).

some time before the dryer reaches normal conditions. Fig. 6.14 shows the performance of the controller during the start-up of the dryer. The moisture content of wet grain was assumed to be 20% and 25% w.b.. Initially, the outlet moisture content did not change; once the grain exited the drying section, the outlet moisture content of the dryer rapidly approached the set point. After some mild oscillations, the outlet moisture content stabilized at the set point.

To imitate the real situation in a dryer, a random inlet moisture pattern was generated and fed to the virtual dryer to test the performance of the controller. Fig. 6.15 shows the inlet and outlet moisture contents of the dryer. The inlet moisture varied in the range of 20-26% with different frequencies; the outlet moisture content was well controlled around the set point.

6.5 Conclusions

A model-predictive controller was developed for a crossflow grain dryer. Two feedforward algorithms (i.e. ZAE and LSE) were tested. Both perform well although the ZAE algorithm showed a slightly smaller control error and the LSE a slightly smoother control action. An estimator for the drying constant was tested. Computer analysis established that the controller compensates well for a change in drying-air temperature, and is robust under various disturbances. The MC controller should be able to work in concert with a grain-quality controller witch manipulates the drying-air temperature according to a grain-quality requirement.

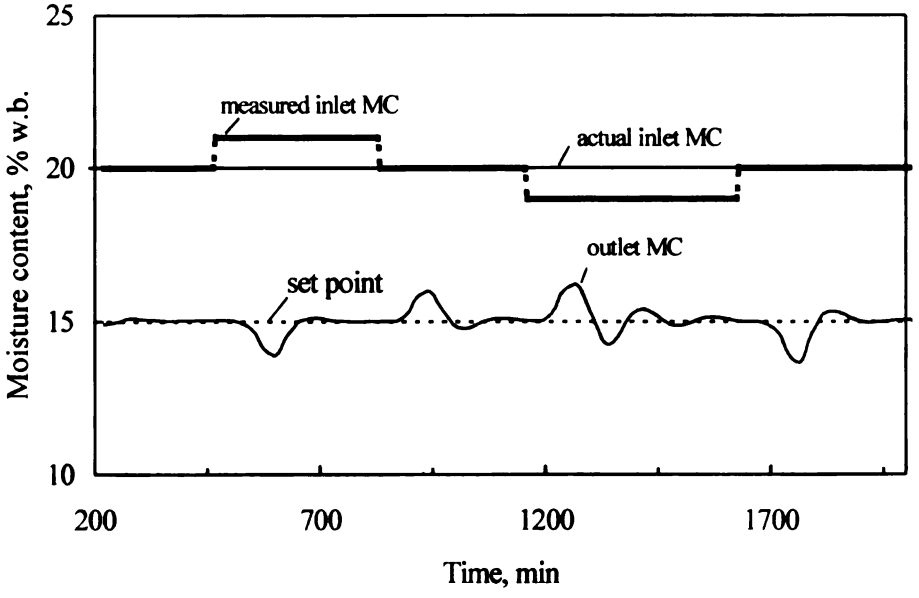

Fig. 6.12 Simulated control response with the presence of drift in the inlet moisture sensor (drying-air temperature = 85°C, filter factor β=0.5).

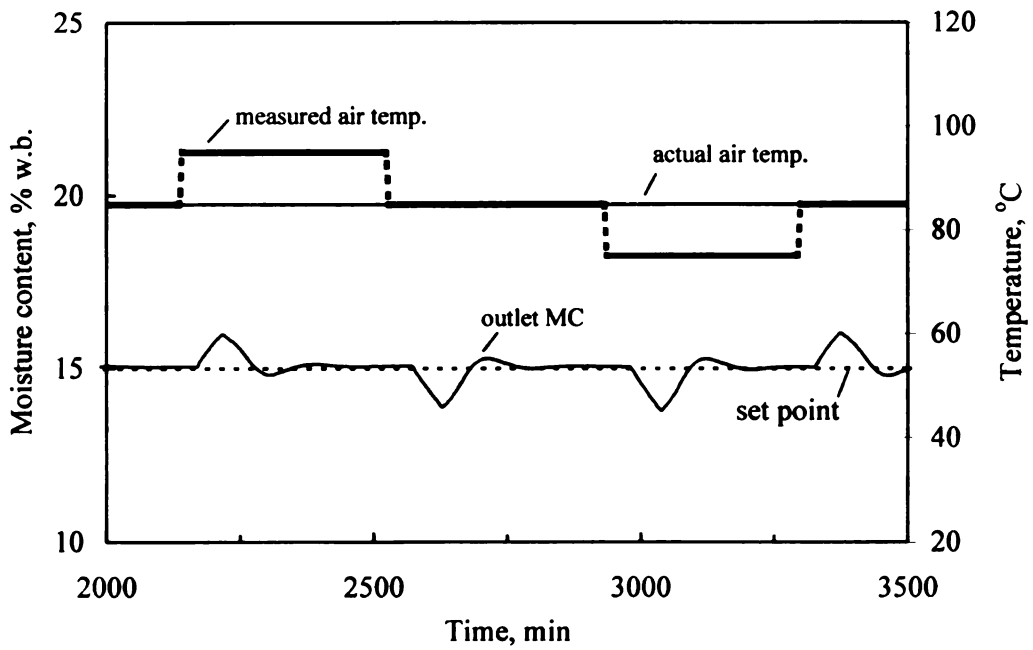

Fig. 6.13 Simulated control response with the presence of drift in the temperature sensor (inlet grain moisture content = 20%w.b., filter factor β=0.5)

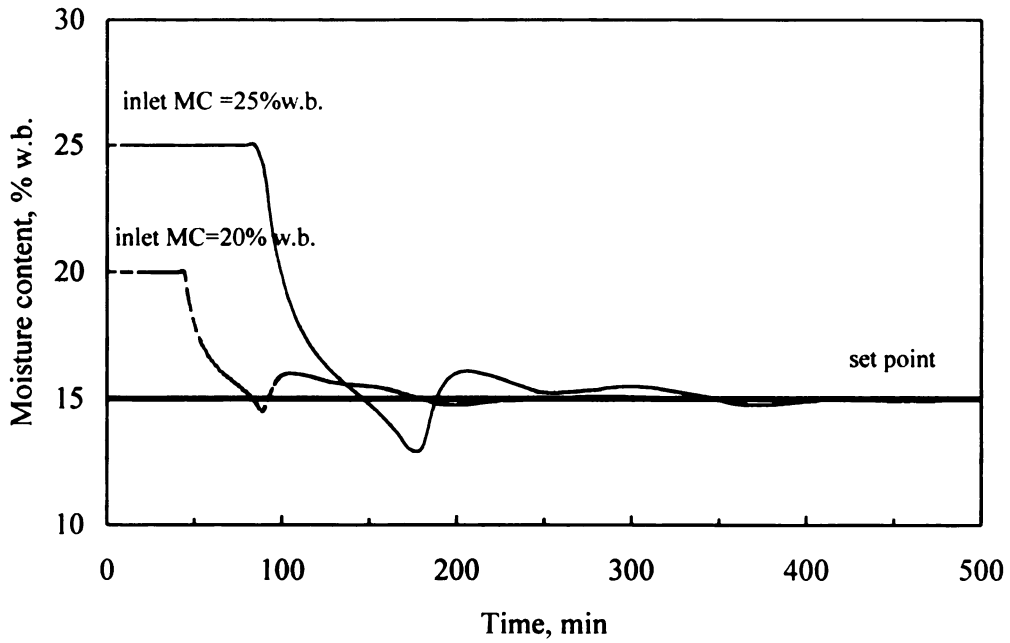

Fig. 6.14 Simulated control response at the start-up period of the dryer (drying-air temperature =85°C, filter factor β=0.5).

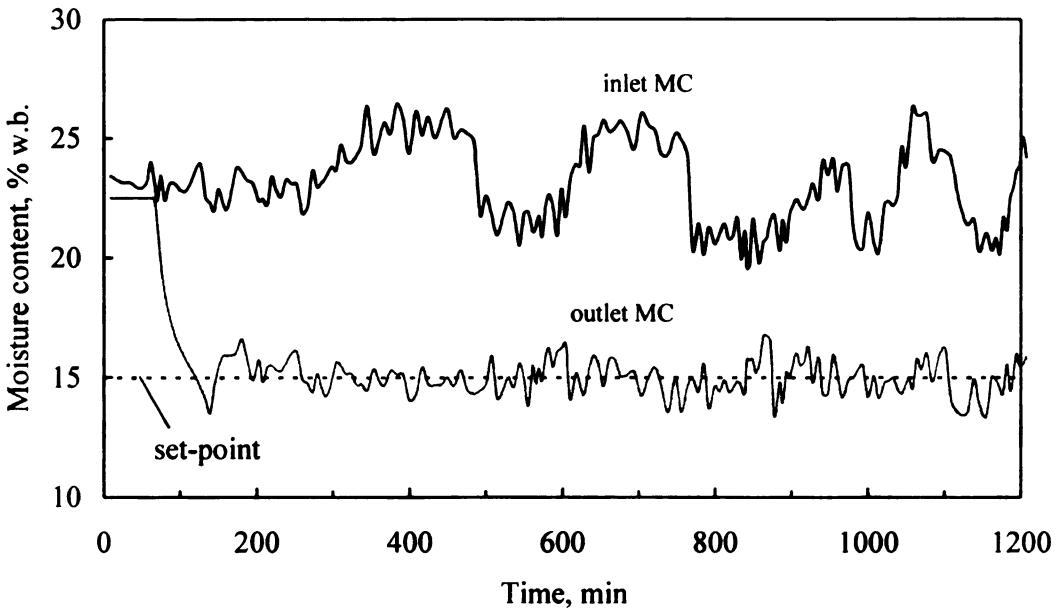

Fig. 6.15 Simulated control response with randomly changing inlet grain moisture content (drying-air temperature = 85°C, filter factor β=0.5).

References

Bosley J. R., T. F. Edgar, A. A. Patwardhan, G. T. Wright. 1992. Model-based control: A survey. IFAC Symposia Series 8: 127-136.

Bruce, D. M., N. J. B. McFarlane. 1993. Control of mixed-flow grain dryers: an improved feedback-plus-feedforward algorithm. J. agric. Enging Res. 56:225-238.

Camacho E. F., C. Bordons. 1995. Model predictive control in the process industry. Springer, London, UK.

Courtois, F., J. L. Nouafo, G. Trystram. 1995. Control strategies for corn mixed-flow dryers. Drying Technology 13(5-7):1153-1165.

Eltigani, A. Y. 1988. Automatic control of commercial crossflow grain dryers. Ph. D Dissertation, Michigan State University, East Lansing, MI.

Forbes, J. F., B. A. Jacobson, E. Rhodes, G. R. Sullivan. 1984. Model based control strategies for commercial grain drying systems. Canadian Journal of Chemical Engineering 62:773-779.

Garcia G. E., D. M. Prett, M. Morari. 1989. Model predictive control: theory and practice - a survey. Automatica 25:335-348.

Johnson, G. W. 1997. LabVIEW graphical programming : practical applications in instrumentation and control. McGraw-Hill, New York, NY.

Marchant, J. A. 1985. Control of high temperature continuous flow grain dryers. Agricultural Engineer 40(4):145-149.

McFarlane, N. J. B., D. M. Bruce. 1991. Control of mixed-flow grain dryers: development of a feed-back-plus-feedforward algorithm. J. agric. Eng. Res. 49:243-258.

Olesen, H. T. 1987. Controlling drying percentage. Chapter 3, Appendix E, of *Grain Drying.* Innovation Development Engineering APS, Thisted, Denmark.

Pabis, S., S. M. Henderson. 1961 Grain drying theory: II. A critical analysis of the drying curve of shelled maize. J. agric. Eng. Res. 6:272-277

Perry, R. H., D. W. Green. 1997. Perry's Chemical Engineers' Handbook. McGraw-Hill Companies Inc., New York, NY.

Platt, D., A. Palazoglu, T. R. Rumsey. 1992. Dynamics and control of cross-flow dryers II. A feedforward-feedback control strategy. Drying Technology 10(2):333-363.

Shinskey, F.G. 1994. Feedback Controllers for the Process Industries. McGraw-Hill, Inc., New York, NY.

Whitfield, R. D. 1986. An unsteady-state simulation to study the control of concurrent and counter-flow dryers. J. agric. Eng. Res. 32:171-178.

Whitfield, R. D. 1988a. Control of a mixed-flow drier Part 1: Design of the control algorithm. J. agric. Eng. Res. 41:275-287.

Whitfield R. D. 1988b. Control of a mixed-flow drier Part 2: Test of the control algorithm. J. agric. Eng. Res. 41:289-299.

Zhang, Q., J. B. Litchfield. 1993. Fuzzy logic control for a continuous crossflow grain dryer. Food Process Engineering 16:59-77.

CHAPTER 7. FIELD TESTS OF THE CONTROLLER

Abstract

The model-predictive control system developed in Chapter 5 was implemented and tested on a commercial crossflow grain dryer. Both Zero-Average-Error and Lest-Squire-Error algorithms showed good accuracy and stability. The moisture content of was controlled within ± 1.3% of the set point, at inlet moisture contents ranging from 21 to 32% w.b. and the drying-air temperatures from 85 to120°C. The controller also showed excellent compensation to changes in the drying-air temperature.

7.1 Introduction

A distributed-parameter process model (c.o.d.) for high-temperature grain drying was developed in Chapter 5. In Chapter 6, a model predictive controller for a crossflow dryer was developed. Two feedforward algorithms, i.e. Zero Average Error (ZAE, Eq. 5.5) and Least Square Error (LSE, Eq. 5.8), were designed with the feedback loop consisting an estimator (Eqs. 5.10,11) with a filter (Eq. 2.12). The range of the filter factor β of the modifier was found to be 0.3-0.8. Computer simulations of the control of a virtual grain dryer showed that the controller has good accuracy and robustness.

This Chapter reports the implementation and field tests of the controller.

7.2 Implementation

7.2.1 Grain dryer

The controller has been implemented and tested on a ZIMMERMANN VT1210 grain dryer (manufactured by ffi Co., Indianapolis) located at the Jorgensen Elevator, Williamston, MI. The dryer has a cylindrical shape with the drying-air flowing through the grain column from the inside to the outside. The dryer consists of a drying section, cooling section, unload system, fan and burner (Fig. 7.1). The upper part of the tower serves as drying section, with a grain turn-flow located midway in the drying column; the lower part of the tower consists of the cooling section in which ambient air is used to cool the grain before it leaves the dryer. The air exiting the cooling section is directed to the

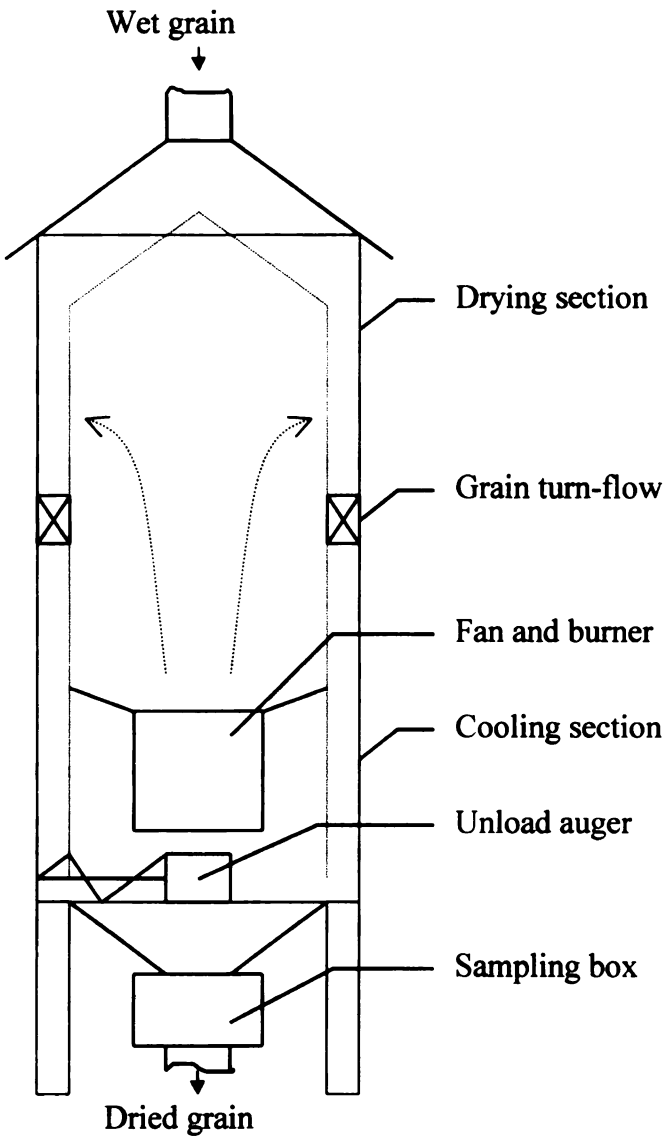

inlet of the burner and is recycled. The specifications of the dryer are listed in Table 5.1

Fig. 7.1 Schematic of ZIMMERMANN VT1210 grain dryer.

in Chapter 5.

A sampling box was added to the outlet of the dryer to facilitate installation of a moisture sensor. The function of the sampling box is to keep the probe of the sensor surrounded by a constant flow of grain. The grain flowrate in the box is adjustable with a slide gate in the bottom of the sampling box. Extra grain overflows the box through a by-pass.

A 100 m^3 garner bin is used for temporary storage of wet grain. The dryer receives grain directly from the dump pit when a truck is dumping grain. Otherwise the dryer receives grain from the wet garner bin.

7.2.2 Control system

The control system consists of the moisture and temperature sensors, the unload mechanism of the dryer, and the computer plus software (Fig. 7.2).
The control algorithms are implemented on a personal computer (Gateway 2000, 4DX2-66, 16MB RAM). The computer communicates with the sensors and the drive motor through a Lab-PC-1200/AI Data Acquisition Card (DAQ) of National Instrument (Austin, TX). The card has 24 digital I/O, one 12-bit ADC with eight analog inputs and two 12-bit DACs with voltage outputs. One digital I/O is used to control the auto-control contact, three analog inputs are used by the sensors (two for moisture and one for temperature), and one analog output is for the motor control of the unload auger.

The rpm of the unload auger is proportional to a 0-5 voltage input to the controller of the unload motor. The maximum speed of the auger at 5 V input is 293 rpm and results

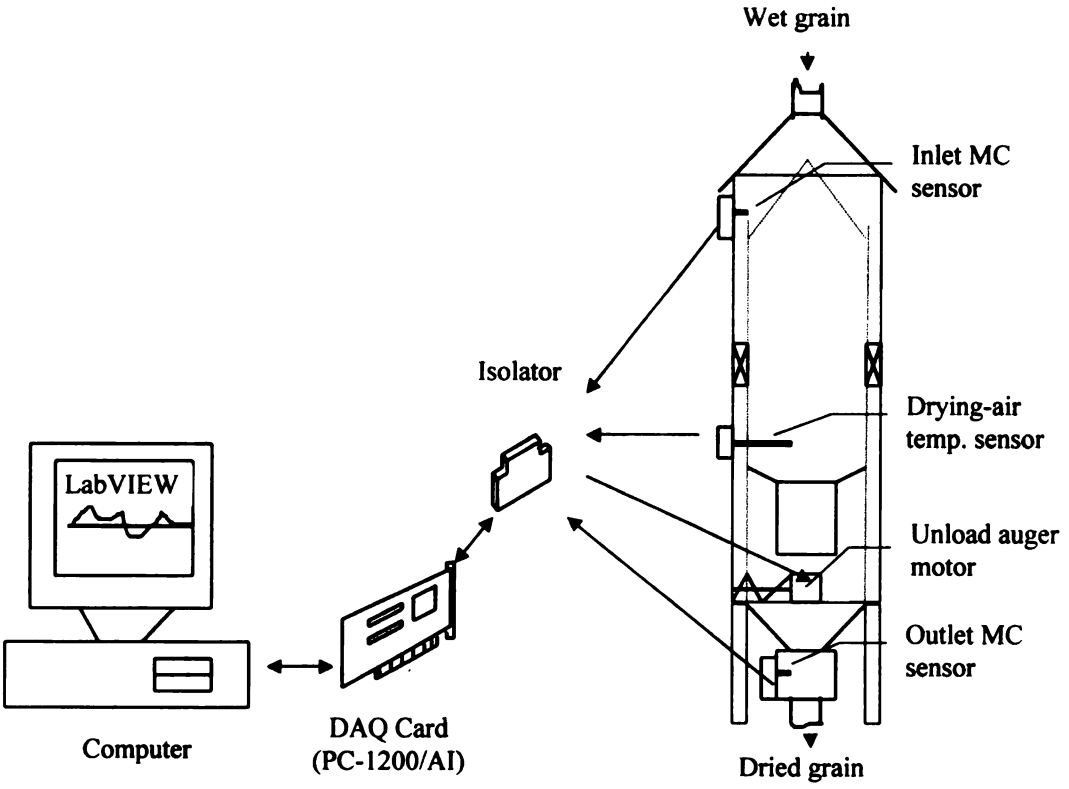

Fig. 7.2 Implementation of the controller.

in the maximum discharge capacity of 60.2 tonne/h (51.2 tonne of dry matter per hour).

Two moisture sensors (TRIME-GW, MESA Systems Co., Framingham, MA) were employed to measure the inlet and outlet grain moisture contents. The TRIME-GW grain moisture sensor is based on time-domain reflectometry technology; two metal probes are emerged in the grain column; a high frequency pulse is generated and propagated along the probes; at the end of the probes, the pulse is reflected back to its source. The moisture content of grain is related to the transit time of the pulse in the probes. The inlet sensor was placed at the top of the dryer, and the outlet sensor in the sampling box (Fig. 7.2).

An 8 m long PT100 Resistance Temperature Detector (RTD) was installed in the drying-air plenum to measure the average drying-air temperature. A G418 RTD conditioner was used to convert the temperature signal to 0-5V output.

7.2.3 Programming

The 12.92 m long grain column between the inlet moisture sensor and the end of the cooling section was conceptually divided into 20 stacked beds each with a length of 0.646m. The control action was updated each time the grain had moved down 0.646m. The residence time for the grain in a 0.646m high grain bed was calculated by:

$$\tau = \frac{\rho_g^{ave}(\Delta H)A}{\Phi(G_{max})} \tag{7.1}$$

where τ = residence time of grain in one bed, h

ΔH = height of one bed, 0.646 m

A = cross-sectional area of the grain column, 3.25 m^2

Φ = relative discharge rate of the unloading auger, % G_{max}

G_{max} = maximum discharge rate of the unloading auger, 51.2 tonne of dry matter per hour

ρ_g^{ave} = average density of the grain in the dryer, kg (dry matter) m^{-3}

The average density of the grain is based on the moisture distribution of the grain in the dryer, and was calculated using the following relationship (Lorenzen,1958):

$$\rho_g = (816 - 5.9543M)(1 - \frac{M}{100}) \tag{7.2}$$

where ρ_g = density of grain, kg (dry matter) m^{-3}

M = grain moisture content, % w.b.

The program was written in LabVIEW 4.1, a graphic programming language for data acquisition and control (Johnson, 1997). A virtual control panel of the grain dryer was generated on the computer. The dryer could be either manually operated or automatically controlled from the virtual control panel. The process data were displayed in real time, in terms of numbers and/or charts and was recorded on disk as text files. The flowchart of the control program is shown in Fig. 7.3. The computer (i.e. the controller) takes over the control of the unloading auger (i.e. the dryer) by sending a digital high signal to the auto control contact. Then, the controller enters the cycle of: (1) measuring the inlet/outlet grain moisture contents and the drying-air temperature, (2) calculating and updating the control action, and (3) waiting for the next sampling period. The period of each cycle is the time for grain to move down one bed, and is calculated with Eq. 7.1. In the last two minutes of each cycle, 20 readings, one reading every 6

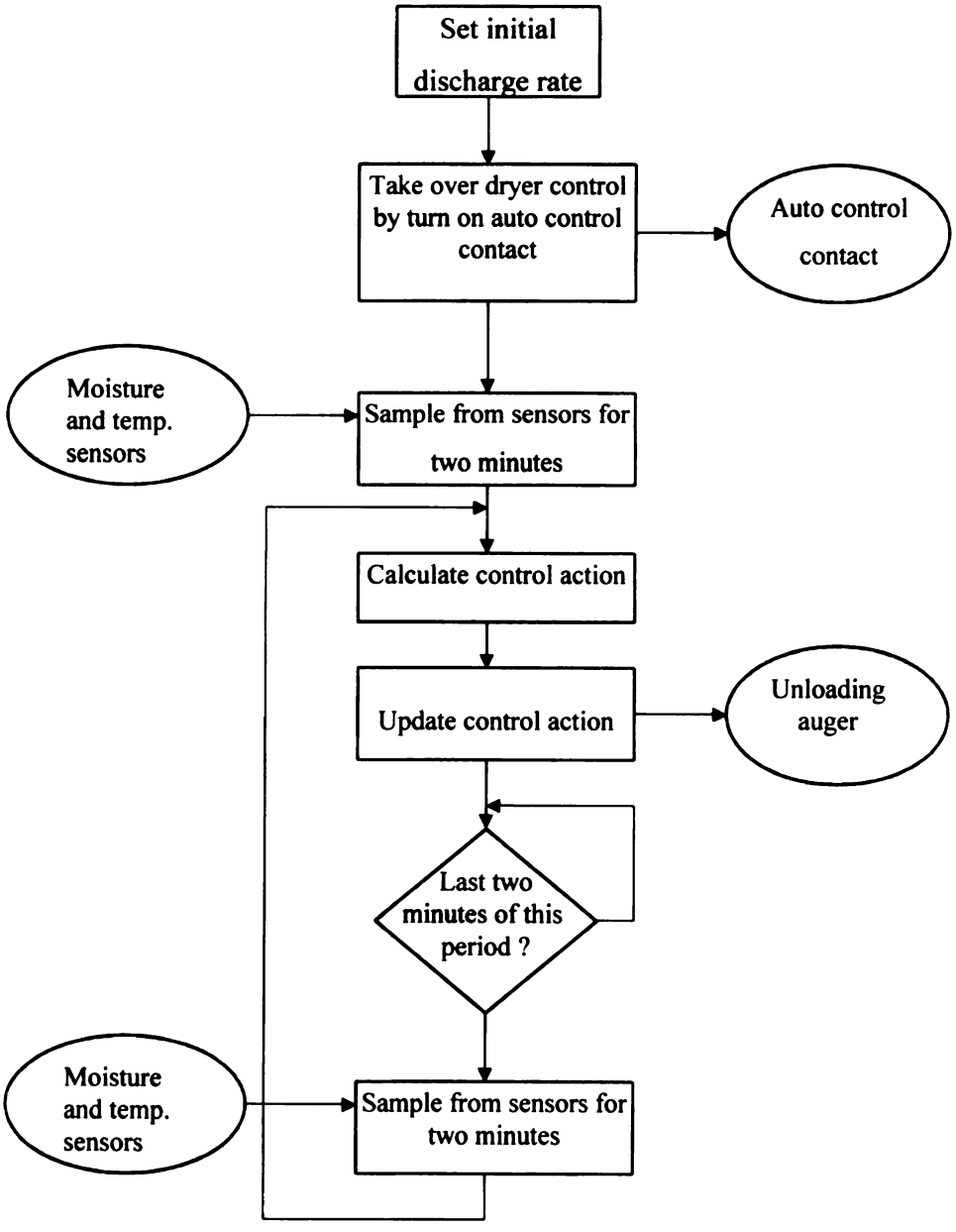

Fig. 7.3 Flowchart of the control program.

seconds, are obtained from each sensor, and their averages are used in the calculation of the control action during the next cycle.

7.3 Results and Discussion

There were three phases in the control test: (1) on-line calibration of the moisture sensors, (2) preliminary testing of the control algorithm, and (3) testing the controller under various operating conditions. Initially, the dryer was manually controlled. Next, the dryer was auto-controlled under close supervision, and was adjusted when necessary. Finally, the dryer was totally controlled by the controller.

The control tests were conducted during Oct.-Dec., 1997. More than 100 hours of data were collected while the dryer operated under automatic control, with the inlet moisture content ranging from 21 to 32%, the drying-air temperature from 85 to 120°C, and the ambient temperature from –5 to 10°C.

7.3.1 On-line calibration of the moisture sensors

The inlet and outlet moisture sensors were calibrated during manual operation of the dryer. Grain samples were collected manually at the inlet and outlet sensors at the same time that the controller was reading the voltage signals from the sensors. The moisture contents of the samples were measured immediately after sampling using a BURROWS Grain Moisture Meter(Seedburo Equipment Company, Chicago, IL). The meter measures the capacitance of a 250g grain sample, and relates it to the moisture content. The BURROWS meter was calibrated with the standard oven method (ASAE, 1991); it has a precision of ± 0.25% near 15% w.b. and ± 0.4% near 25% w.b.. The

calibration relations for the inlet and outlet sensors were developed by regression analysis of the data, and were used in the moisture measurement of the sensor.

Fig. 7.4 compares the readings of the BURROWS meter and the calibrated moisture sensors. The BURROWS meter shows larger fluctuations because only one reading was obtained for each sample, whereas the sensor took 20 measurements during a 2-minute period.

To check the stability of the moisture sensors, grain samples were taken regularly during the control tests and their moisture contents were measured with the BURROWS meter. The outlet sensor was found to be reasonably stable during the testing. The inlet sensor worked acceptably during the first half of the test period, but was found to be unstable near the end of the tests. In a few control tests, the inlet sensor was discarded and the inlet moisture contents were manually entered on the computer. The drift of the inlet sensor occurred mainly under extreme weather conditions (i.e. cold and windy) due to water condensation on the sensor.

7.3.2 Control tests

(1) Initial value of the multiplier

An initial value is assigned to the multiplier of the drying constant (γ , see Eq. 6.9) before starting the controller. The multiplier is modified by the feedback loop during the dryer operation to compensate for the model error. If there is no information on the error in the control model, a reasonable choice for the initial value of the multiplier is 1.0 (i.e. the model error will not be compensated). If a better initial value of the multiplier can

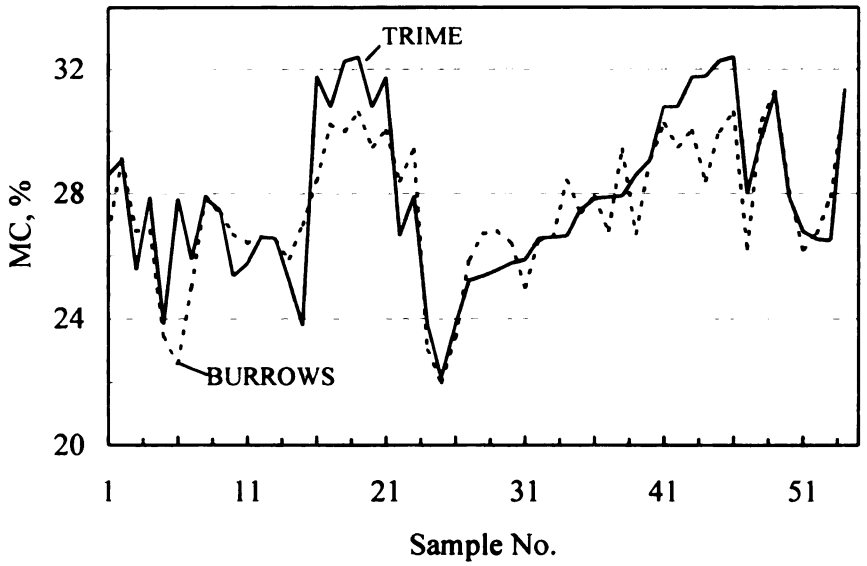

(a) Inlet sensor

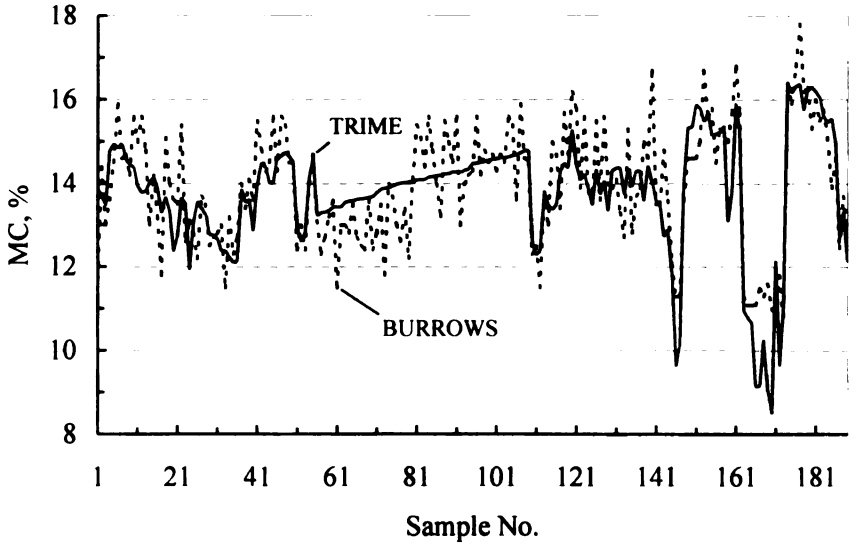

(b) Outlet sensor

Fig. 7.4 Comparison of the readings of the TRIME sensors and the BURROWS meter: (a) inlet moisture, and (b) outlet moisture.

be provided, the transition period for modification of the multiplier will be shorter, and the desired control precision is reached more rapidly.

Fig. 7.5 shows a test in which the initial value of the multiplier was chosen as 0.9. The feedback loop was disabled and the multiplier did not change during the first residence time. After 22:00 of the time, the multiplier decreased because the predicted outlet moisture content was higher than the measured value. It required another residence time before the multiplier reached the steady-state value of 0.75.

Several preliminary tests indicated that at steady state the multiplier for the ZIMMERMAN VT1210 falls in the range of 0.6-0.8.

(2) Tests of the control algorithms

Fig. 7.6 shows a test of the grain dryer operating at 105°C and controlled with Zero-Average-Error (ZAE) algorithm with β=0.5 and γ_0=0.7, the set-point was 14% w.b.. During the start-up period (the first 3 hours), the dryer was manually controlled. The controller was switched on at 15:40. In the next 22 hours of the test, the inlet moisture content varied from about 30% at the beginning to about 23% w.b. at the end. The inlet moisture content fluctuated greatly during the first 8 hours of the tests when grain was delivered directly to the dryer from the field. Less fluctuation occurred in the inlet moisture content at night when grain entered the dryer from the garner bin. The fluctuation in the inlet moisture content is reflected in the outlet moisture content after one residence time (about 2.5-3.5 hours). Excluding the start-up period, the outlet moisture content was controlled in the range of 13.2-15.5% with an average of 14.08%,

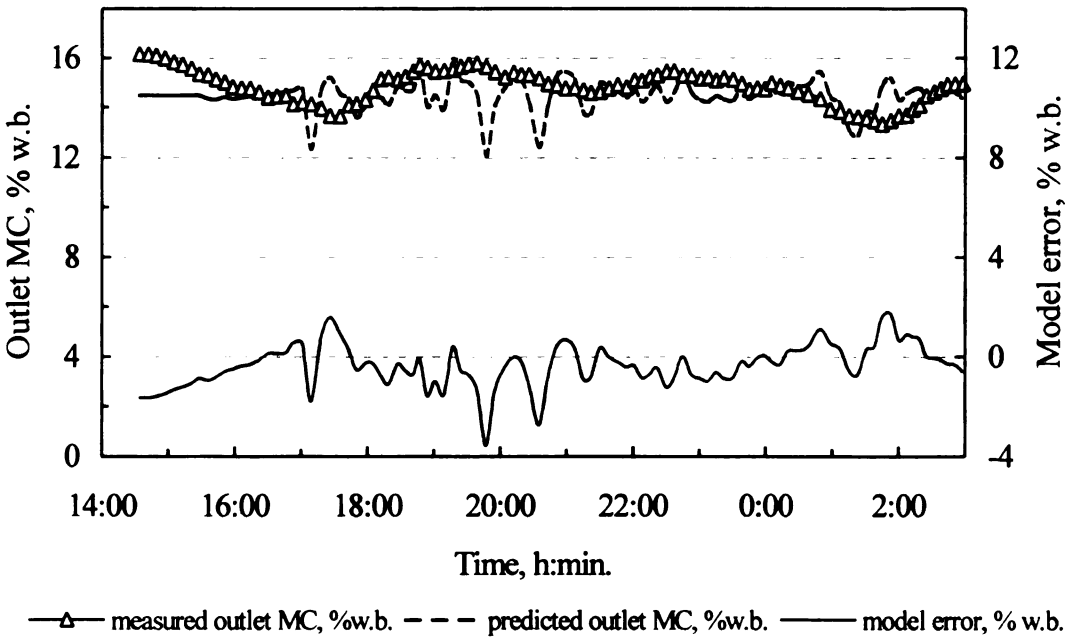

Fig. 7.5 Measured and predicted outlet moisture contents and the value of the multiplier of the maize drying constant in a crossflow dryer operating under ZAE control (drying-air temperature = 105°C, set point =14.5% w.b., filter factor β = 0.5).

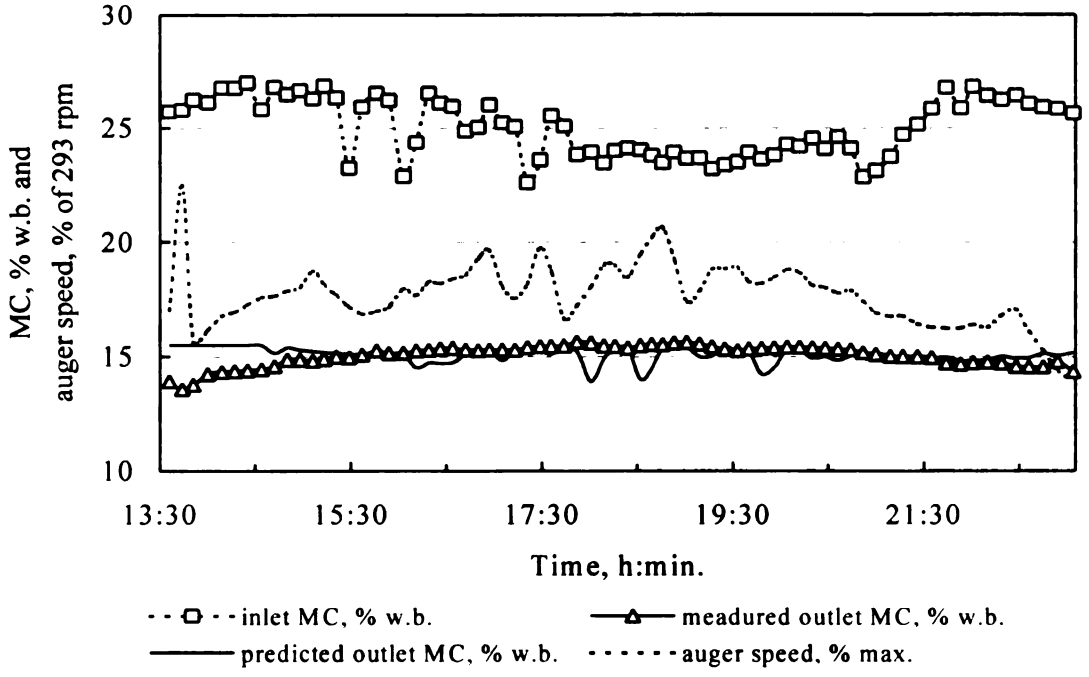

Fig. 7.6 Inlet and outlet moisture contents, and the auger speed during automatic control of a crossflow dryer with ZAE control (drying-air temperature = 105°C, filter factor β = 0.5, initial multiplier γ_0 = 0.7, residence time=2.5-3.5 hours).

which is in the range of –1.3% to +1.0% around the set-point. The auger rpm varied from 40 to 62 rpm.

Fig. 7.7 shows a test with the ZAE algorithm with β=0.5 and γ_0=0.6. The inlet moisture content ranged from 29% to 18% w.b.. The outlet moisture content was controlled within13.3 -15.8% with an average of 14.8% (i.e. the offset is –1.2 to +1.3% w.b.). The set point of the test was 14.5% w.b.. Comparing Fig. 7.6 and 7.7, no significant difference is found in the control results although different initial values of the multiplier (i.e. 0.7 for Fig. 7.6 and 0.6 for Fig. 7.7) were assigned.

The measured and predicted outlet moisture contents in the test illustrated in Fig. 7.7, and the difference between them (i.e. the model error), are shown in Fig. 7.8. There occurs a spike in the predicted outlet moisture content after one residence time for each spike in the inlet moisture content. However, the spikes in the measured outlet moisture content are not as sharp because of the mixing of grain in the dryer, especially in the grain turn-flow section. The mixing of grain is favorable for reducing the variation in the outlet grain moisture content, but exaggerates the model error in Fig. 7.8. It causes a relatively large error in the estimation of the drying constant, and results in the over-modification of the multiplier. Therefore, the following filter was added to the inlet moisture content:

$$M_i^f = M_i^c + 0.5(M_i^l - M_i^c) \tag{7.3}$$

where M_i^f = inlet moisture content after filtering

M_i^c = current sampling value of the inlet moisture content

M_i^l = last value of the inlet moisture content after filtering

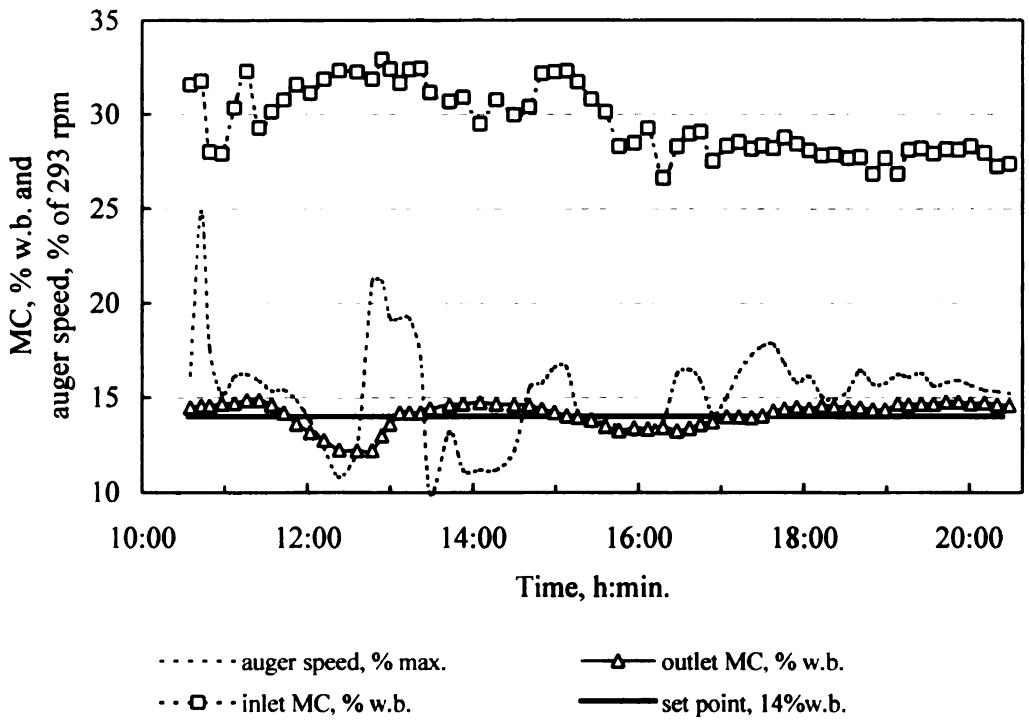

Fig. 7.7 Inlet and outlet moisture contents, and the auger speed during automatic control of a VT1210 dryer with ZAE control (drying-air temperature = 105°C, filter factor β = 0.5, initial multiplier γ_0 = 0.6, residence time =2.0-2.5 hours).

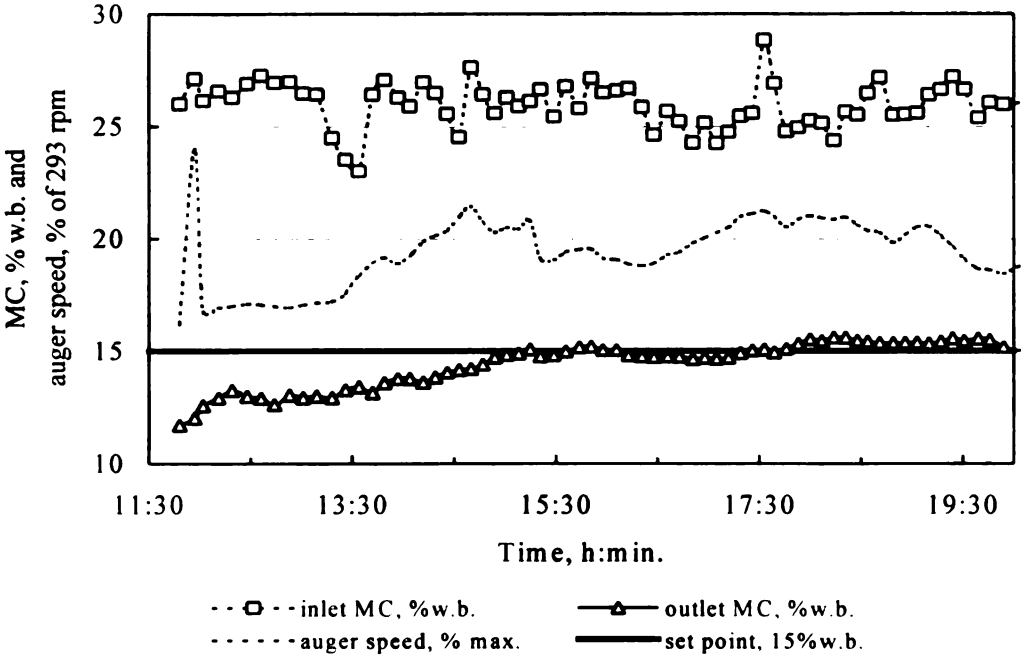

Fig. 7.8 Measured and predicted outlet moisture contents, and the model error (i.e. the measured minus the predicted outlet moisture contents) during the test shown in Fig. 7.7.

Fig. 7.9 shows a control test after the inlet moisture filter had been added. The measured and predicted outlet moisture contents are smoother than in Fig. 7.8. The outlet moisture content was controlled to within ± 0.7% w.b. of the set point. The spikes in the inlet moisture content at 15:30, 16:00 and 17:20 were damped out in the predicted outlet moisture contents at 18:00, 18:30 and 19:40 (i.e. at τ + the residence time).

Fig. 7.10 represents a test with the LSE algorithm without the use of the inlet moisture content filter. The dryer was manually controlled until 13:20. Since the inlet moisture content was high (32%), the auger speed was set low during the start-up period. This caused overdrying between 12:00 to 13:00. After 13:20 the controller took over, and the outlet moisture content was controlled to within ± 0.8% w.b. of the set point.

Comparing Fig. 7.10 to Figs. 7.6 and 7.7, it can be seen that the changes in auger rpm with the LSE algorithm (Fig. 7.10) are less sharp than with the ZAE algorithm. This agrees with the simulation analysis of the controller presented in Chapter 5.

Fig. 7.11 shows a test of the LSE algorithm with the addition of the inlet moisture filter. The inlet moisture content variation was relatively smooth. The outlet moisture content slowly approached the set point after the start-up at 14:20. The outlet moisture content was controlled to within –1.0% to +0.7% w.b. of the set point after the start-up period. Comparing the results of Fig. 7.9 and Fig. 7.11, it is clear again that the variation in the auger rpm is less abrupt with the LSE algorithm than with the ZAE algorithm.

(3) Effects of the drying-air temperature

A step change in the drying-air temperature was introduced intentionally to test controller response. Because the inlet sensor was unstable, the inlet moisture content of

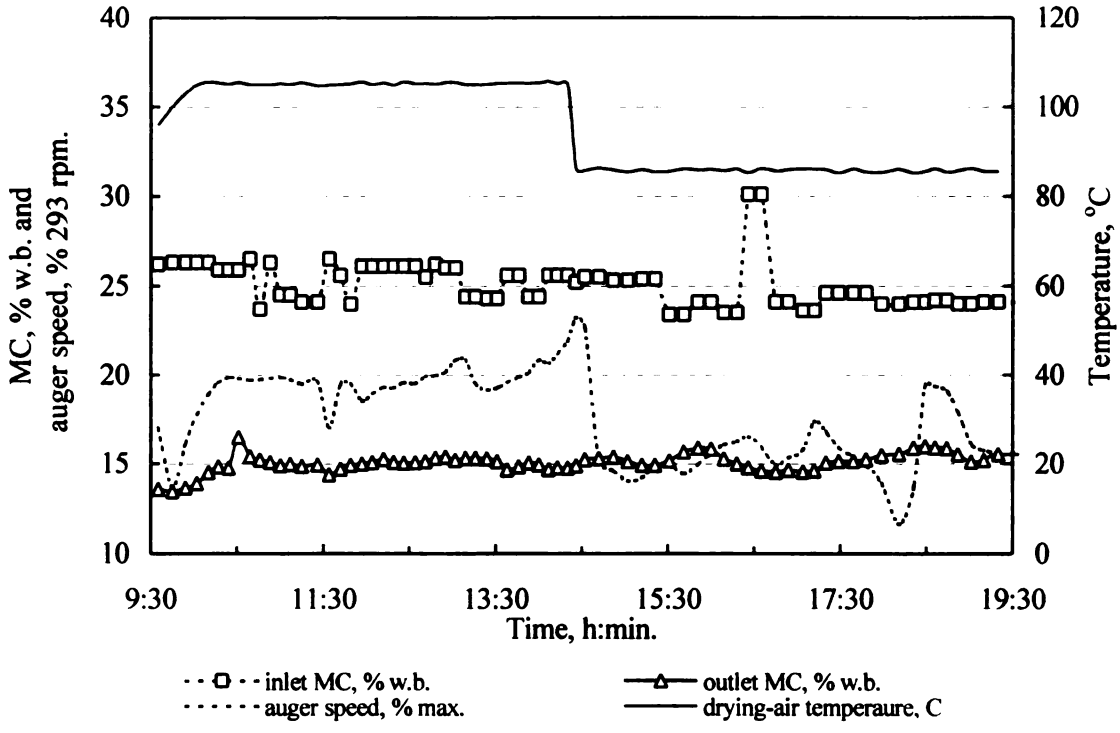

Fig. 7.9 Inlet and outlet moisture contents, and the auger speed, during automatic control of a VT1210 dryer with ZAE control and an inlet moisture filter (drying-air temperature = 105°C, filter factor β = 0.5, initial multiplier γ_0 = 0.7, set point = 15% w.b., residence time=2-2.5 hours).

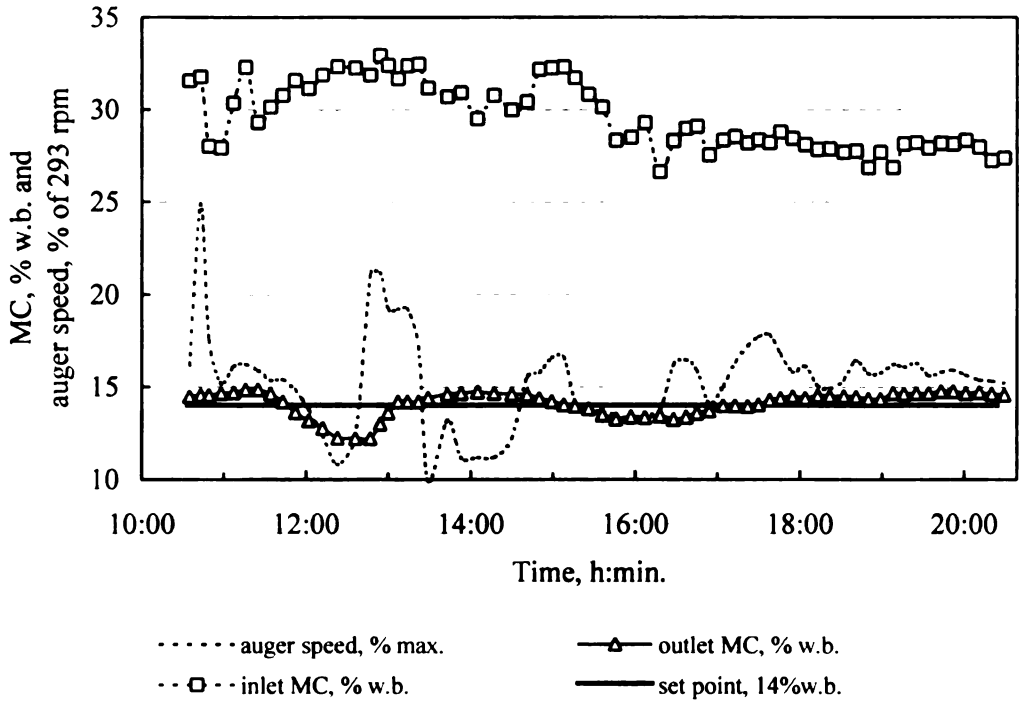

Fig. 7.10 Inlet and outlet moisture contents, and the auger speed, during automatic control of a VT1210 dryer with LSE control (drying-air temperature = 105°C, filter factor β = 0.5, initial multiplier γ_0 = 0.7, residence time = 2.5-3.0 hours).

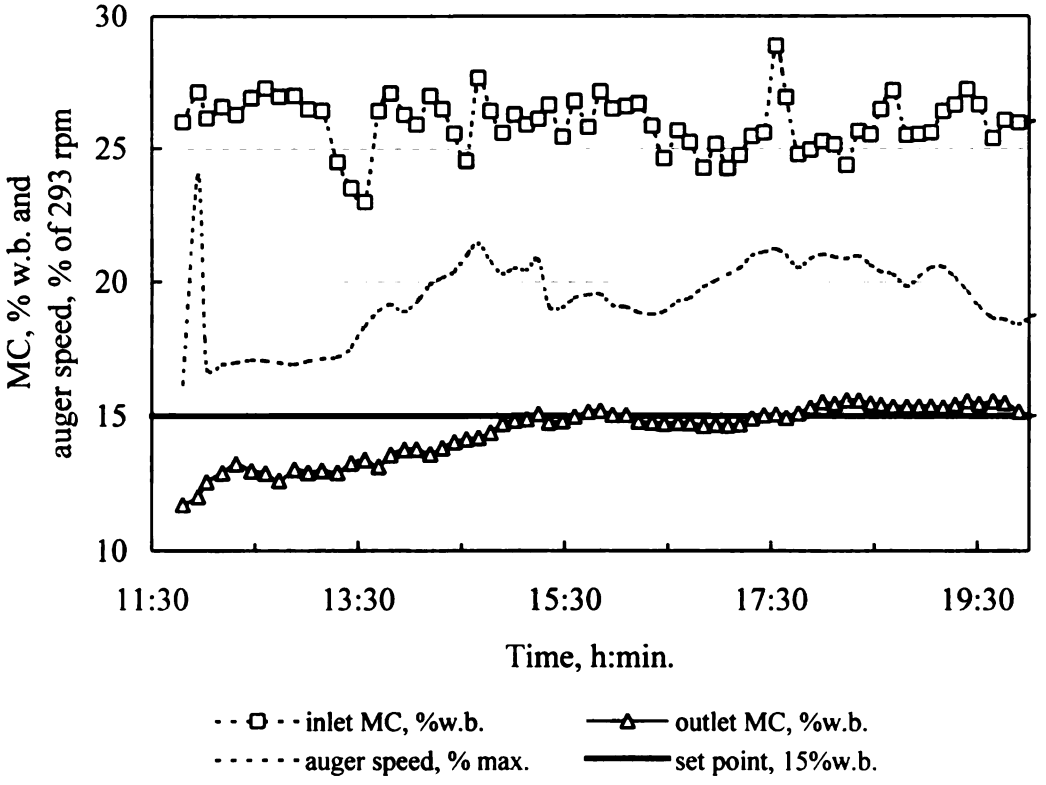

Fig. 7.11 Inlet and outlet moisture contents, and the auger speed during automatic control of a crossflow dryer with LSE control and the inlet moisture filter (drying-air temperature = 105°C, filter factor β = 0.5, initial multiplier γ_0 = 0.7, residence time = about 2.5 hours).

grain was measured manually with the BURROWS meter and was entered to the controller from the virtual control panel. The moisture content of the inlet grain samples was taken every sampling period, and was assumed to be constant during the sampling period.

Fig. 7.12 shows the response of the controller with the ZAE algorithm to a sudden drop of 20°C in the drying-air temperature at 14:30. The immediate response of the auger rpm to the change in the air temperature was significant, but the outlet moisture content was hardly affected. The outlet moisture content was controlled to within –0.5% to +0.9% w.b. of the set point. Thus, the controller compensated well for the temperature change.

Fig. 7.13 shows the response of the controller with the LSE algorithm to the 20°C step up in the drying-air temperature at 11:30. The controller again compensated well for the temperature change. The outlet moisture content was controlled within –1.3% to +0.7% w.b. of the set point

In the test shown in Fig. 7.13, there was a step increase in the inlet moisture content at 14:50, and then a step drop at 16:00. The auger speed and the outlet moisture first decreased to a minimum point at 16:50, and then increased. During the transition period, the simulated and measured moisture contents followed a similar trend (see Fig. 5.3 in Chapter 5).

(4) Control of the start-up period of the dryer

During the first run of the dryer in a drying season, the moisture content of all grain in the dryer is the same. The simulation analysis in Chapter 5 (Fig. 5.14) shows that the controller can quickly steer the outlet moisture content to the set point after a period

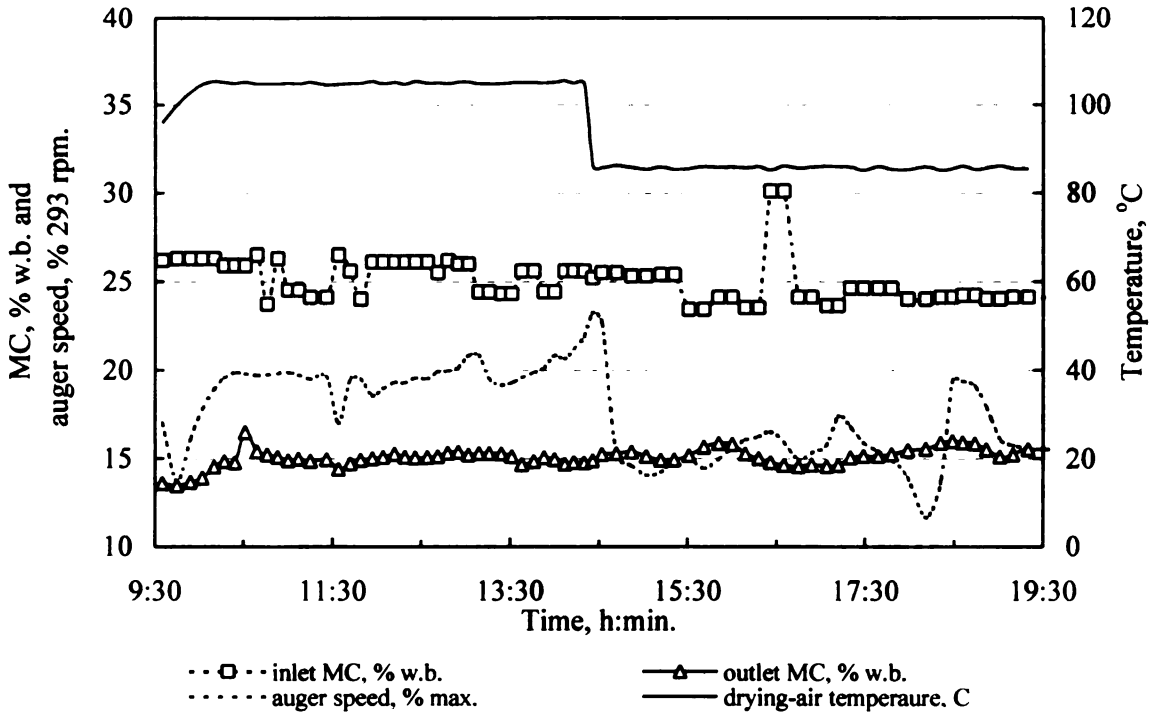

Fig. 7.12 Response to a step change in the drying-air temperature of a VT1210 dryer from 105 to 85°C with ZAE control (set point =15% w.b., filter factor β = 0.5, initial multiplier γ_0 = 0.7, residence time = about 2.5 hours).

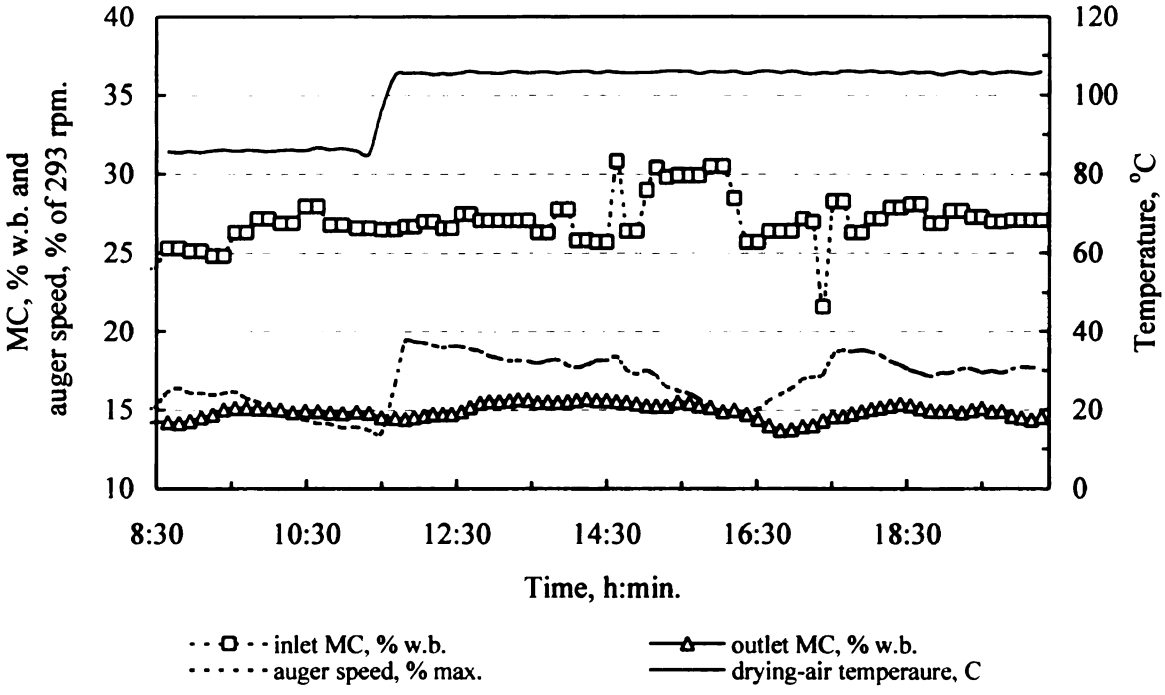

Fig. 7.13 Response to a step change in the drying-air temperature of a VT1210 dryer from 85 to 105°C with LSE control (set point = 15% w.b., filter factor β = 0.5, initial multiplier γ_0 = 0.7, residence time = 2.5-3.0 hours).

equal to the average residence time of the grain in the dryer. Initially, the moisture content of the grain is too high and has to be recycled to the inlet of the dryer.

No experimental test was conducted on the control of the start-up period of the first run of the dryer in 1997 drying season. As this start-up period occurs only once a season, its control is less important for automatic control.

Most dryers are shut down at the end of the day without emptying the grain in the dryer, and the drying process is restarted the next day. If the controller does not memorize the moisture distribution in the dryer when it is shut down, it can not make the correct decision during the first residence time period (daily start-up period) after the dryer is restarted.

There are two choices to control the dryer during the daily start-up period: (a) by manually control, (b) by providing the controller with the current moisture distribution in the dryer.

Manual control is not only inconvenient, but is also inaccurate. [The daily start-up periods in Figs 7.5,6,8,9 were manually controlled, and large over-/under-drying was observed].

A semi-empirical algorithm was developed for the automatic control of the dryer during the daily start-up period. After the dryer is restarted, the inlet and outlet moisture contents of the grain are measured for ten minutes. When the controller is switched on, the grain moisture distribution is approximated as linear from the inlet and outlet. The test in Fig. 7.13 was a restart after 13 hours shut-down of the test in Fig. 7.12. The semi-empirical start-up algorithm was used in the start-up period of Fig. 7.13, and resulted in the outlet moisture content continuing smoothly.

The best way for the control of the daily start-up period is to record the moisture distribution when the dryer is a shut down, and re-enter the value before the dryer is restarted.

7.4 Conclusions

(1) The moisture controller showed excellent accuracy and stability in all the experimental tests. The outlet moisture content of grain was controlled to within ± 1.3% of the set point with the inlet moisture content ranging from 21 to 32% w.b. and the drying-air temperature from 85 to 120°C.

(2) Both the ZAE and LSE control algorithms worked well although the auger rpm changes less abruptly with the LSE algorithm. No conclusion was drawn which algorithm is superior.

(3) A filter on the inlet moisture measurement is necessary to reduce exaggerated model errors.

(4) The controller compensated well for a variation in the drying-air temperature when the grain quality needs to be controlled.

(5) The predicted performance of the controller was validated during the field tests.

(6) Reliable on-line moisture sensors for the controller, especially for inlet grain to the dryer, still need to be developed before the dryer control system can be commercialized.

References

ASAE Standards, 38th Ed. 1991. D352.2-Moisture measurement-Ungrounded grain and seeds. Am. Soc. Agric. Eng., St. Joseph, MI.

Lorenzen, C. 1958. The effect of moisture on weight-volume relationships of small grain. ASAE Paper No. 58-111, Am. Soc. Agric. Eng., St Joseph, MI.

Johnson, G. W. 1997. LabVIEW Graphical Programming : Practical Applications in Instrumentation and Control. McGraw-Hill, New York, NY.

CHAPTER 8. GRAIN QUALITY CONTROL IN HIGH-TEMPERATURE DRYERS

Abstract

The drying-air temperature is usually determined for conventional grain dryers by rule-of-thumb and is usually not adjusted during dryer operation. The quality of dried grain is uncertain since it fluctuates with the residence time of grain in the dryer. The objective of this Chapter was to develop a control strategy for optimizing the quality of dried grain by varying the drying-air temperature. A neural network model was developed to relate the quality of dried grain to the drying conditions. A control algorithm was tested which varies the drying-air temperature so that the grain quality approaches the quality set-point at the outlet of the dryer. Simulation tests showed that the grain-quality controller results in improved grain quality in crossflow drying.

8.1 Introduction

High temperature drying may cause significant quality damage to the grain. The major factors influencing the grain quality damage in dryers are the drying-air temperature and the grain-residence time. The residence time of grain (i.e. dryer capacity) needs to be controlled to keep the moisture content of the grain at the outlet of the dryer close to the set-point. Decreasing the drying-air temperature is will reduce the quality damage to the grain, but it will decrease the dryer capacity and energy efficiency. The optimal drying-air temperature is the highest temperature at which the grain quality is still acceptable; it is conventionally determined by rule-of-thumb based on the intended usage of the grain (i.e. for food, feed or seed).

The drying-air temperature is usually kept constant during the dryer operation. However, the moisture content of the grain entering a continuous-flow dryer changes randomly, depending on the variety, growing conditions and the harvest time. The residence time of the grain in the dryer is varied accordingly; therefore, the quality of the dried grain will vary significantly because the drying-air temperature is not adjusted. To achieve the desired and uniform quality of the dried grain, the drying air temperature needs to be optimized and regulated along with the speed of the unload auger.

The best way to determine the "optimal" drying-air temperature in a grain dryer is by modeling the quality change in the dryer. The grain-quality models developed in Chapter 4 of this thesis can not be directly employed for quality control because of the large computation requirements. First, a control-oriented model relating the quality of dried grain to the inlet grain moisture content and the drying air temperature, has to be developed.

A potential problem for quality control is the disturbance to the moisture control. The quality control requires frequent regulating of the drying-air temperature, which may degrade the performance of the moisture controller. This problem has been addressed in the design of the moisture controller (see Part III, Chapters 5-7). It was shown in simulation and field tests that the moisture controller is robust under conditions of moderate changes in the drying-air temperature.

The objectives of this Chapter are to develop control-oriented grain-quality models and the grain-quality control algorithm for grain dryers.

8.2 Control-oriented Quality Models

Comprehensive simulation tests for the crossflow drying of maize are described in Chapter 4; the results are presented in Tables 4.4a-e. The drying conditions were: air-temperature 50-120°C, airflow rate 32-96 $m^3 m^{-3} min^{-1}$, and initial grain moisture content 17.5-35% w.b.. The thickness of the grain column was 30.5 cm. The final grain moisture content of 15% w.b. after drying was searched for by simulation. The standard deviation of the initial moisture content of grain was chosen as 3% w.b., which is common for maize entering a dryer. The change in the percentage of denatured protein (PDP) was chosen as the quality criterion in this Chapter because of its importance in several maize-processing industries.

Two models are developed based on the data in Tables 4a-e, i.e. a quality *simulation model* and a quality *control model*. In the simulation model, the drying conditions (i.e. drying-air temperature, airflow rate and initial grain moisture content) are the inputs and the grain quality is the output. The control model predicts the drying-air

temperature for the desired grain quality at a particular airflow and inlet grain moisture content.

A conventional function approximator (e.g. a polynomial) has been shown to be effective only in a small range of drying conditions (Liu et al., 1997). Thus, another approximation technique had to be employed to properly represent the strong non-linear relationship between the variables in Tables 4.4a-e.

Neural network (NN) approximation has been successful in representing complex non-linear relationships between multiple inputs and outputs. Huang et al.(1993) developed a NN model for a tissue-paper dryer; the model was developed with data obtained from simulation tests, and closely represented the trends of the test data. Trelea et al. (1997) employed a NN model to predict the drying and the wet-milling degradation of maize; the agreement between the experimental data and the NN model was good.

The development of the NN models for quality control of crossflow grain dryers was used. A feed-forward neural network was employed in developing the model. The architecture of the model is shown in Fig. 8.1. There are two visual layers and one hidden layer in the network, with three inputs and one output. The neuron number in the hidden layer, n, was searched.

The mathematical description of the quality *simulation model* is:

$$Q = \phi_2\{W2[\phi_1(W1\begin{bmatrix} G \\ T \\ M_0 \end{bmatrix} + B1)]\} + B2 \qquad (8.1)$$

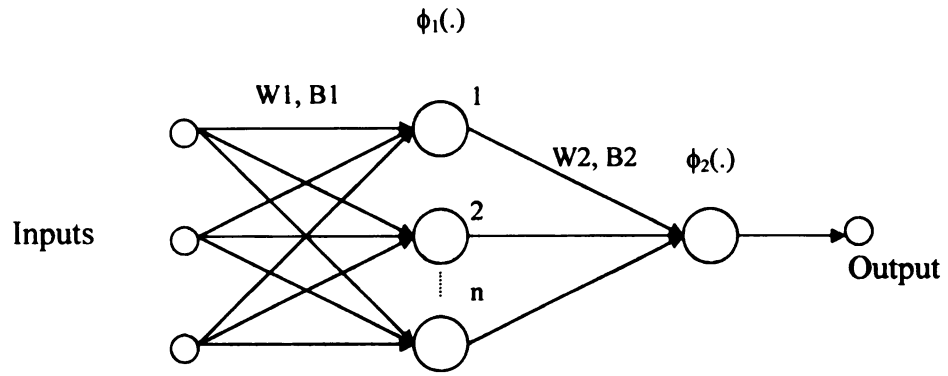

Fig. 8.1 The structure of the NN model.

and of the *quality control model* :

$$T = \phi_2\{W2[\phi_1(W1\begin{bmatrix} G \\ M_0 \\ Q \end{bmatrix} + B1)]\} + B2 \tag{8.2}$$

where

G = scaled airflow rate

T = scaled drying air temperature

M_0 = scaled initial grain moisture content

Q = scaled grain quality

W1, W2 = weight matrices

B1, B2 = bias vectors

ϕ_1, ϕ_2 = functions

n = number of neurons in hidden layer

The inputs and outputs were scaled to 0-1 by dividing the maximum values in the training data. The maximum values of the parameters were found to be 96 $m^3m^{-3}min^{-1}$ for

airflow rate, 120°C for drying-air temperature, 35% w.b. for inlet grain moisture content, and 35% for denatured protein. ϕ_1 was chosen as the hyperbolic tangent function and ϕ_2 as the pure linear function. The model parameters of W1, W2, B1 and B2 were determined by "training" the NN model with the training data in Tables 4.4a-e. A back-propagation algorithm was used to train the NN model with the function of *trainbpx* in the Neural Networks Toolbox of Matlab [Demuth et al., 1992]. The training process continued until the sum of the square error (SSE) of the NN model had stabilized.

The number of hidden neurons *n* was searched during the training. Fig. 8.2 shows the SSE of the control model after 6000 epochs of training at different numbers of hidden neurons. A higher number of neurons in the hidden layer constitutes a smaller SSE of the model. It was decided to use three hidden neurons in both models.

The results for the *simulation model* were (final SSE=0.14):

$$W1 = \begin{bmatrix} 0.0634 & 0.1158 & -4.0228 \\ 1.0417 & 2.3108 & 1.8126 \\ 0.1604 & 1.0965 & -4.5147 \end{bmatrix}$$

$$B1 = \begin{bmatrix} 2.5246 \\ -4.6694 \\ 2.5674 \end{bmatrix}$$

$$W2 = [-0.9223 \quad 0.4245 \quad 0.7375]$$

$$B2 = [0.3521]$$

Fig. 8.3 compares the simulation model to the training data at an airflow rate of 64 $m^3\ m^{-3}\ min^{-1}$. The agreement between the NN model and the training data is good.

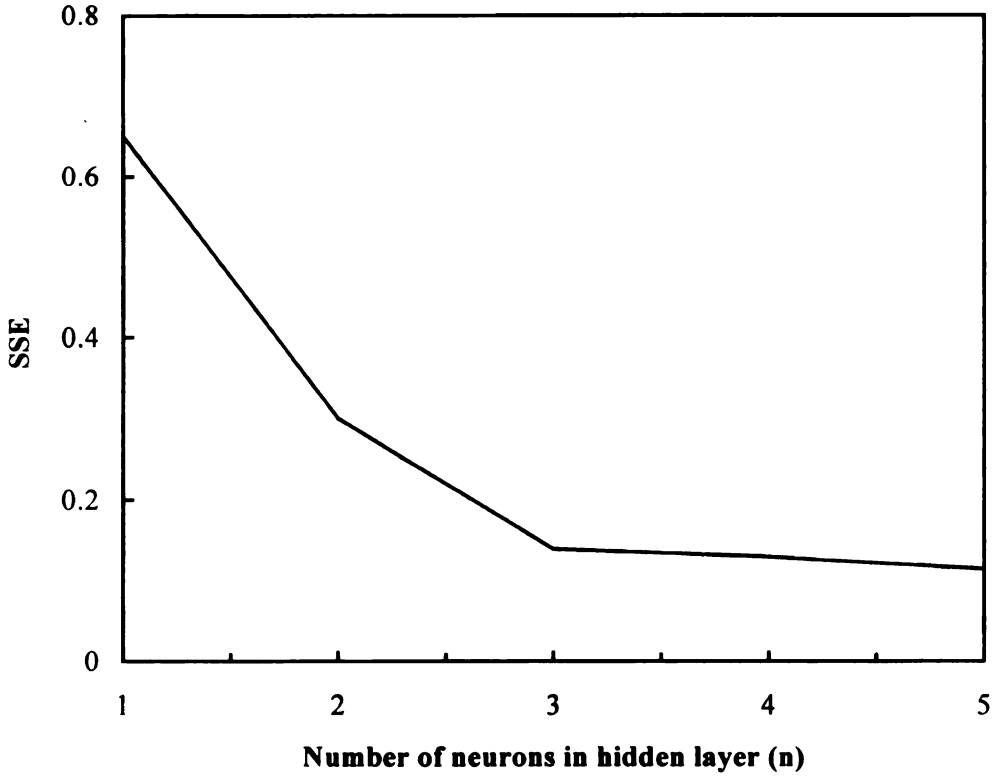

Fig. 8.2 Sum of the square error (SSE) of the neural network *control model* vs. the number of neurons (n) in hidden layer.

The results for the *control model* were (final SSE=0.15):

$$W1 = \begin{bmatrix} 1.2487 & 3.6306 & 0.4423 \\ 1.1707 & -3.2809 & -1.5777 \\ 0.1555 & -1.0397 & -1.3205 \end{bmatrix}$$

$$B1 = \begin{bmatrix} -3.1249 \\ 1.3498 \\ 0.4837 \end{bmatrix}$$

$$W2 = [-0.4020 \quad 0.5225 \quad -1.8377]$$

$$B2 = 0.1893$$

Fig. 8.4 compares the control model to the training data. The NN control model follows the training data well except in the lower and upper ranges of the drying temperature. Additional neurons in the hidden layer and different nonlinear functions were investigated but did not improve the results. The fundamental reason is that the temperature does not change smoothly but in steps in the training data, and thus it was a severe test for the NN model to fully represent the multiple-step function shown in Fig. 8.4. The accuracy of the NN model is acceptable in the range of 60 to 100°C temperature range.

8.3 Quality Control Algorithm

In the development of the quality control algorithm, it was assumed that the moisture content of the grain at the outlet of the dryer is always controlled to the set point (i.e. 15% w.b.) by an "ideal" moisture controller. This allows the design of the quality controller to be independent of the moisture control, and simplifies the problem. Because

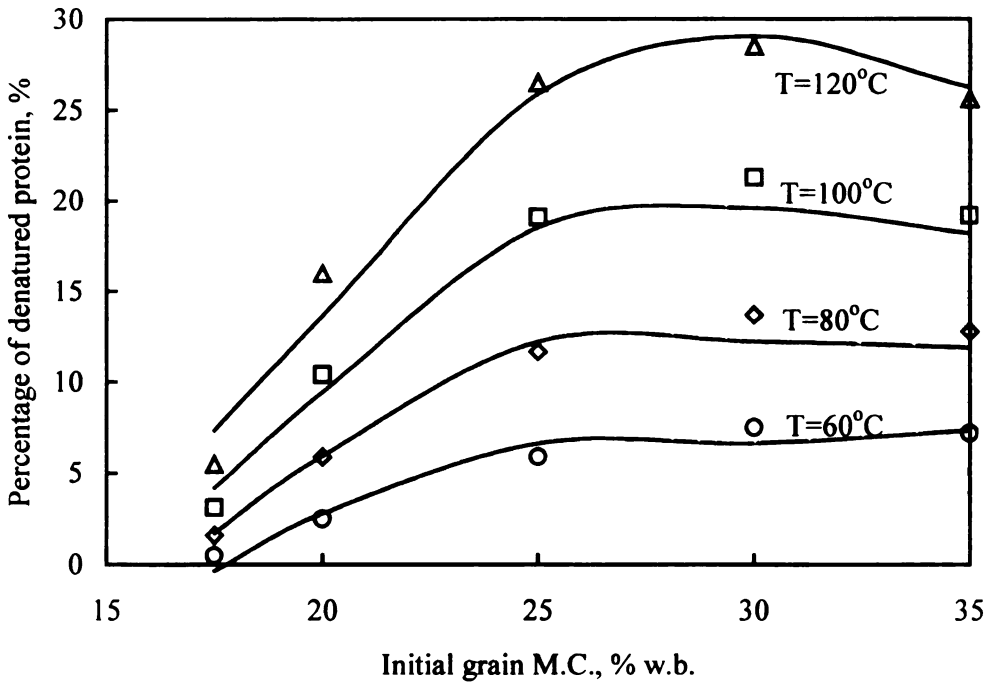

Fig. 8.3 The percentage of denatured protein of maize after crossflow drying as predicted by the neural-network *simulation model* (solid lines) and the training data (marks), at an airflow rate of 64 $m^3m^{-3}min^{-1}$.

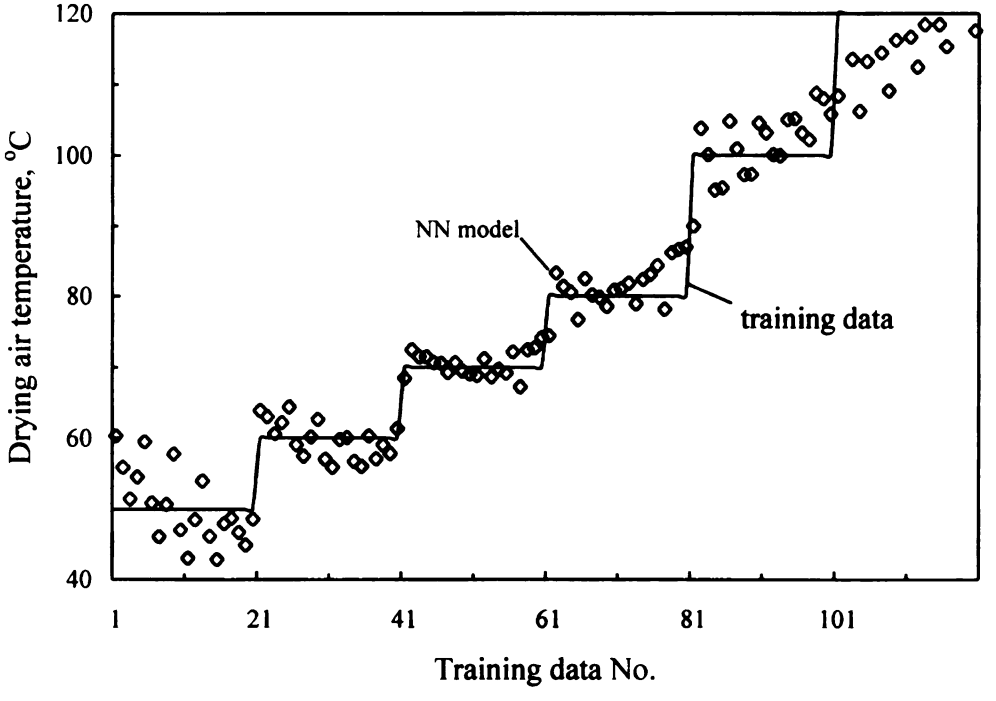

moisture controller can not be "ideal", the accuracy of the quality control depends on the

Fig. 8.4 Comparison of the neural-network *control model* and the training data.

performance of the moisture controller.

Since accurate on-line measurement of grain quality is not (yet) commercially the available, no feedback algorithm could be implemented in the quality controller. Thus, a model-based feedforward control algorithm was used.

If the desired grain quality at the outlet of the dryer is known, the NN control model can determine the required drying-air temperature corresponding to the inlet grain moisture content (as measured by a moisture sensor at the inlet of the dryer). At each sampling period, the inlet grain moisture content is measured and the desired drying-air temperature is calculated. However, this temperature can not be directly used to control the air temperature of the dryer because the residence time of the grain in the dryer is usually much longer than the sampling period. The grain currently in the dryer is the grain which enters the dryer during previous sampling periods, possibly with different initial moisture contents each requiring different drying-air temperatures. Therefore, the drying-air temperature for controlling the dryer needs to be optimized by considering the grain entering the dryer *and* the grain currently in the dryer.

To optimize the temperature, a weighted average of the temperatures required by the grain currently in the dryer is selected. If the residence time of grain in the dryer constitutes n sampling periods there will be n desired temperatures, i.e. one for grain entering the dryer at each sampling period. Then, the optimized drying-air temperature is:

$$T = \sum_{i=1}^{n} \alpha_i T_i \tag{8.3}$$

where α_i = weights, i=1, 2, ..., n

T_i = temperature for ith sampling period, i=1, 2, ..., n

T = optimized temperature

The optimized temperature is recalculated every sampling period.

Fig. 8.5 shows the optimized drying-air temperature for different PDP values, using Eq 8.3 for the crossflow drying of maize at an airflow rate of 64 $m^3\ m^{-3}\ min^{-1}$. All the temperatures were equally weighted (i.e. $\alpha_i = 1/n$). The drying column was conceptually divided into 10 beds; the sampling period was chosen as the time for grain to move through one bed; therefore, the residence time of grain in the dryer was equal to 10 sampling periods. The inlet grain moisture content ranged from 20-30% w.b. with 5% step changes, the outlet grain moisture content was controlled at 15% w.b. The optimized temperatures varied with the inlet grain moisture content and the set-point of the dried grain quality. When the percentage of denatured protein was changed from 8% to 12%, and from 12% to 16%, the optimized drying-air temperature increased about 15°C. When the inlet grain moisture content was changed from 20% to 30% w.b., the drying-air temperature had to be decreased by about 30°C to maintain the required grain quality. Conventionally, the drying-air temperature is seldom adjusted in crossflow dryers. Fig. 8.6 shows the predicted outlet grain quality of a crossflow dryer when the drying air temperature was maintained at 103°C. The grain quality was predicted using the grain-quality simulation model (Eq. 8.1). The PDP increased from about 10% to 20% when the inlet grain moisture content changed from 20% to 30%. *Thus, the quality of grain dried in a crossflow dryer varies significantly if the drying-air temperature is not adjusted.*

The dried grain quality was relatively uniform when a quality controller was employed to regulate the drying-air temperature for a set-point of the outlet grain quality

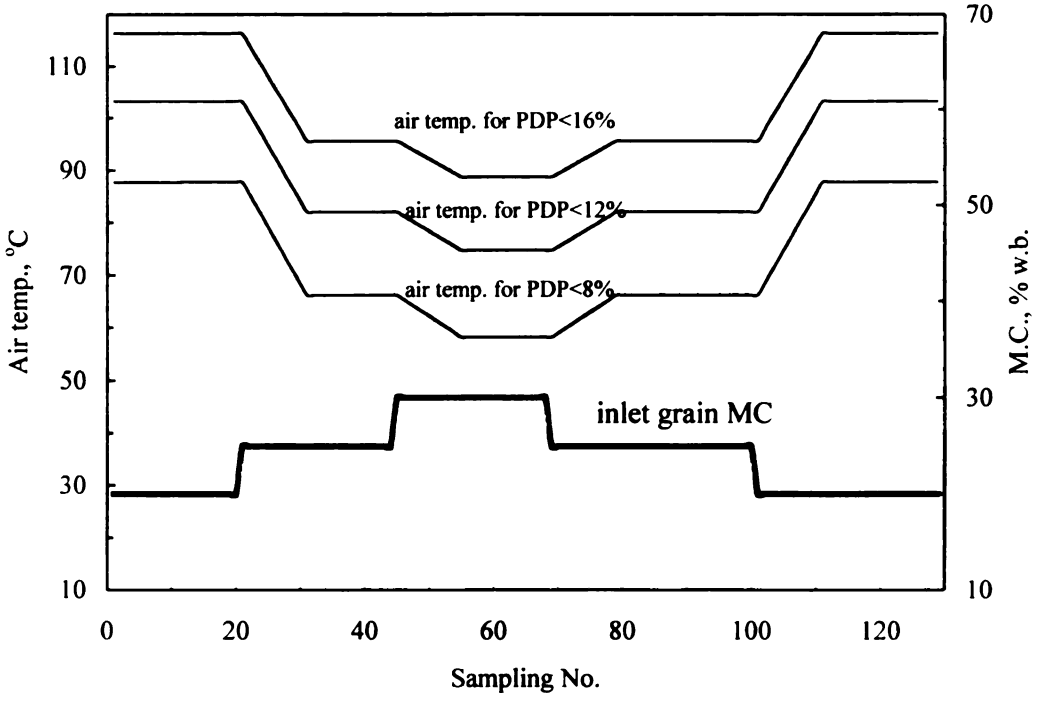

Fig. 8.5 Optimized drying-air temperature for crossflow drying of maize at different set-points of the outlet grain PDP- percentage of denatured protein (outlet grain moisture content = 15% w.b., airflow rate = 64 $m^3m^{-3}min^{-1}$).

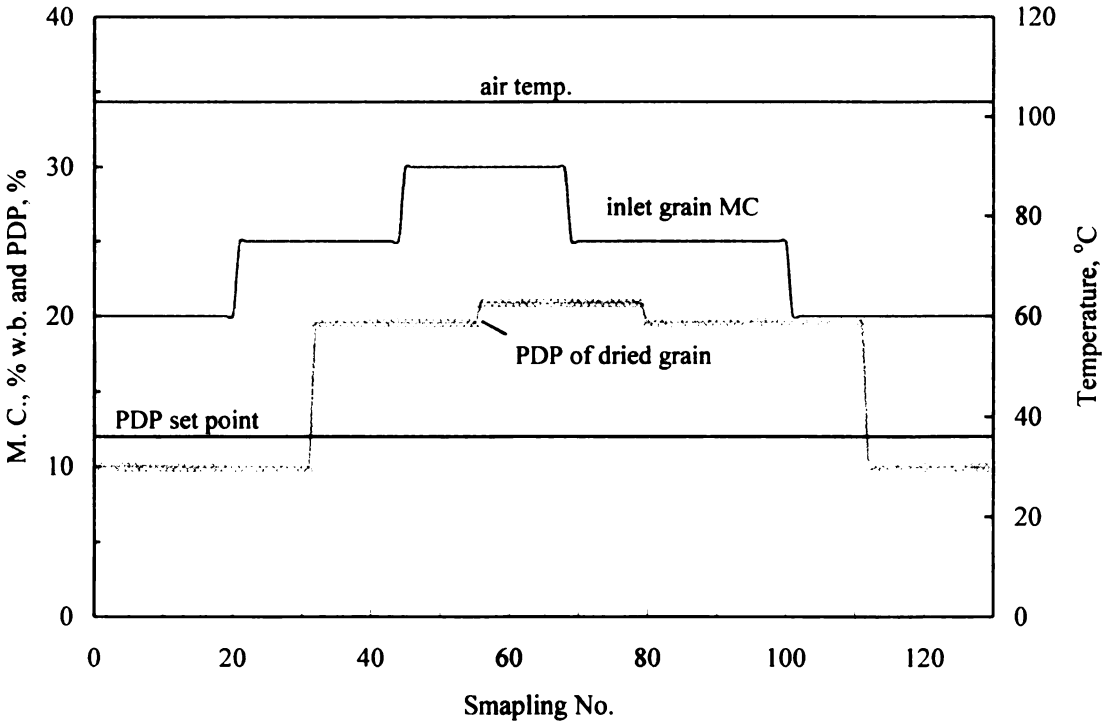

Fig. 8.6 Inlet grain moisture content and predicted outlet grain quality of maize crossflow-dried at 103°C (PDP = percentage of denatured protein, outlet grain moisture content = 15% w.b., set-point of the PDP = 12% of denatured protein, airflow rate = 64 $m^3m^{-3}min^{-1}$).

of 12% denatured protein (as shown in Fig. 8.7). For the same pattern of the inlet grain moisture content as in Fig. 8.6, the variation of the outlet grain quality was small and the average close to the set-point. There was a small steady-state error in the outlet grain-quality because different models (i.e. Eq. 8.1 for simulation and Eq. 8.2 for control) were used for prediction and control of the grain quality, and no feedback was employed in the quality controller.

8.4 Conclusions

(1) Neural-network models were used for simulating the changes in grain quality in a crossflow maize dryers.

(2) A model-based feedforward grain-quality controller was developed for controlling the grain quality of crossflow-dried maize.

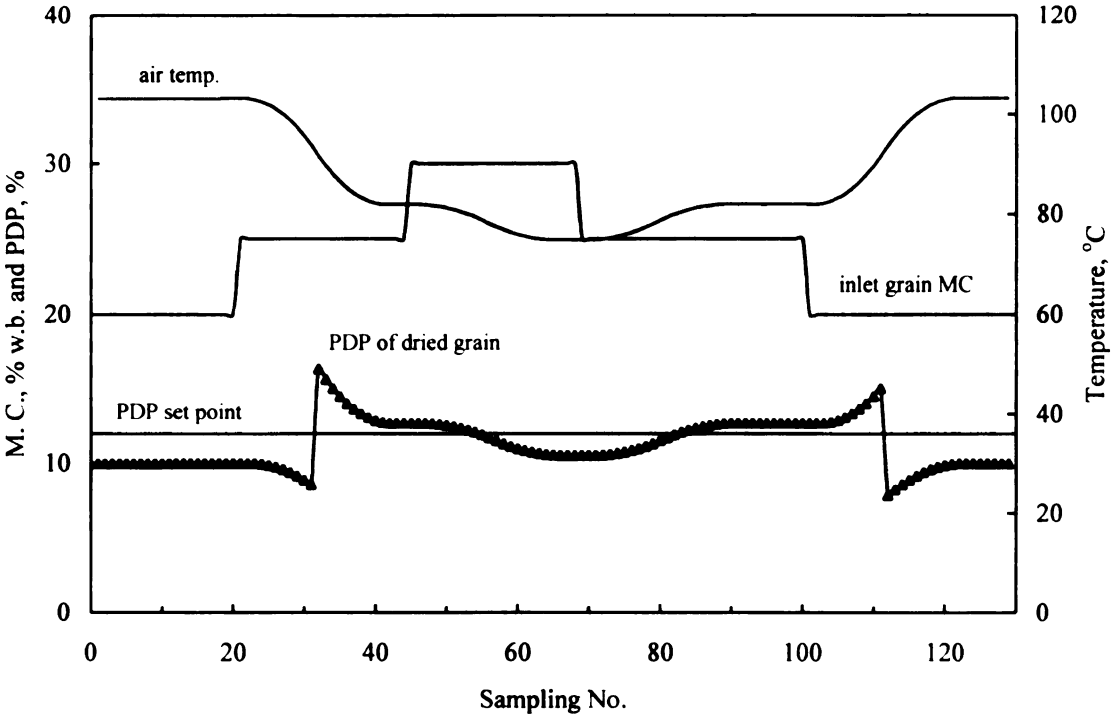

Fig. 8.7 Inlet grain moisture content, optimized drying-air temperature and predicted outlet maize quality in a crossflow dryer operated with a grain-quality controller (PDP = percentage of denatured protein, set point of grain moisture content = 15% w.b., set-point of the PDP = 12% of denatured protein, airflow rate = 64 $m^3m^{-3}min^{-1}$).

References

Liu, Q., F. W. Bakker-Arkema. 1997. Stochastic simulation and control of grain quality in crossflow grain dryers. Paper No. 97-6030. Am. Soc. of Agric. Eng., St. Joseph, MI.

Huang, B., A. S. Mujumdar. 1993. Use of neural network to predict industrial dryer performance. Drying Technology 11(3):524-541.

Demuth, H., M. Beale. 1992. Neural Networks Toolbox User's Guide. The MathWorks, Inc., Natick, MA.

Trelea, I. C., F. Courtois, G. Trystram. 1997. Dynamic models for drying and wet-milling quality degradation of corn using neural networks. Drying Technology 15(3&4): 1095-1102.

CHAPTER 9. SUMMARY

9.1 Stochastic Drying Modeling

The variation of moisture content among grain kernels is significant before, during and after drying. The stochastic nature of the moisture content of maize in the drying process was explored experimentally and analytically. Stochastic grain drying models were developed of the distribution of the moisture content of maize kernels dried in concurrent-flow, counter-flow and crossflow dryers. The models simulate, in addition to the average final moisture content, the moisture content distribution and standard deviation of the grain exiting these dryers.

Deterministic grain drying models assume a uniform inlet moisture content while the stochastic models presume a more realistic normal distribution of the moisture content in the grain entering a dryer. Only stochastic modeling can provide essential design information on the degree of overdrying and of underdrying occurring in grain dryers.

9.2 Grain-quality Models

The changes in the denatured protein content and in the germination of maize during crossflow drying were successfully modeled by combining thin-layer drying/quality models with the MSU stochastic grain-drying model. The application of quality models was illustrated in the analysis of crossflow drying.

Due to lack of quantitative relationships between the dryer parameters and grain quality, the grain quality is not accounted for in the conventional design of grain dryers. Usually, the drying-air temperature is compromised between the dryer capacity and grain quality. The grain-quality models provide an advanced tool to optimize the dryer parameters so that the dryer reaches maximum capacity and energy efficiency while still producing grain of acceptable quality.

9.3 Moisture Controller

A distributed-parameter process model of crossflow drying was developed. The model is more flexible and accurate than the commonly-used lumped-parameter models, and is of adequate simplicity for use in a dyer-control system.

A model-predictive controller was developed for a crossflow grain dryer consisting of a feedforward loop and an indirect feedback loop. The controller has an effective compensation mechanism to changes in the drying-air temperature, and is robust under various disturbances.

9.4 Grain-quality Controller

A neural-network model was employed for developing process model of grain-quality in a crossflow dryer. The neural-network model was good in representing the non-linear relationship between the grain quality and the drying parameters, i.e. air temperature, airflow rate and the initial grain moisture content. Model-based feedforward quality controller was developed for controlling the quality of crossflow-dried maize. The

grain-quality controller optimizes the drying-air temperature, resulting in acceptable and uniform grain quality.

9.5 Suggestions for Future Study:

(1) To employ the stochastic drying and grain-quality models for the optimal design of grain dryers.

(2) To improve the reliability of on-line grain moisture sensors.

(3) To test the quality-control algorithm on commercial dryers.

(4) To develop and test the control systems for mixed-flow and concurrent-flow dryer models.